2

Two-dimensional patterns, lattices and symmetry

2.1 Approaches to the study of crystal structures

In Chapter 1 we developed an understanding of simple crystal structures by first considering the ways in which atoms or ions could pack together and then introducing smaller atoms or ions into the interstices between the larger ones. This is a pragmatic approach as it not only provides us with an immediate and straightforward understanding of the atomic/ionic arrangements in some simple compounds, but also suggests the ways in which more complicated compounds can be built up.

However, it is not a systematic and rigorous approach, as all the possibilities of atomic arrangements in all crystal structures are not explored. The rigorous, and essentially mathematical approach is to analyse and classify the geometrical characteristics of quite general two-dimensional patterns and then to extend the analysis to three dimensions to arrive at a completely general description of all the patterns to which atoms or molecules or groups of atoms or molecules might conform in the crystalline state.

These two distinct approaches—or strands of crystallographic thought—are apparent in the literature of the nineteenth and early twentieth centuries. In general, it was the metallurgists and chemists, such as Tammann* and Pope,* who were the pragmatists, and the theoreticians and geometers, such as Fedorov* and Schoenflies,* who were the analysts. It might be thought that the analytical is necessarily superior to the pragmatic approach because its generality and comprehensiveness provides a much more powerful starting point for progress to be made in the discovery and interpretation of the crystal structures of more and more complex substances. But this is not so. It was, after all, the simple models of sodium chloride and zinc blende of Pope (such as we also constructed in Chapter 1) that helped to provide the Braggs* with the necessary insight into crystal structures to enable them to make their great advances in the interpretation of X-ray diffraction photographs. In the same way, 40 years later, the discovery of the structure of DNA by Watson and Crick was based as much upon structural and chemical knowledge and intuition, together with model building, as upon formal crystallographic theory.

However, a more general appreciation of the different patterns into which atoms and molecules may be arranged is essential, because it leads to an understanding of the important concepts of symmetry, motifs and lattices. The topic need not be pursued rigorously—in fact it is unwise to do so because we might quickly 'lose sight of the wood for the trees!' The essential ideas can be appreciated in two dimensions, the

* Denotes biographical notes available in Appendix 3.

The Basics of Crystallography and Diffraction. Fourth Edition. Christopher Hammond.

subject of this chapter. The extension to three dimensions (Chapters 3 and 4) which relates to 'real crystal structures', should then present no conceptual difficulties.

2.2 Two-dimensional patterns and lattices

Consider the pattern of Fig. 2.1 (a), which is made up of the letter **R** repeated indefinitely. What does **R** represent? Anything you like—a 'two-dimensional molecule', a cluster of atoms or whatever. Representing the 'molecule' as an **R**, an *asymmetric* shape, is in effect representing an *asymmetric* molecule. We shall discuss the different types or elements of symmetry in detail in Section 2.3 below, but for the moment our general everyday knowledge is enough. For example, consider the symmetry of the letters **R M S.** **R** is asymmetrical. **M** consists of two equal sides, each of which is a reflection or mirror image of the other, there is a **mirror line** of symmetry down the centre indicated by the letter m, thus M←m . There is no mirror line in the **S**, but if it is rotated 180° about a point in its centre, an identical **S** appears; there is a **two-fold rotation axis** usually called a **diad axis** at the centre of the **S**. This is represented by a little lens-shape at the axis of rotation: S .

In Fig. 2.1(a) **R**, the repeating 'unit of pattern' is called the **motif**. These motifs may be considered to be situated at or near the intersections of an (imaginary) grid. The grid is called the **lattice** and the intersections are called **lattice points**.

Let us now draw this underlying lattice in Fig. 2.1(a). First we have to decide where to place each lattice point in relation to each motif: anywhere will do—above, below, to one side, in the 'middle' of the motif—the only requirement is that the *same* position with respect to the motif is chosen every time. We shall choose a position a little below the motif, as shown in Fig. 2.1(b). Now there are an infinite number of ways in which the lattice points may be 'joined up' (i.e. an infinite number of ways of drawing a lattice

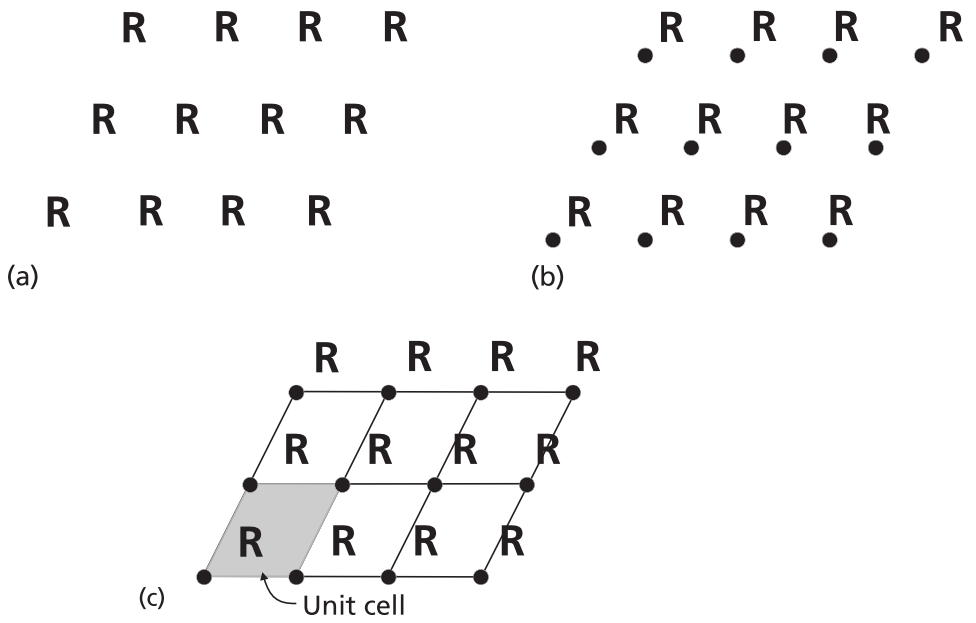

Fig. 2.1. (a) A pattern with the motif **R**, (b) with the lattice points indicated and (c) the lattice and a unit cell outlined. (Drawn by K. M. Crennell.)

or grid of lines through lattice points). In practice, a grid is usually chosen which 'joins up' adjacent lattice points to give the lattice as shown in Fig. 2.1(c), and a unit cell of the lattice may also be outlined. Clearly, if we know (1) the size and shape of the unit cell and (2) the motif which each lattice point represents, including its orientation with respect to the lattice point, we can draw the whole pattern or build up the whole structure indefinitely. The unit cell of the lattice and the motif therefore define the whole pattern or structure. This is very simple: but observe an importance consequence. Each motif is identical and, for an infinitely extended pattern, the environment (i.e. the spatial distribution of the surrounding motifs, and their orientation) around each motif is identical. This provides us with the definition of a lattice (which applies equally in two and three dimensions): *a lattice is an array of points in space in which the environment of each point is identical.* Again it should be stressed that by environment we mean the spatial distribution and orientation of the surrounding points.

Like all simple definitions (and indeed ideas), this definition of a lattice is often not fully appreciated; there is, to use a colloquial expression, 'more to it than meets the eye!' This is particularly the case when we come to three-dimensional lattices (Chapter 4), but, for the two-dimensional case, consider the patterns of points in Fig. 2.2 (which should be thought of as extending infinitely). Of these only (a) and (d) constitute a lattice; in (b) and (c) the points are certainly in a *regular* array, but the surroundings of each point are *not* all identical.

Figures 2.2(a) and (d) represent two two-dimensional lattice types, named **oblique** and **rectangular**, respectively, in view of the shapes of their unit cells. But what is the distinction between the oblique and rectangular lattices? Surely the rectangular lattice is just a special case of the oblique, i.e. with a 90° angle?

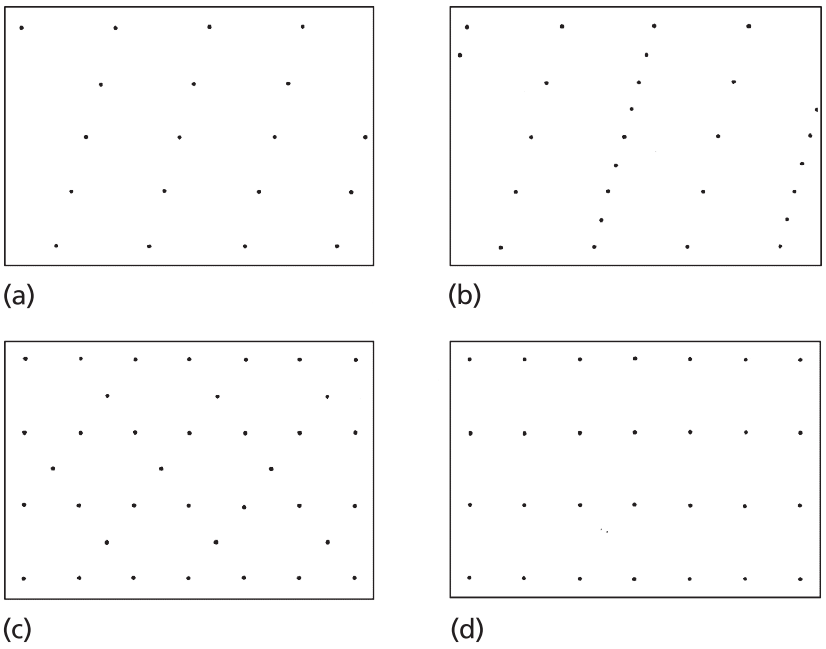

Fig. 2.2. Patterns of points. Only (a) and (d) constitute lattices.

The distinction arises from different symmetries of the two lattices, and requires us to extend our everyday notions of symmetry and to classify a series of symmetry elements. This precise knowledge of symmetry can then be applied to both the motif and the lattice and will show that there are a limited number of patterns with different symmetries (only seventeen) and a limited number of two-dimensional lattices (only five).

2.3 Two-dimensional symmetry elements

The clearest way of developing the concept of symmetry is to begin with an asymmetrical 'object'—say the **R** of Fig. 2.1—then to add successively mirror lines and axes of symmetry and to see how the **R** is repeated to form different patterns or groups. The different patterns or groups of **R**s which are produced correspond, of course, to objects or projections of molecules (i.e. 'two-dimensional molecules') with different symmetries which are not possessed by the **R** alone.

The patterns or groups which arise and which as explained below are of concern in crystallography are shown in Fig. 2.3. On the left are the patterns of **R**s, in the centre are decorative motifs with the same symmetry, and on the right are projections of molecules. Figure 2.3(1) shows the **R** 'on its own' and, as an example, the asymmetrical projection of the CHFCClBr molecule. Figure 2.3(2) shows 'right-' and 'left'-handed **R**s reflected in the 'vertical' mirror line between them. This pair of **R**s has the same mirror symmetry as the projection of the *cis*-difluoroethene molecule. Now add another 'horizontal' mirror line as in Fig. 2.3(3). A group of four **R**s (two right- and two left-handed) is produced. This group has the same symmetry as the projection of the ethene molecule.

The **R** may be repeated with a diad (two-fold rotation) axis, as in Fig. 2.3(4). The two **R**s (both right handed) have the same symmetry as the *trans*-difluoroethene molecule. Now look back to the group of **R**s in Fig. 2.3(3); notice that they also are related by a diad (two-fold rotation axis) at the intersection of the mirror lines: the action of reflecting the **R**s across two perpendicular mirror lines 'automatically' generates the two-fold symmetry as well. This effect, where the action of two symmetry elements generates another, is quite general as we shall see below.

Mirror lines and diad axes of symmetry are just two of the symmetry elements that occur in two dimensions. In addition there are three-fold rotation or **triad** (3) axes (represented by a little triangle, ▲, four-fold rotation or **tetrad** (4) axes (represented by a little square, ■), and six-fold (6) or **hexad** axes (represented by a little hexagon, ⬢). Asymmetrical objects are represented as having a one-fold or **monad** (1) axis of symmetry (for which there is no little symbol)—which means in effect that one 360° rotation brings the object into coincidence with itself.

Figure 2.3(5) shows the **R** related by a triad (three-fold) axis. The projection of the trifluoroalkylammonia molecule also has this same symmetry. Now add a 'vertical' mirror line as in Fig. 2.3(6). Three more left-handed **R**s are generated, and at the same time the **R**s are mirror related not just in the vertical mirror line but also in two lines inclined at 60° as shown; another example of additional symmetry elements (in this case mirror lines) being automatically generated.

This procedure (of generating groups of **R**s which represent motifs with different symmetries) may be repeated for tetrad (four-fold) axes (Fig. 2.3(7)); plus mirror lines (Fig. 2.3(8)); for hexad (six-fold) axes (Fig. 2.3(9)); plus mirror lines (Fig. 2.3(10)). Notice that not only do these axes of symmetry 'automatically' generate mirror lines at 90° (for tetrads) and 60° (for hexads) but also 'interleaving' mirror lines at 45° and 30° as well.

The ten arrangements of **R**s (and the corresponding two-dimensional motifs or projections of molecules) are called the **ten two-dimensional crystallographic or plane point groups**, so called because all the symmetry elements—axes (perpendicular to the page) and mirror lines (in the page)—pass through a point. The ten plane point groups are labelled with 'shorthand' symbols which indicate, as shown in Fig. 2.3, the

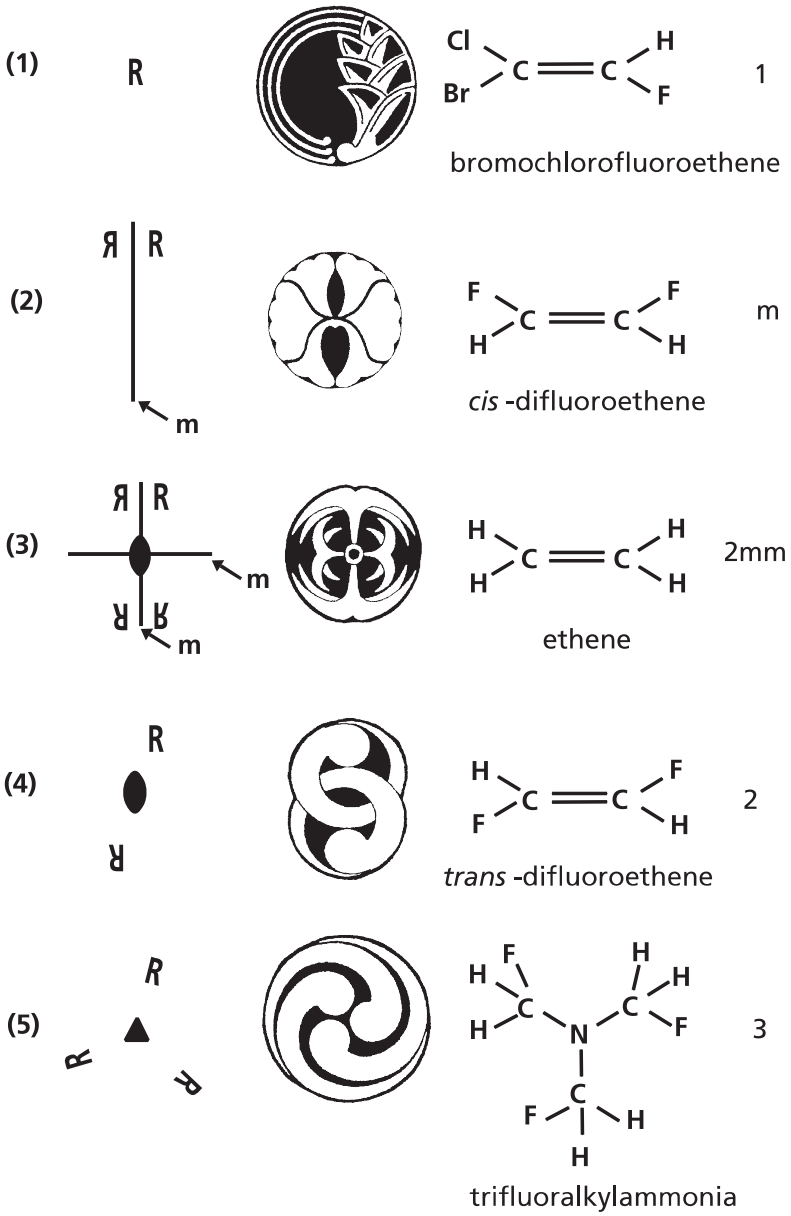

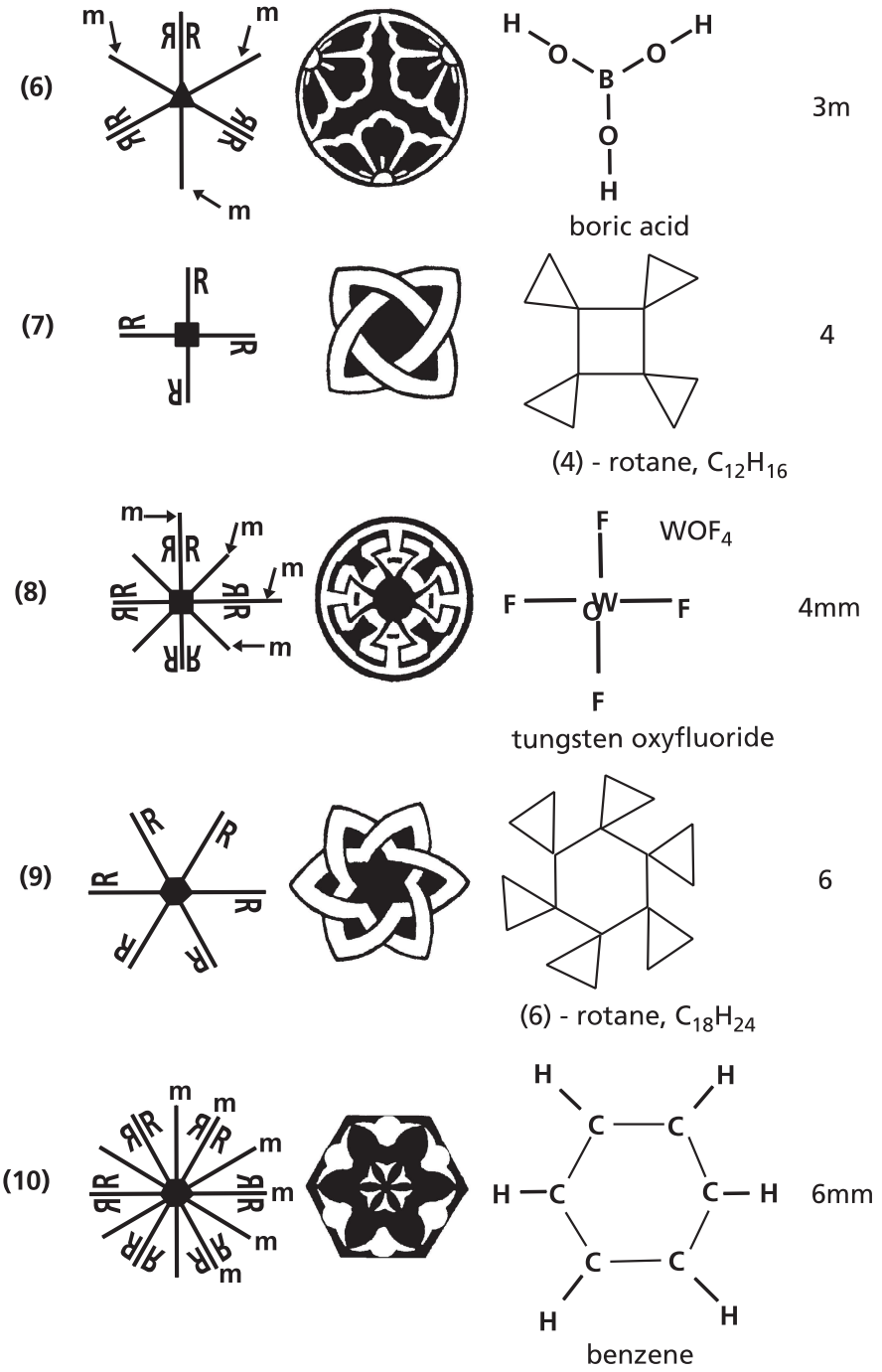

Fig. 2.3. The ten plane point groups showing left to right, the symmetry which arises based on an asymmetrical object **R**; examples of motifs; examples of molecules and ions (drawn as projections) and the point group symbols. (Drawn by K. M. Crennell.)

symmetry elements present: 1 for a monad (no symmetry), *m* for one mirror line, *mm* (or 2*mm*) for two mirror lines (plus diad), 2 for a diad, 3 for a triad, 3*m* for a triad plus three mirror lines, 4 for a tetrad, 4*mm* for a tetrad plus four mirror lines, 6 for a hexad and 6*mm* for a hexad plus six mirror lines (the extra '*m*' in the symbols referring to the 'interleaving' mirror lines).

Now, in deriving these ten plane point groups we have ignored groups of **R**s with fivefold (**pentad**), seven-fold (**heptad**) etc. axes of symmetry with and without mirror lines. Such plane point groups are certainly possible and are widely represented in nature—the pentagonal symmetry of a starfish for example. However, what makes the ten plane point groups in Fig. 2.3 special or distinctive is that *only* these combinations of axes and mirror lines can occur in regular repeating patterns in two dimensions as is explained in Sections 2.4 and 2.5 below. Hence they are properly called the two-dimensional *crystallographic* point groups as indicated above. Patterns with pentagonal symmetry are necessarily non-repeating, non-periodic or 'incommensurate' and consequently have in the past been rather overlooked by crystallographers. However, with the realization that groups of atoms (or viruses) can form 'quasicrystals' with five-fold symmetry elements (see Section 4.9), the study of non-periodic two-dimensional patterns has become of increasing interest and importance (see Section 2.9). A simple way at this stage of 'seeing the difference' is to compare, for example, the arrangement of six lattice points equally spaced around a central lattice point (hexagons) with the arrangement of five 'lattice' points equally spaced around a central point (pentagons). In the former case the arrangement of points can be put together to form a lattice (a pattern or *tiling* of hexagons with 'no gaps' and 'no overlaps'). In the latter case the points cannot be put together to form a lattice—there are always 'gaps' or 'overlaps' between the tiling of pentagons. Try it and see!

2.4 The five plane lattices

Having examined the symmetries which a two-dimensional motif may possess we can now determine how many two-dimensional or plane lattices there are. We will do this by building up patterns from the ten motifs in Fig. 2.3 with the important condition that the symmetry elements possessed by the single motif must also extend throughout the whole pattern. This condition is best understood by way of a few examples. Consider the asymmetrical motif **R** (Fig. 2.3(1)); there are no symmetry elements to be considered and the **R** may be repeated in a pattern with an oblique unit cell (i.e. the most asymmetrical) arrangement of lattice points. Now consider the motif which possesses one 'vertical' mirror line of symmetry (Fig. 2.3(2)). This mirror symmetry must extend throughout the whole pattern from motif to motif which means that the lattice must be rectangular. There are two possible arrangements of lattice points which fulfil this requirement: a simple rectangular lattice and a centred rectangular lattice as shown in Fig. 2.4(a).

These rectangular lattices also possess 'horizontal' mirror lines of symmetry corresponding to the motif with the two sets of mirror lines as shown in Fig. 2.3(3). Now consider the motifs with tetrad (four-fold) symmetry (Figs 2.3(7) and (8)). This four-fold symmetry must extend to the surrounding motifs which means that they must be arranged in a square pattern giving rise to a square lattice (Fig. 2.4(a)).

Altogether, five two-dimensional or plane lattices may be worked out, as shown in Fig. 2.4(a). They are described by the shapes of the unit cells which are drawn between lattice points—oblique p, rectangular p, rectangular c (which is distinguished

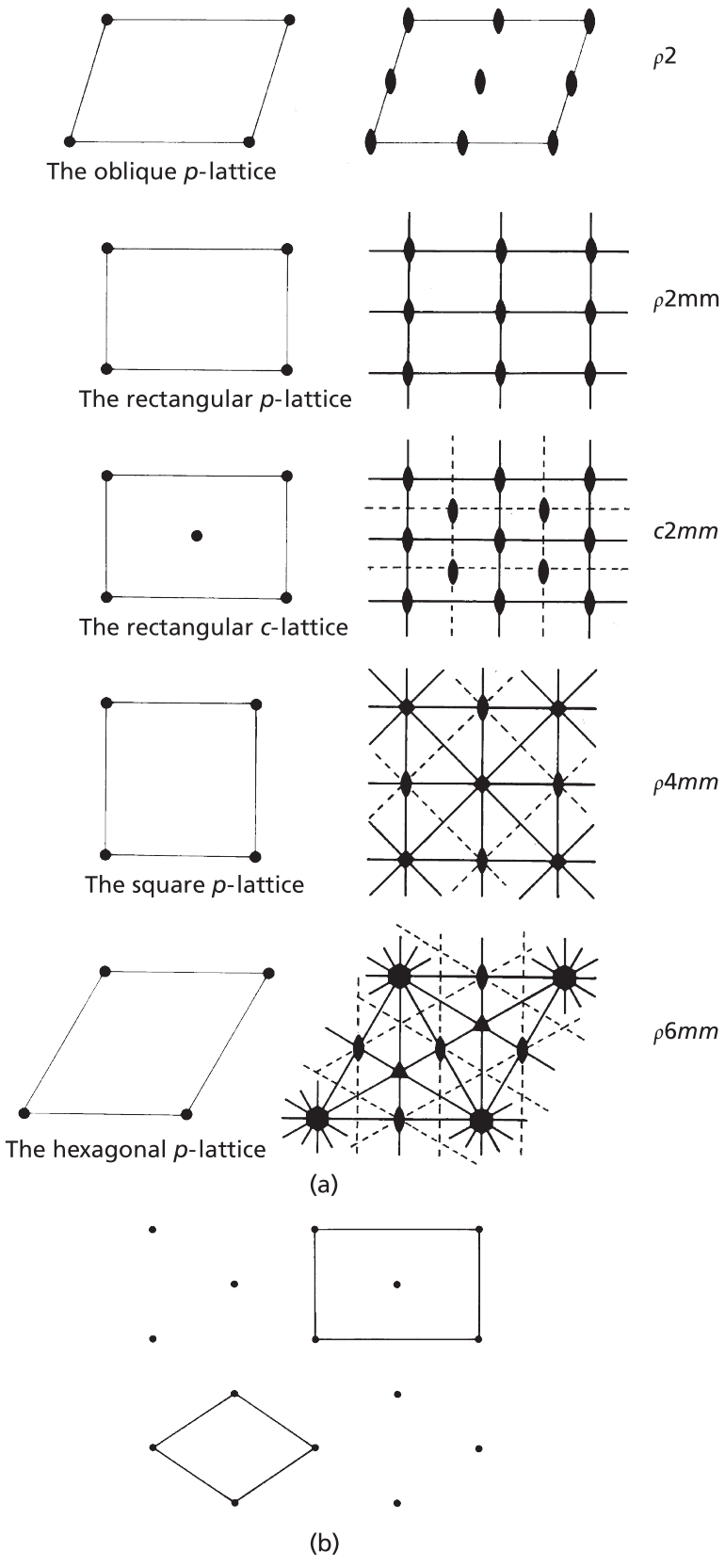

Fig. 2.4. (a) Unit cells of the five plane lattices, showing the symmetry elements present (heavy solid lines indicate mirror lines, dashed lines indicate glide lines) and their plane group symbols (from *Essentials of Crystallography*, by D. McKie and C. McKie, Blackwell, 1986). (b) The rectangular *c* lattice, showing the alternative primitive (rhombic *p* or diamond *p*) unit cell.

from rectangular *p* by having an additional lattice point in the centre of the cell), square *p* and hexagonal *p*. Notice again that additional symmetry elements are generated 'in between' the lattice points as shown in Fig. 2.4(a) (right). For example, in the square lattice there is a tetrad at the centre of the cell, diads halfway along the edges and vertical, horizontal and diagonal mirror lines as well as the tetrads situated at the lattice points.

All two-dimensional patterns must be based upon one of these five plane lattices; no others are possible. This may seem very surprising—surely other shapes of unit cells are possible? The answer is 'yes', a large number of unit cell shapes are possible, but the pattern of lattice points which they describe will always be one of the five of Fig. 2.4(a). For example, the rectangular *c* lattice may also be described as a rhombic *p* or diamond *p* lattice, depending upon which unit cell is chosen to 'join up' the lattice points (Fig. 2.4(b)). These are just two alternative descriptions of the *same* arrangement of lattice points. So the choice of unit cell is arbitrary: *any* four lattice points which outline a parallelogram can be joined up to form a unit cell. In practice we take a sensible course and mostly choose a unit cell that is as small as possible—or 'primitive' (symbol *p*)—which does not contain other lattice points within it. Sometimes a larger cell is more useful because the axes joining up the sides are at 90°. Examples are the rhombic or diamond lattice which is identical to the rectangular centred lattice described above and, to take an important three-dimensional case, the cubic cell (Fig. 1.6(c)) which is used to describe the ccp structure in preference to the primitive rhombohedral cell (Fig. 1.7(c)).

Now we combine the ten plane point group symmetries (Fig. 2.3) with the appropriate plane lattices (Fig. 2.4) in order to work out the total number of two-dimensional patterns. For example, plane point group symmetries 4 and 4*mm*, combined with the square lattice, give two patterns *p*4 and *p*4*mm* (Fig. 2.6). Notice that in these (and other) patterns additional mirror lines and axes of symmetry are 'automatically' generated within the unit cell (Fig. 2.6(b)). Notice also that there are two possible combinations of plane point symmetry 3*m* with the plane hexagonal lattice: the triad axes generated within the unit cell either have mirror lines passing through them (*p*3*m*1) or not (*p*31*m*). Continuing in this way we generate thirteen two-dimensional patterns known as the **symmorphic plane groups**. However, there is a complication: the combination of a point group symmetry with a lattice can give rise to an additional symmetry element called a **glide line**. Consider the two patterns in Fig. 2.5, both of which have a rectangular lattice. In Fig. 2.5(a) the motif has mirror symmetry as in Fig. 2.3(2); it consists of a pair of right- and left-handed **R**s. In Fig. 2.5(b) there is still a reflection—still pairs of right- and left-handed **R**s—but one set of **R**s has been translated, or glided half a lattice spacing. This symmetry is called a **reflection glide** or simply a **glide line of symmetry**. Notice that glide lines also arise automatically in the centre of the unit cell of Fig. 2.5(b) as do mirror lines in Fig. 2.5(a). Glide lines are, of course, as familiar to us as mirror lines; they represent the pattern of our footprints in the snow when we walk in a straight line!

The presence of the glide lines also has important consequences regarding the symmetry of the motif. In Fig. 2.5(a) the motif has mirror symmetry but in Fig. 2.5(b) it does not: the pair of right- and left-handed **R**s is asymmetric. It is the repetition of the

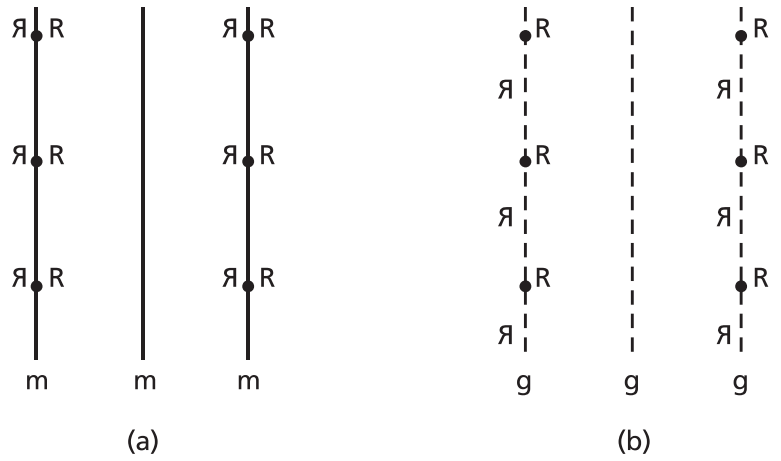

Fig. 2.5. Patterns with (a) reflection symmetry and (b) glide-reflection symmetry. The mirror lines (*m*) and glide lines (*g*) are indicated.

translational symmetry elements—the glide lines—that determines the overall rectangular symmetry of the pattern. The glide lines which are present in the five plane lattices are shown (in addition to the axes and mirror lines of symmetry) in Fig. 2.4(a).

2.5 The seventeen plane groups

Glide lines give rise to four more two-dimensional patterns (*pg*, *pmg*, *pgg*, and *p*4*g*—Fig. 2.6)—the **non-symmorphic plane groups** giving seventeen in all—the seventeen **plane groups**. On a macroscopic scale the glide symmetry in a crystal would appear as simple mirror symmetry—the shift between the mirror-related parts of the motif would only be observable in an electron microscope which was able to resolve the individual mirror-related parts of the motif, i.e. distances of the order of 0.5–2 Å (50–200 pm).

The seventeen plane groups are shown in Fig. 2.6(a). They are labelled by 'shorthand' symbols which indicate the type of lattice (*p* for primitive, *c* for centred) and the symmetry elements present, *m* for mirror lines, *g* for glide lines, 4 for tetrads and so on. The symmetry elements within a unit cell are shown in Fig. 2.6(b). It is a good exercise in recognizing the symmetry elements present in the 17 plane groups to lay a sheet of tracing paper over Fig. 2.6(a), to indicate the positions of the axes, mirror and glide lines of symmetry in an (arbitrary) unit cell and then to compare your 'answers' with those shown in Fig. 2.6(b).

It is essential to practice recognizing the motifs, symmetry elements and lattice types in two-dimensional patterns and therefore to find to which of the seventeen plane groups they belong. Any regular patterned object will do—wallpapers, fabric designs, or the examples at the end of this chapter. Figure 2.7 indicates the procedure you should follow. Cover up Fig. 2.7(b) and examine only Fig. 2.7(a); it is a projection of molecules of $C_6H_2(CH_3)_4$. You should recognize that the molecules or groups of atoms are *not* identical in this two-dimensional projection. The motif is a *pair* of such molecules and this is the 'unit of pattern' that is repeated. Now look for symmetry elements and (using a piece of tracing paper) indicate the positions of all of these on the pattern. Compare

your pattern of symmetry elements with those shown in Fig. 2.7(b). If you did not obtain the same result you have not been looking carefully enough! Finally, insert the lattice points—one for each motif. Anywhere will do, but it is convenient to have them coincide with a symmetry element, as has been done in Fig. 2.7(b). The lattice is clearly oblique and the plane group is $p2$ (see Fig. 2.6).

Another systematic way of identifying a plane pattern is to follow the 'flow diagram' shown in Fig. 2.8. The first step is to identify the highest order of rotation symmetry present, then to determine the presence or absence of reflection symmetry and so on through a series of 'yes' and 'no' answers, finally identifying one of the seventeen plane patterns whose plane group symbols are indicated 'in boxes', corresponding to those given in Fig. 2.6.

2.6 One-dimensional symmetry: border or frieze patterns

Identifying the number of one-dimensional patterns provides us with a good exercise in applying our more general knowledge of plane patterns. It is also a useful exercise in that it tells us about the different types of patterns that can be designed for the borders of wallpapers, edges of dress fabrics, friezes and cornices in buildings, and so on.

In plane patterns the symmetry operations and symmetry elements are (clearly) repeated in a plane; in one-dimensional patterns they can only be repeated in or along a line—i.e. the line or long direction of the border or frieze. This restriction immediately rules out all rotational symmetry elements with the exception of diads: two-fold symmetry alone can be repeated in a line: three-, four-, and six-fold symmetry elements require the repetition of a motif in directions other than the line of the border. For the same reason glide-reflection lines of symmetry, other than that along the line of the border, are ruled out. Mirror lines of symmetry are restricted to those along, and perpendicular to, the line of the border.

These restrictions result in seven one-dimensional groups, shown in Fig. 2.9. It is a good and satisfying exercise for you to derive these from first principles as outlined above. It is also useful to compare Fig. 2.9 with Fig. 2.6; the bracketed symbols in Fig. 2.9 indicate from which plane pattern the one-dimensional pattern may be derived. Notice that in one case two one-dimensional patterns—these with 'horizontal' and 'vertical' mirror planes—are derived from one plane pattern (pm). This is because the mirror lines in the plane group pm can be oriented either along, or perpendicular to, the line of the one-dimensional pattern.

Figure 2.23 (see Exercise 2.6) also shows examples of some of the border patterns. You can practice recognizing such patterns either by overlaying the pattern with a piece of tracing paper, and indicating the positions of the diads, mirror and glide lines as described above for plane patterns or by following the flow diagram (Fig. 2.10).

2.7 Symmetry in art and design: counterchange patterns

We have a rich inheritance of plane and border patterns in printed and woven textiles, wallpapers, bricks and tiles which have been designed and made by countless craftsmen

Fig. 2.6. (*continued*)

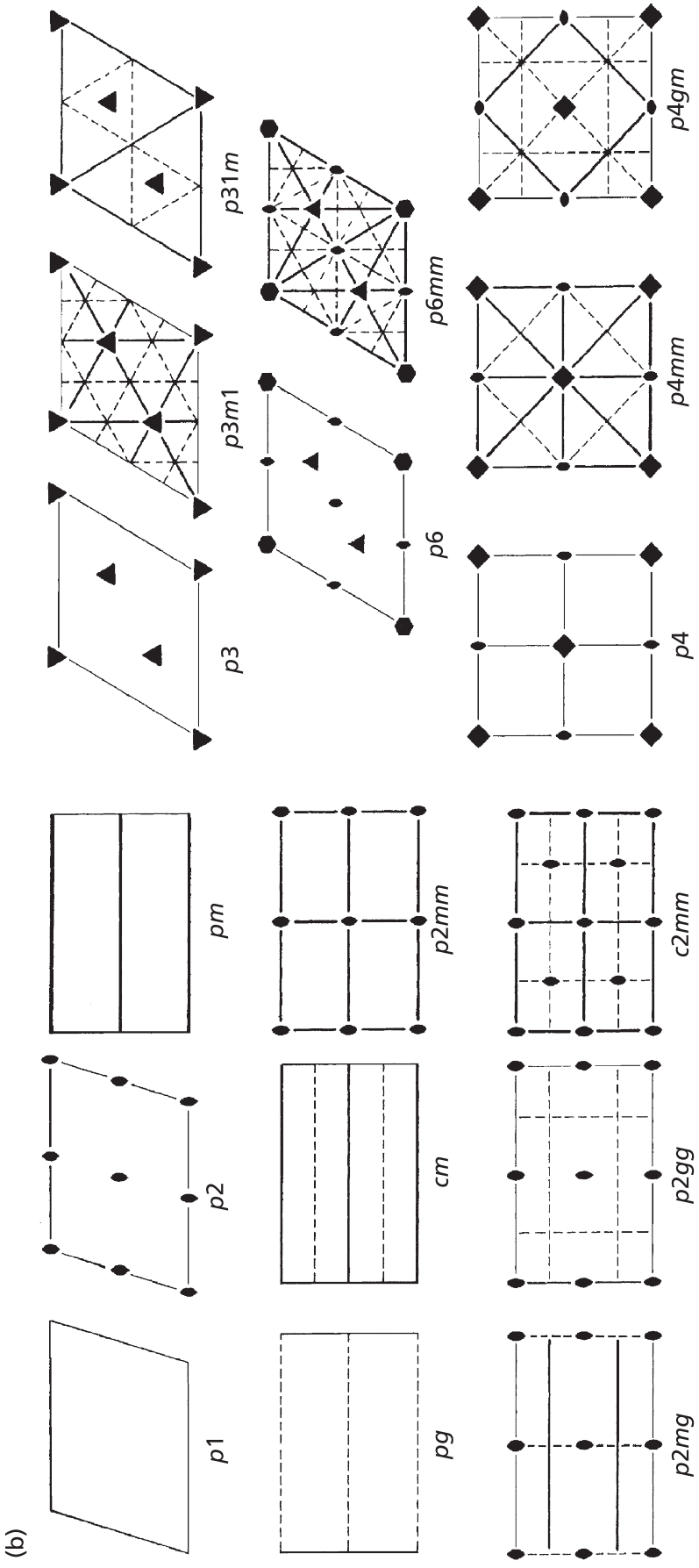

Fig. 2.6. (a) The seventeen plane groups (from *Point and Plane Groups* by K. M. Crennell). The numbering 1–17 is that which is arbitrarily assigned in the International Tables. Note that the 'shorthand' symbols do not necessarily indicate all the symmetry elements which are present in the patterns, (b) The symmetry elements outlined within (conventional) unit cells of the seventeen plane groups, heavy solid lines and dashed lines represent mirror and glide lines respectively (from *Manual of Mineralogy* 21st edn, by C. Klein and C. S. Hurlbut, Jr., John Wiley, 1999).

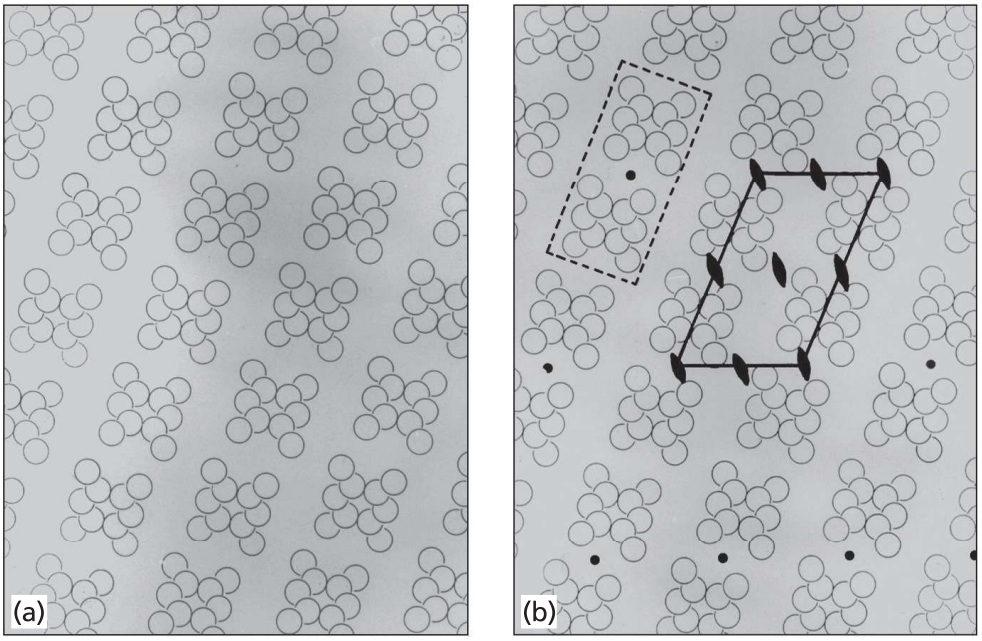

Fig. 2.7. Projection (a) of the structure of $C_6H_2(CH_3)_4$ (from *Contemporary Crystallography*, by M. J. Buerger, McGraw-Hill, 1970), with (b) the motif, lattice and symmetry elements indicated.

and artisans in the past 'without benefit of crystallography'. The question we may now ask is: 'Have all the seventeen plane groups and seven one-dimensional groups been utilized in pattern design or are some patterns and some symmetries more evident than others? If so, is there any relationship between the preponderance or absence of certain types of symmetry elements in patterns and the civilization or culture which produced them?'

Questions such as these have exercised the minds of archaeologists, anthropologists and historians of art and design. They are, to be sure, questions more of cultural than crystallographic significance, but patterns play such a large part in our everyday experience that a crystallographer can hardly fail to be absorbed by them, just as he or she is absorbed by the three-dimensional patterns of crystals.

The study of plane and one-dimensional patterns (and indeed three-dimensional (space) patterns) is complicated by the question of colour—'real' colours in the case of plane and one-dimensional patterns, or colours representing some property, such as electron spin direction or magnetic moment, in space patterns (Chapter 4). Colour changes may also be analysed in terms of symmetry elements in which colours are alternated in a systematic way. Clearly, the greater the number of colours, the greater the complexity. The simplest cases to consider are two-colour (e.g. black and white) patterns. Figure 2.11 shows the generation of plane motifs through the operation of what are called counter-change or colour symmetry elements,[1] which are distinguished from ordinary (rotation) axes and mirror lines of symmetry by a prime superscript. For example, the operation of a $2'$ axis is a twice repeated rotation of an asymmetric

[1] These are a special case of what are sometimes known as *anti-symmetry* elements, which relate the symmetry of opposites—black/white in this case.

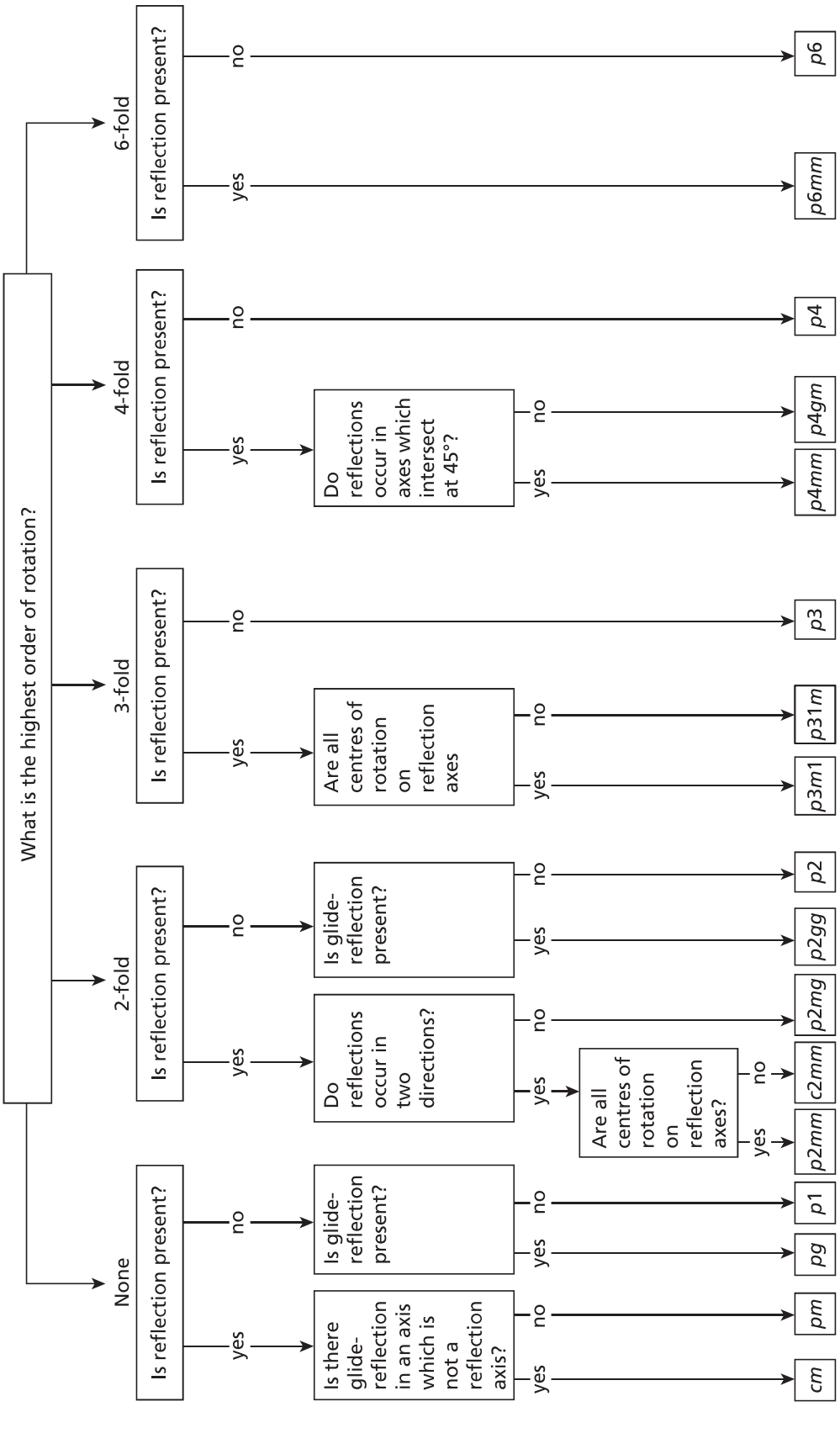

Fig. 2.8. Flow diagram for identifying one of the seventeen plane patterns (redrawn from *The Geometry of Regular Repeating Patterns* by M. A. Hann and G. M. Thomson, the Textile Institute, Manchester, 1992). The numbering is that which is arbitrarily assigned in the International Tables (see Fig 2.6).

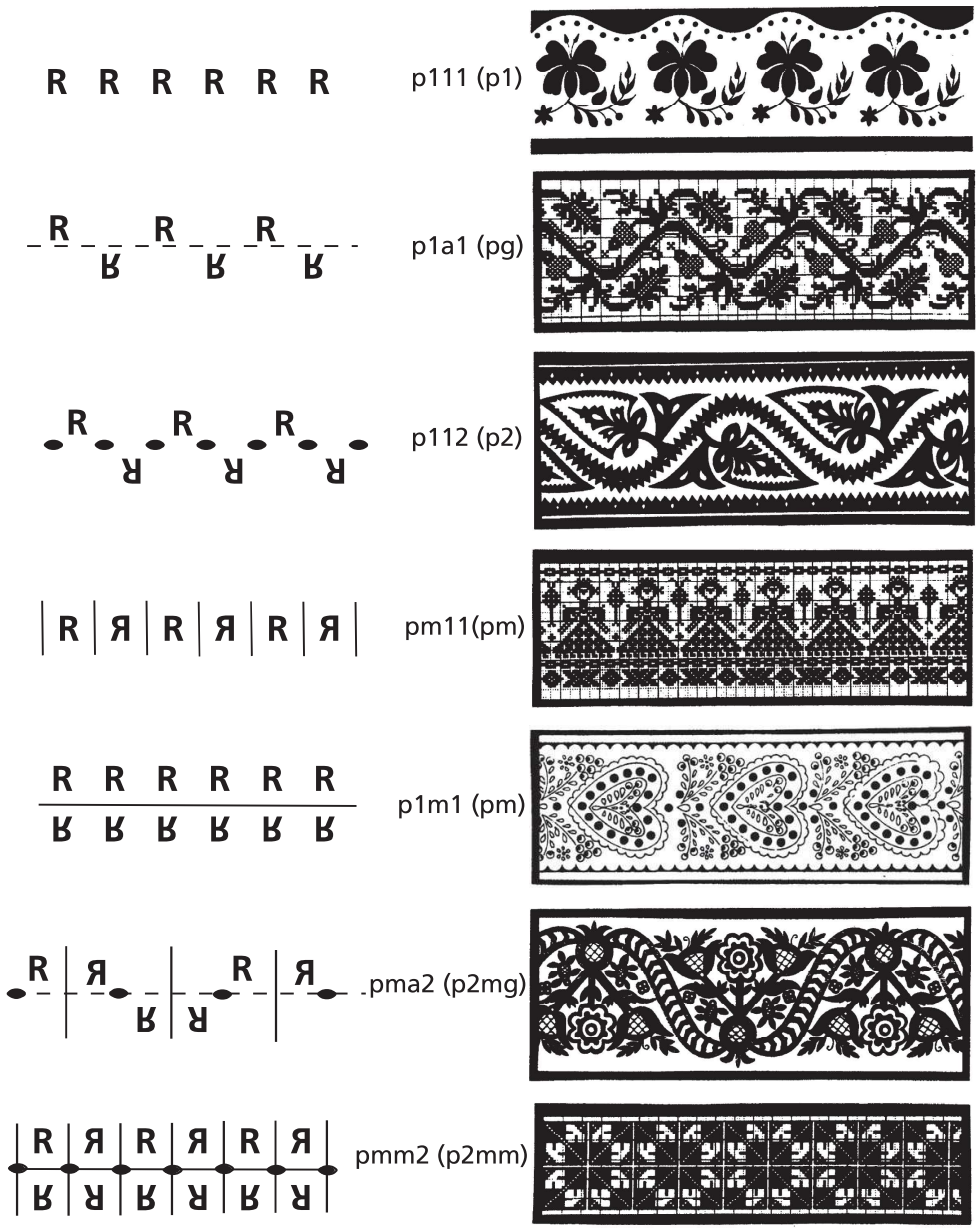

Fig. 2.9. (*Left*) the seven one-dimensional groups or classes of border or frieze patterns (drawn by K. M. Crennell); (solid lines indicate mirror lines, dashed lines (symbol a) indicate glide lines and ⬬ symbols indicate diads); (*centre*) their symmetry symbols and (*bracketed*) the plane groups from which they are derived; and (*right*) examples of Hungarian needlework border patterns (from *Symmetry Through the Eyes of a Chemist* 3rd edn. by M. and I. Hargittai, Springer, New York and London 2008).

object by 180° plus a colour change at each rotation; the operation of an m′ mirror line is a reflection plus colour change. Altogether there are eleven counterchange point groups (Fig. 2.11) compared with the ten plane point groups (Fig. 2.3). Note that there are **no** counterchange point groups corresponding to the plane point groups with only odd-numbered axes of symmetry (the monad and the triad), but that there are in each case two possible counterchange point groups corresponding to the plane point groups with symmetry 2*mm*, 4*mm* and 6*mm*.

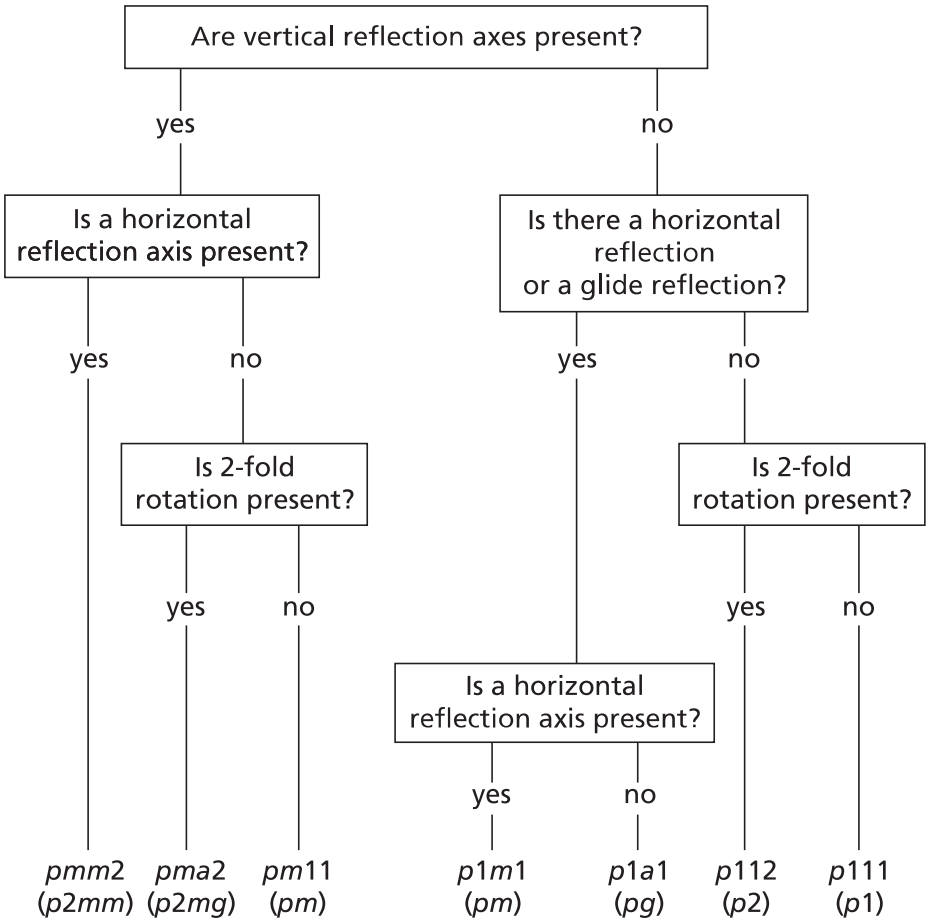

Fig. 2.10. Flow diagram for identifying one of the seven border patterns (from *The Geometry of Regular Repeating Patterns*, in brackets the plane groups from which they are derived. loc. cit.).

The derivation of the counterchange one- and two-dimensional patterns also involves the operation of a g' glide line which involves a reflection plus a translation of half a lattice spacing **plus** a colour change and gives (to extend our footprint analogy) a sequence of black/white (i.e. right/left footprints).

Accounting for two-colour symmetry gives rise to a total of forty-six (rather than seventeen) plane patterns and seventeen (rather than seven) one-dimensional patterns. Figure 2.12 shows an example of plane group pattern $p2gg$ (No. 8—see Fig. 2.6(a), (b)) and the two possible counterchange patterns (symbols $p2'\ gg'$ and $p2g'\ g'$) which are based upon it.

Probably the most influential and pioneering study of patterns was *The Grammar of Ornament* by Owen Jones, first published in 1856.[2] Owen Jones attempted to categorize both plane and border patterns in terms of the different cultures that produced them, and although the symmetry aspects of patterns are touched on in the most fragmentary

[2] Owen Jones. *The Grammar of Ornament*, Day & Sons Ltd., London, reprinted by Studio Editions, London (1986).

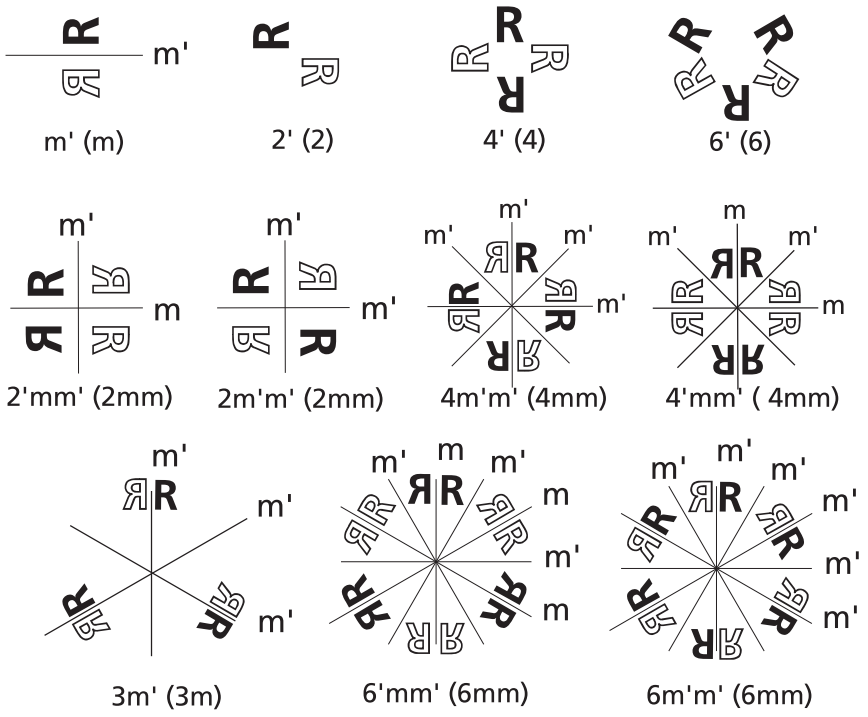

Fig. 2.11. The eleven counterchange (black/white) point groups and (bracketed) the point group symbols for the plane point groups to which they correspond (see Fig. 2.3). The counterchange symmetry elements are denoted by prime superscripts. (Drawn by K. M. Crennell.)

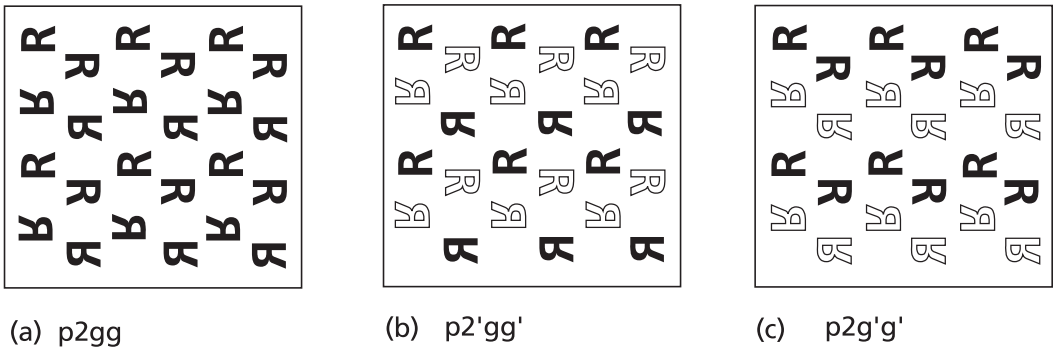

Fig. 2.12. (a) Plane group $p2gg$ and (b) and (c) the two counterchange plane groups $p2'\,gg'$ and $p2g'g'$ respectively which are based upon it. (Drawn by K. M. Crennell.)

way, there is no doubt that the superb illustrations and encyclopaedic character of the book provided later writers with material which could be classified and analysed in crystallography terms. Perhaps the best known of these was M. C. Escher (1898–1971) who drew inspiration for his drawings of tessellated figures from visits to the Alhambra in the 1930s, and also presumably from Owen Jones' chapter on 'Moresque Ornament' in which he describes the Alhambra as 'the very summit of Moorish art, as the Parthenon

is of Greek art'. Escher's patterns encompass all the seventeen plane groups, eleven of which are represented in the Alhambra.*

More recent work has identified clear preponderances of certain plane symmetry groups, and the absences of others.[3] For example, nearly 50% of traditional Javanese batik (wax-resist textile) patterns belong to plane group $p4mm$ (Fig. 2.6), others, such as $p3$, $p3m1$, $p31m$ and $p6$ are wholly absent. In Jacquard-woven French silks of the last decade of the nineteenth century, nearly 80% of the patterns belong to plane group pg. In Japanese textile designs of the Edo period *all* plane groups are represented, with a marked preponderance for groups $p2mm$ and $c2mm$. What these differences mean, or tell us about the cultures which gave rise to them, is, as the saying goes, 'another question'.

In X-ray crystallography crystal structures are frequently represented as two-dimensional projections (electron density maps—see Section 13.2). The beauty and variety of these patterns led Dr Helen Megaw*, a crystallographer at Birkbeck College, London, to suggest that they be made the basis for the design of wallpapers and fabrics in the same way that William Morris used flowers and birds in his pattern designs. Her suggestion eventually bore fruit in the work of the *Festival Pattern Group* of the 1951 Festival of Britain and the production of a remarkable variety of patterned wallpapers, carpets and fabrics based upon crystal structures as diverse as haemoglobin, insulin and apophyllite. These patterns, recently republished,[4] provide a rich source of material for plane group recognition.

2.8 Layer (two-sided) symmetry and examples in woven textiles

Woven textiles consist of interlacing warp 'north-south' threads and weft 'east-*weft*' threads. The various combinations of interlacings, which give rise to the different patterns of cloths, are very wide indeed, ranging from the simplest 'single cloth', plain weave fabric, where individual warp and weft threads pass over and under each time (Fig. 2.13), to more complex cloth structures. Common structures include twills (e.g. Fig. 2.14), herringbones, sateens, etc. Clearly, there are symmetry relationships between the 'face' and 'back' of such woven fabrics and the study of such relationships introduces us to what are known as *layer-symmetry groups* or classes.

We will not describe all the layer-symmetry groups or classes (of which there are a total of 80) but just some of the general principles of their construction. Readers who wish to follow this topic further should refer to the book by Shubnikov and Koptsik or the papers by Scivier and Hann.[5] However, we may note here that the 80 layer-symmetry

* Denotes biographical notes available in Appendix 3.

[3] M. A. Hann. *Symmetry of Regular Repeating Patterns: Case Studies from various cultural settings.* Journal of the Textile Institute (1992), Vol. 83, pp. 579–580.

[4] L. Jackson. *From Atoms to Patterns, Crystal Structure Designs from the 1951 Festival of Britain.* Richard Dennis Publications, Shepton Beauchamp, Somerset (2008).

[5] J.A. Scivier and M.A. Hann (2000) *The application of symmetry principles to the classification of fundamental simple weaves*, Ars Textrina **33**, 29 and (2000) *Layer symmetry in woven textiles*, Ars Textrina **34**, 81.

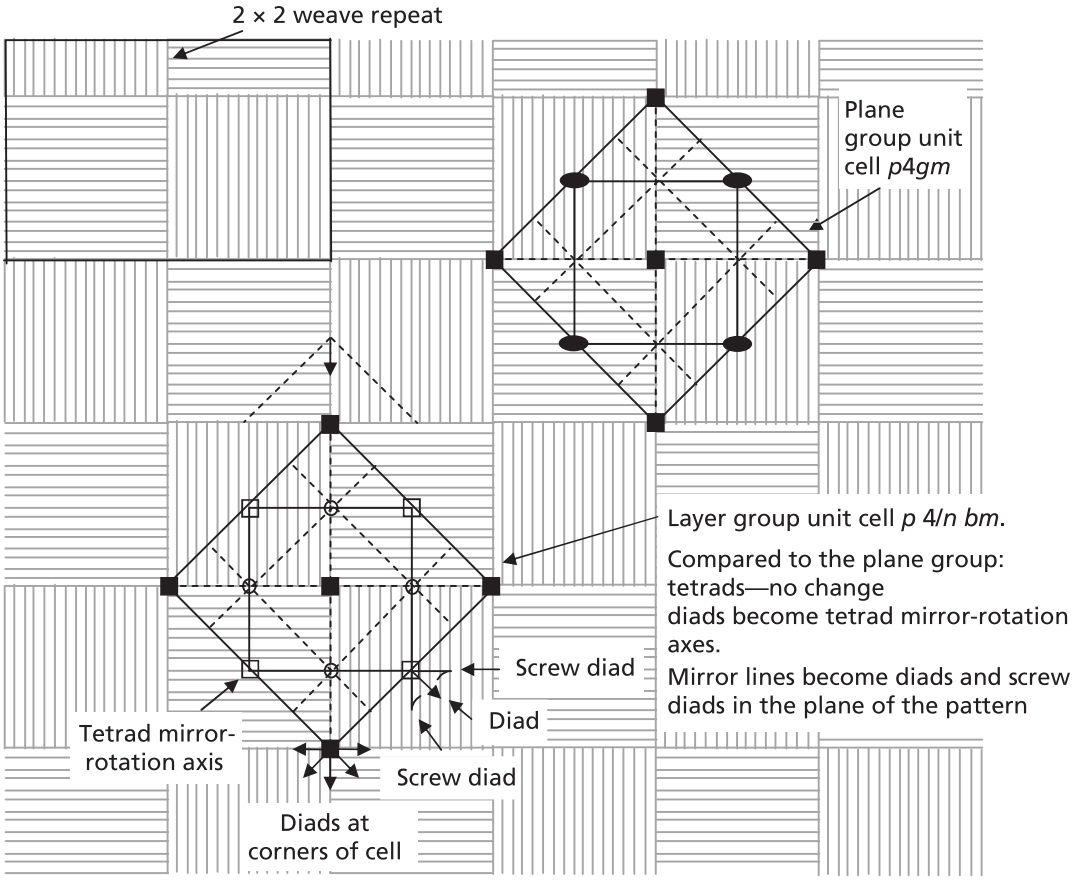

Fig. 2.13. Diagrammatic representation of a plain weave and (superimposed) the plane group unit cell *p*4*gm* (see also Fig. 2.6) and the layer-symmetry group unit cell *p*4/*nbm*. Note the differences between the symmetry elements in these unit cells: the diads and mirror lines in *p*4*gm* become tetrad mirror-rotation axes and screw diads respectively (in the plane) in *p* 4/*n bm*. (Drawn by C. McConnell.)

groups are sub-groups of the 230 space groups (Section 4.6) and that the 17 plane groups are, in turn, sub-groups of the 80 layer-symmetry groups.

Because of the structural restrictions imposed by the warp and weft character, the five plane groups with three or six fold symmetry are not applicable to woven fabrics and, correspondingly, neither are 16 of the 80 layer-symmetry groups.

As we have seen, in describing the 17 plane groups we are restricted to rotation axes perpendicular to the plane and reflection (mirror) and glide lines of symmetry within the plane. In describing layer-symmetry groups further symmetry elements or operations are required which relate the 'face' and 'back' of the fabric. These are (i) rotation-reflection (alternating) axes of symmetry perpendicular to the plane which consist of a rotation plus a reflection in the plane. These symmetry operations correspond to the black/white counterchange point groups (Fig. 2.11) in which the symbol **R** is now understood to have two sides—black on the face and white on the back. Again, because of the structural restrictions imposed by woven fabrics, only two such rotation-reflection axes are applicable—$2'$ and $4'$ (Fig. 2.11). (ii) Diad axes lying *within* the

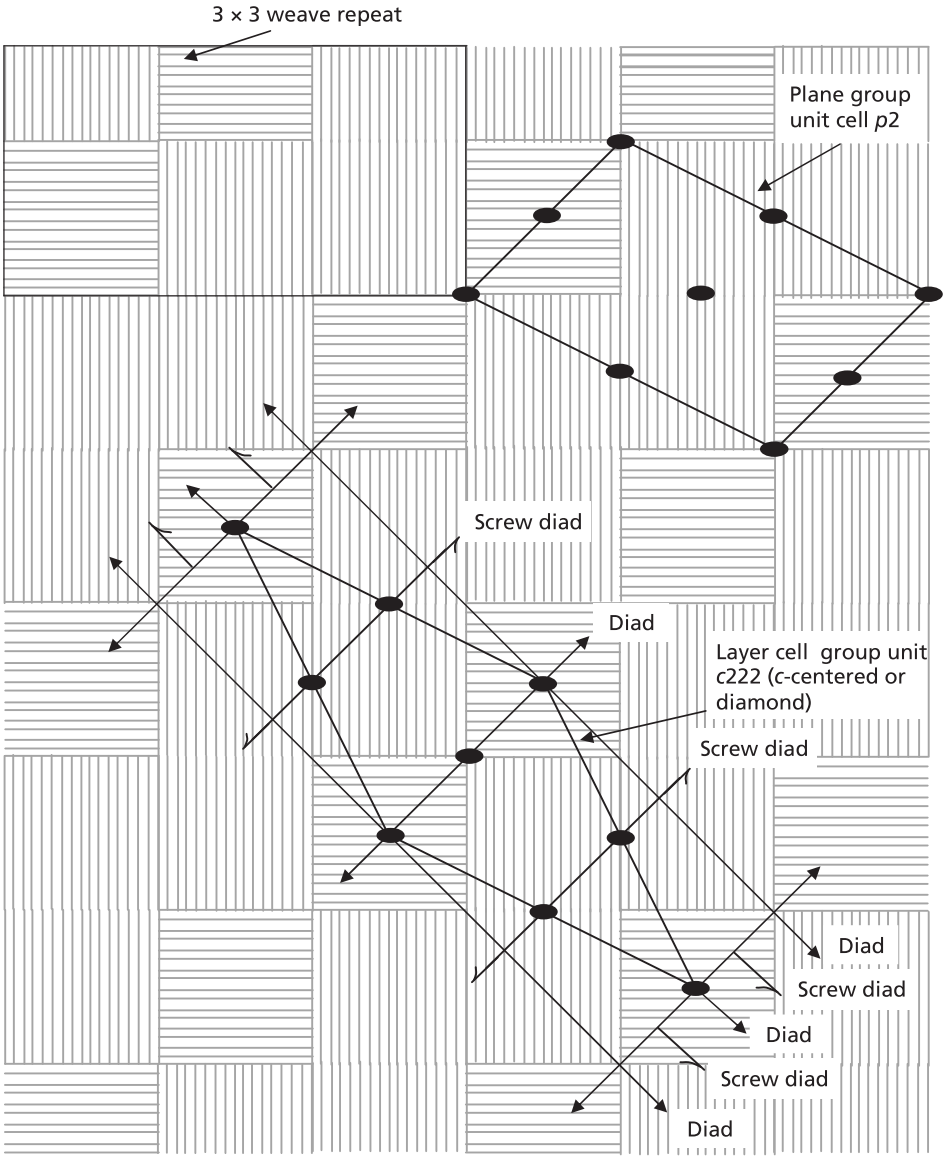

Fig. 2.14. Diagrammatic representation of a twill weave with a 3 × 3 repeat and (superimposed) the plane group unit cell $p2$ and the layer-symmetry group unit cell $c222$. Note the differences between these unit cells: $c222$ is a rectangular c-centred or 'diamond' unit cell (see Fig. 2.4) and contains diads and screw diads lying in the plane of the pattern. (Drawn by C. McConnell.)

plane—both the simple diad axes which we have already met and also *screw diad* axes which involve a rotation plus a translation (like glide lines) of half a lattice spacing (screw diad axes are but one example of screw axes which we shall meet in our description of three-dimensional symmetry and space groups). In both cases, because the axes lie in the plane, they 'turn over' the black face of the **R** to its white face. The operations of these in-plane axes are shown in Fig. 2.15. Notice that the operation of the diad is identical to that of the counterchange mirror line m' (Fig. 2.11). (iii) Planes (not lines) of symmetry coinciding with the plane; both reflection (mirror) planes (which are not

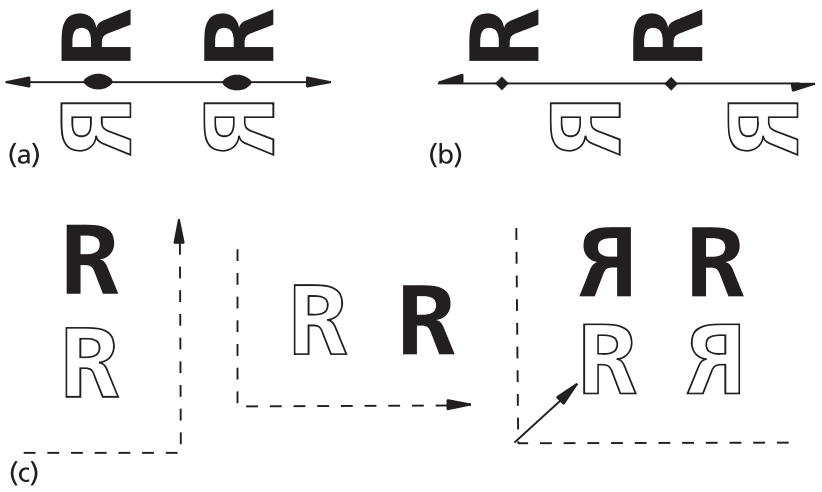

Fig. 2.15. The additional symmetry operations for the 52 layer-symmetry groups applicable to woven fabrics (plus the counterchange symmetry operations $2'$ and $4'$ (Fig. 2.11). The 'face' and 'back' of the **R** symbols are shown here as black and white, respectively. (a) Operation of an in-plane diad axis (double arrow-head) (identical to counterchange symmetry element m'—see Fig. 2.11) and (b) an in-plane screw diad axis (single arrow-head). (c) Operation of in-plane glide planes (dashed lines) for three different orientations of the glide directions—along the axes and diagonally. (Drawn by K. M. Crennell.)

applicable to woven textiles because the back of the cloth is not identical to the front[6]) and glide-reflection planes (which are applicable to woven textiles). These symmetry operations are also shown in Fig. 2.15.

We will now apply these ideas to the plain weave and twill illustrated in Figs 2.13 and 2.14. The 'weave repeat' is the smallest number of warp and weft threads on which the weave interlacing can be represented; it is a 2×2 square for the plain weave (Fig. 2.13) and a 3×3 square for this example of a twill weave (Fig. 2.14). It is important to note that these weave repeat squares *do not* correspond with the unit cells of the plane patterns. These unit cells and the plane group symmetry elements are also shown in Figs 2.13 and 2.14. As can be seen, the plain weave has plane symmetry $p4gm$ and the twill plane symmetry $p2$ (see Fig. 2.6).

Figures 2.13 and 2.14 also show the unit cells and layer symmetry elements for these two weaves and the standard notation (which we will not describe in detail) which goes with them. Notice that for the plain weave that the unit cell is identical to that for the plane group symmetry but for the twill it is different—the primitive (p) lattice becomes a centred (c) or diamond lattice. Notice also that the layer-group symmetry of the plain weave is much more 'complicated' than that of the twill. It includes tetrad rotation-reflection axes perpendicular to the plane as well as diads and screw diads within the plane. The twill, by contrast, has no mirror lines of symmetry at all.

[6] This restriction further reduces (by 12) the number of layer-symmetry groups applicable to woven textiles, leaving a total of $80 - 16 - 12 = 52$. Still a lot!

Fig. 2.16. Operation of a tetrad rotation-reflection axis showing an **R** superimposed on a 'float' of the plain weave fabric (Fig. 2.13). The operations of reflection-rotation are of course repeated three times. (Drawn by K. M. Crennell.)

Finally, look carefully at the positions of the tetrad rotation–reflection axes in the centres of the plain weave warp and weft 'floats'. These axes help us to visualize the relation between the face and back of the fabric: for example, rotate a warp float 90° and we have a weft float, reflect it (black to white) and you have the weft float in the back face of the fabric as shown in Fig. 2.16.

2.9 Non-periodic patterns and tilings

Johannes Kepler was the first to show that pentagonal symmetry would give rise to a pattern which was non-repeating. Figure 2.17 is an illustration from perhaps his greatest work *Harmonices mundi* (1619) which shows in the figures captioned 'Aa' and 'z' a pattern or tiling of pentagons, pentagonal stars and 10 and 16-sided figures which radiate out in pentagonal symmetry from a central point. Grünbaum and Shephard[7] have shown how the tiling 'Aa' can be extended indefinitely giving long-range orientational order but the pattern does not repeat and cannot be identified with any of the seventeen plane groups (Fig. 2.6). A. L. Mackay[8] has shown how a regular, but non-periodic pattern, can be built up from regular pentagons in a plane with the triangular gaps covered by pieces cut from pentagons, which he describes with the title (echoing Kepler) *De nive quinquangula*—on the pentagonal snowflake.

These are but two examples of non-periodic or 'incommensurate' tilings, the mathematical basis of which was largely developed by Roger Penrose and are generally named after him. Figure 2.18 shows how a Penrose tiling may be constructed by linking together edge-to-edge 'wide' and 'narrow' rhombs or diamond-shaped tiles of equal edge lengths. The angles between the edges of the tiles (as shown in Fig. 2.18(a)) are not arbitrary but arise from pentagonal symmetry as shown in Fig. 2.18(b) (where the tiles are shown shaded in relation to a pentagon); nor are they linked together in an arbitrary fashion but according to local 'matching rules', shown in Fig. 2.18(a) by little triangular 'pegs' and 'sockets' along the tile edges. These are omitted in the resultant tiling (Fig. 2.18(c)), partly for clarity and partly because their work in constructing the

[7] B. Grünbaum and G. C. Shephard. *Tilings and Patterns: An Introduction*. W. H. Freeman, New York, 1989.

[8] A.L. Mackay (1976) *De nive quinquangula.* Physics Bulletin, p. 495.

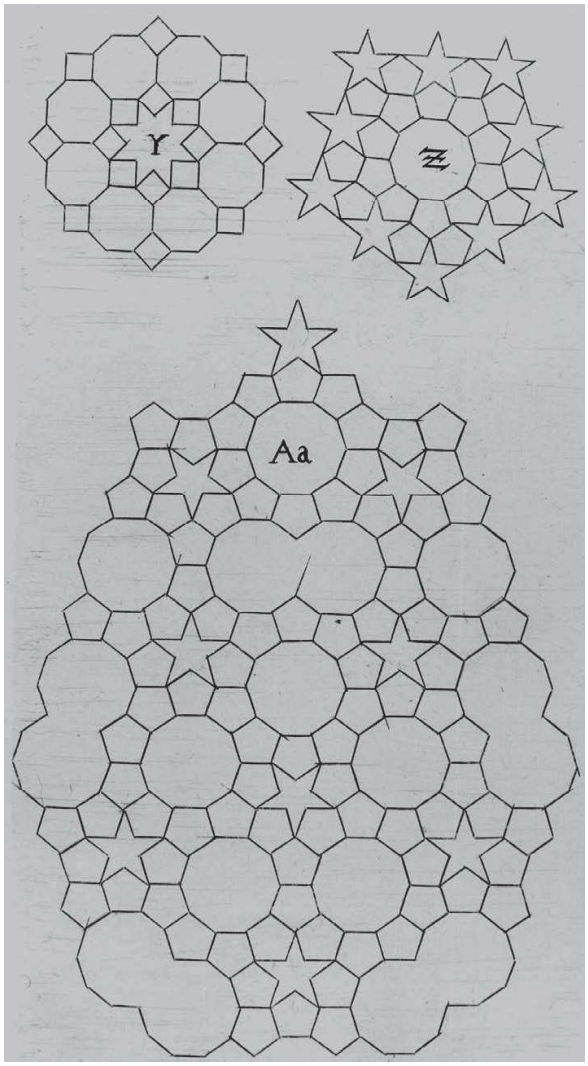

Fig. 2.17. Non-periodic tiling patterns 'z' and 'Aa' (from *Harmonices Mundi* by Johannes Kepler, 1619, reproduced from the copy in the Brotherton Library, University of Leeds, by courtesy of the Librarian).

pattern is done. (An alternative of showing how the tiles must be fitted together is to colour or shade them in three ways and then to match the colours, like the pegs and sockets, along the tile edges.) The tiling can be viewed as a linkage of little cubes where we see three cube faces; the 'front' and 'top' faces (represented by the 'wide' diamonds) and 'side' face (represented by the 'narrow' diamond).

However, building up a perfect Penrose tiling by adding wide and narrow tiles one-by-one is not a straightforward task. Even if we strictly adhere to the edge-matching rules, we soon find that 'blind alleys' are available at every step; nor is it easy to recognize the point at which a mistake has been made until further tiles have been added. In order to build a Penrose tiling without mistakes we need to invoke what are called **vertex matching rules**: these are discussed in C. Janot's book *Quasicrystals* (see Further Reading).

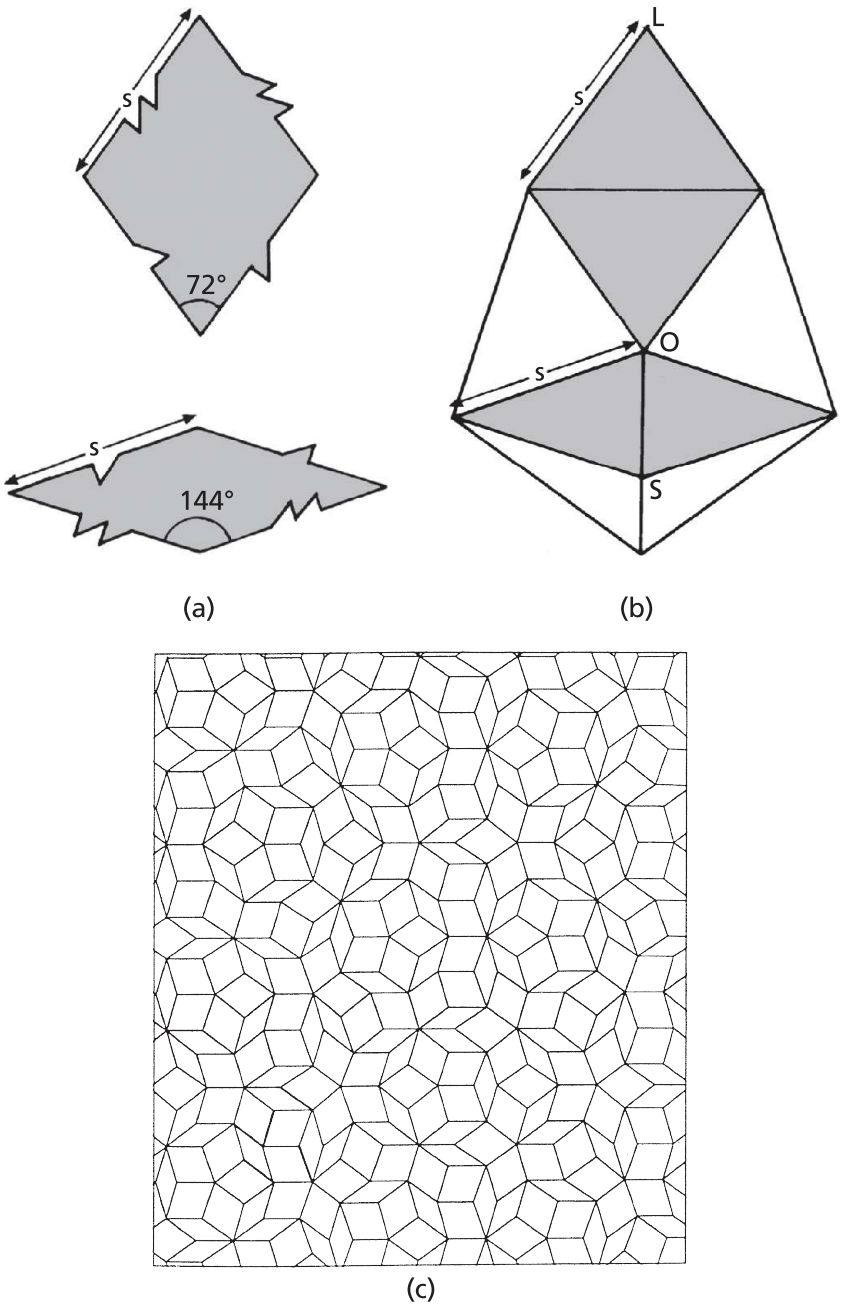

Fig. 2.18. (a) The two types ('wide' and 'narrow') tiles for the construction of a Penrose tiling. The triangular 'pegs' and 'sockets' along the tile edges indicate how they should be linked together edge-to-edge. (b) The geometry of the tiles in relation to a pentagon. The ratio OL/s (wide tile) = s/OS (narrow tile) = $(\sqrt{5}+1)/2 = 1.618\ldots$ (c) shows the resultant tiling (pegs and sockets omitted for clarity) (reproduced by courtesy of Prof. Sir Roger Penrose).

The mathematical analysis of non-repeating patterns is rather difficult (especially in three-dimensions—see Section 4.9), but we can perhaps understand their essential 'incommensurate' properties by way of a one-dimensional analogy or example. Consider a pattern made up of a row of arrows and a row of stars extending right and left from an origin O. If the spacings of the arrows and stars are in a ratio of whole numbers then,

depending on the values of these numbers, the pattern will repeat. Figure 2.19(a) shows a simple case where the ratio of spacings is 3/2 and the pattern repeats (i.e. the arrows and stars coincide) every third arrow or second star. If, however, the spacings of the arrows and stars cannot be expressed as a ratio of whole numbers, in other words if the ratio is an *irrational* number, then the pattern will never repeat—the arrows and stars will never come into coincidence. Figure 2.19(b) shows an example where the ratio of spacings is $\sqrt{2} = 1.414213\ldots$ an irrational number, like π, where there is 'no end' to the number of decimal places and no cyclic repetition of the decimal numbers.[9]

In Penrose five-fold or pentagonal tiling it turns out (Fig. 2.18(b)) that the ratio of the diagonal OL to the edge length s (for the wide tile) and the ratio of the edge length s to the diagonal OS (for the narrow tile) are also both equal to an irrational number $(\sqrt{5}+1)/2 = 1.618034\ldots$ called the *Golden Mean* or *Golden Ratio*. The Golden Ratio also occurs as the convergence of the ratio of successive terms in the so-called **Fibonacci series** of numbers where each term is the sum of the preceding two, i.e. 1, 1, 2, 3, 5, 8, 13, 21, 34, 55, ... Not only is the Golden Ratio and Fibonacci series a subject of mathematical interest but it also occurs in nature in, for example, the intersecting spirals of the florets traced in the head of a sunflower or in a pine-cone. In a pine-cone there are, depending on species, 5/3, 8/5, 13/8 right-/left-handed intersecting spirals and in a sunflower, depending on size, 55/34, 89/55 intersecting spirals—all these numbers corresponding to successive terms in the Fibonacci series[10]. The Fibonacci series may also describe the growth rate of molluscan shells (in which new

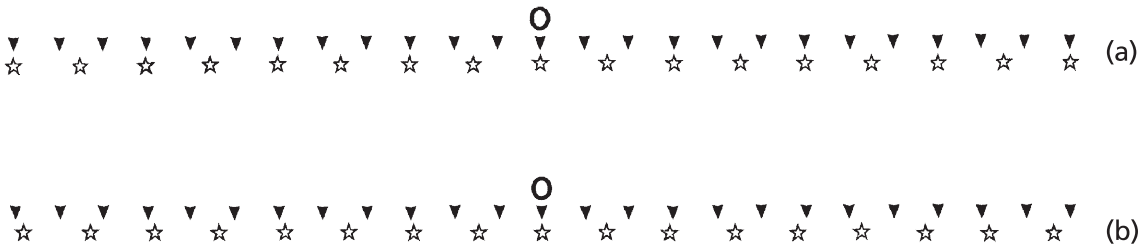

Fig. 2.19. One-dimensional examples of (a) a periodic pattern and (b) a non-periodic pattern. In (a) the pattern repeats every third arrow and second star, in (b) the ratio of the spacings is $\sqrt{2}$ and the pattern never repeats.

[9] The discovery that some numbers are irrational is one of the triumphs of Greek mathematics. The proof that $\sqrt{2}$ is irrational, which is generally attributed to Pythagoras, may be expressed as follows. Suppose that $\sqrt{2}$ *can* be expressed as *a*/*b* where a and b are whole numbers which have no common factor (if they had, we could simply remove it). Hence $\sqrt{2}b = a$ and squaring $2b^2 = a^2$. Now $2b^2$ is an *even* number, hence a^2 is also an even number and, since the square of an even number is even, a is an even number. Now an even number can be expressed as $2 \times$ (any number), i.e. $a = 2c$. Squaring again $a^2 = 4c^2 = 2b^2$, hence $2c^2 = b^2$ and, for the same reason as before, since $2c^2$ is an even number then b is an even number. So, both a and b are even and have a common factor 2 which contradicts our initial hypothesis which therefore must be false.

[10] The configurations produced by the orderly arrangement of leaves and florets around a stem (a subject known as phyllotaxis) and the growth and shapes of shells, horns, and teeth, are fully discussed in the classic text *On Growth and Form* (see Further Reading).

material is added at the growing boundary) or the rate of population increase in animals. Suppose that in an interval of time a young animal (S) becomes an adult (L) and an adult (L) has one offspring (S). Then following the sequence $S \rightarrow L$ and $L \rightarrow LS$ we have: S, L, LS, LSL, $LSLLS$, $LSLLSLSL$, ... Notice that the numbers of L and S individuals in each term are equal to the numbers in the preceding and next-preceding terms: e.g. in the term $LSLLSLSL$ there are $5L$ and $3S$. As the series progresses the ratio L/S again converges to the Golden Ratio. The same is true of the ratio of wide and narrow tiles in a Penrose tiling. The Golden Ratio is also met in architectural proportion and design: a rectangle whose sides are in the (approximate) ratio 1.62:1 seems particularly restful to the eye—not too narrow and not too wide. It occurs in the shapes of window-panes, in the proportions of the facades of Greek temples or, to take a particular example, in the ratio of column spacing to column height (5:8) in the Colosseum in Rome.

It is a simple exercise to show that if a square is cut off a Golden Rectangle, the rectangle which remains also has sides which are in the Golden Ratio and clearly the process can be continued indefinitely (Fig. 2.20). Finally, the rectangle can be used as the template for the construction of an **equiangular spiral** (Fig. 2.20), so called because the tangent at any point on the spiral is at a constant angle to the corresponding radius-vector. This leads to the property of **continued similarity**: the shape remains the same irrespective of size. A large molluscan shell (e.g. of an ammonite or *nautilus*) is the same shape as a small one.

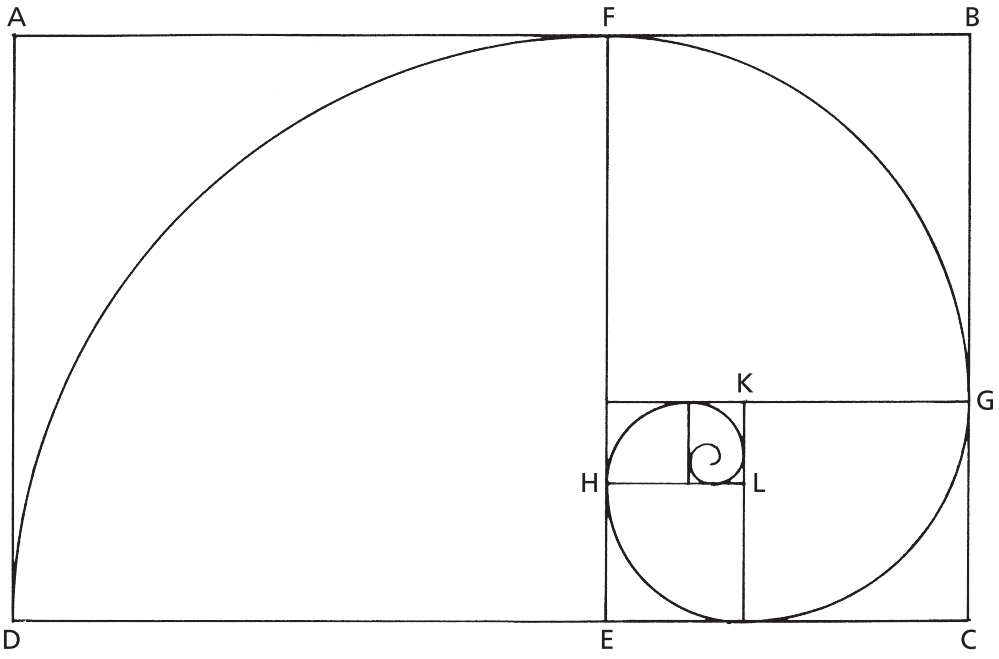

Fig. 2.20. A Golden Rectangle ABCD. Cutting off a square AFED leaves a smaller Golden Rectangle FBCE—and the process may be continued as shown. Notice the **continued similarity** of the inscribed equiangular spiral—e.g. the portion DFG has the same shape as HKL.

Exercises

2.1 Lay tracing paper over the plane patterns in Fig. 2.6. Outline a unit cell in each case and indicate the positions of all the symmetry elements within the unit cell. Notice in particular the differences in the distribution of the triad axes and mirror lines in the plane groups $p31m$ and $p3m1$.

2.2 Figure 2.21 is a design by M. C. Escher. Using a tracing paper overlay, indicate the positions of all the symmetry elements. With the help of the flow diagram (Fig. 2.8), determine the plane lattice type.

2.3 Figure 2.22 is a projection of the structure of FeS_2 (shaded atoms Fe, unshaded atoms S). Using a tracing paper overlay, indicate the positions of the symmetry elements, outline a unit cell and, with the help of the flow diagram in Fig. 2.8, determine the plane pattern type.

2.4 Figure 2.23 is a design by M. C. Escher. Can you see that the two sets of men are related by glide lines of symmetry? Draw in the positions of these glide lines, and determine the plane lattice type.

Fig. 2.21. A plane pattern (from *Symmetry Aspects of M. C. Escher's Periodic Drawings*, 2nd edn, by C. H. MacGillavry. Published for the International Union of Crystallography by Bohn, Scheltema and Holkema, Utrecht, 1976).

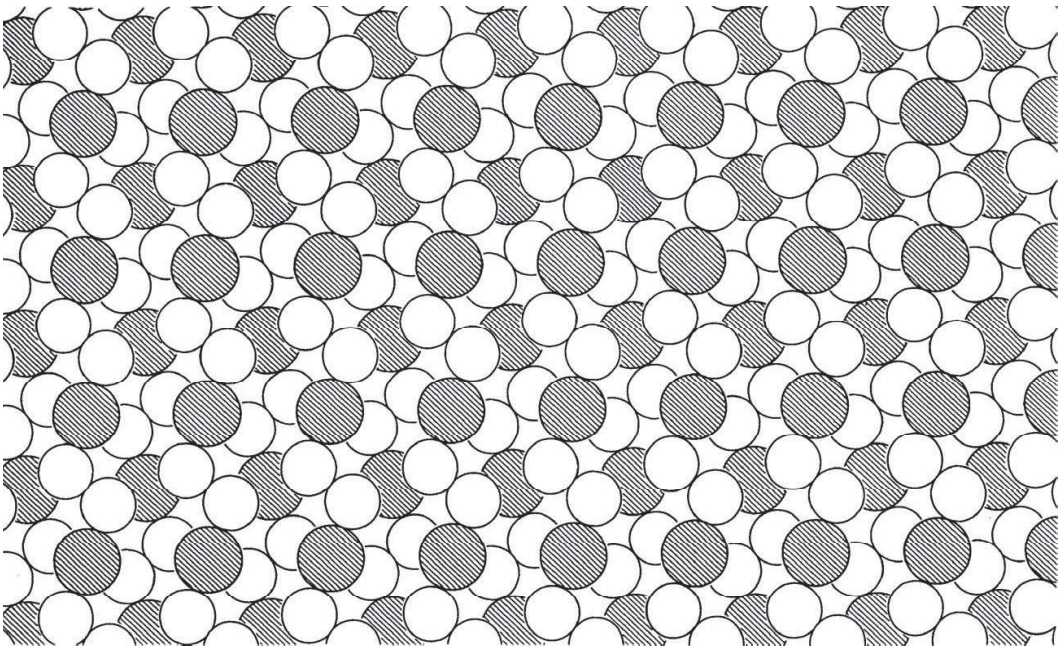

Fig. 2.22. A projection of the structure of marcasite, FeS_2 (from *Contemporary Crystallography* by M. J. Buerger, McGraw-Hill, New York, 1970).

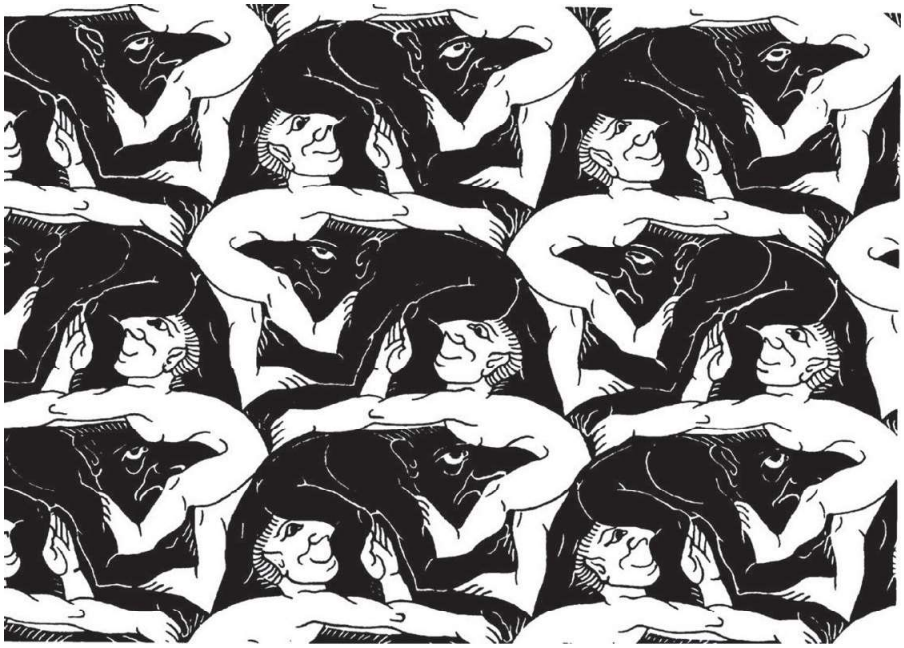

Fig. 2.23. A plane pattern (from C. H. MacGillavry, loc. cit.).

2.5 Determine (with reference to Fig. 2.11) the counterchange (black–white) point group symmetry of a chessboard.

2.6 Figure 2.24 shows examples of border or frieze patterns from *The Grammar of Ornament* by Owen Jones. Using a tracing paper overlay, indicate the positions of the symmetry elements and, with the help of the flow diagram (Fig. 2.10), determine the one-dimensional lattice types.

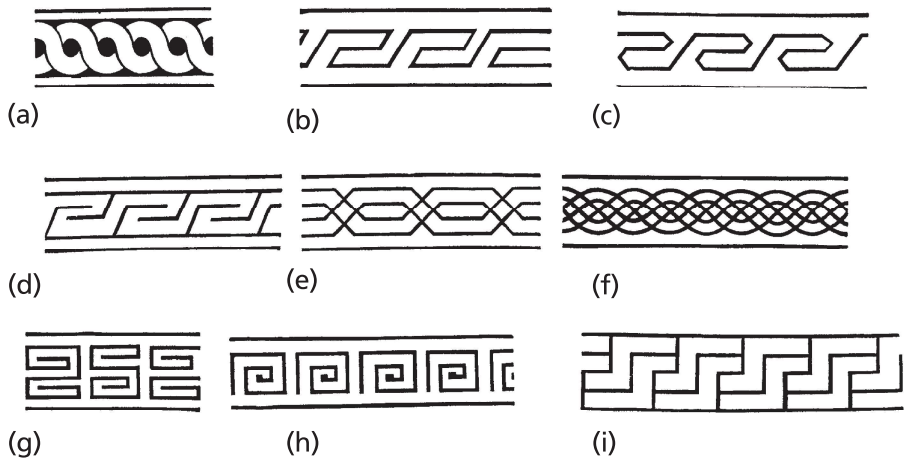

Fig. 2.24. Examples of border or frieze patterns (from *The Grammar of Ornament* by Owen Jones, Day & Son, London 1856, reprinted by Studio Editions, London, 1986). a, b, Greek; c, d, Arabian; e, Moresque; f, Celtic; g, h, Chinese; i, Mexican.

2.7 Figure 2.25(a) is a 'wood block floor' or 'herringbone' pattern with plane group symmetry *p2gg*. Using a tracing-paper overlay (and with the help of Fig. 2.6(b) and the flow chart, Fig. 2.8), locate the positions of the diad axes and glide lines. Now place your tracing paper over the counterchange pattern (Fig. 2.25(b)) and determine which of the symmetry elements become counterchange ($2'$ or g') symmetry elements. To which of the counterchange patterns shown in Fig. 2.12 does this pattern belong?

2.8 The symmetry of border pattern *pma*2 (*p*2*mg*) (Fig. 2.9) consists of a glide line a (or g) along the length of the border with vertical mirror lines and diad axes in between. Derive the two-colour (black and white) counterchange patterns based upon *pma*2 by replacing, in turn, the glide lines, mirror lines and diad axes by the counterchange symmetry elements g', m' and $2'$.

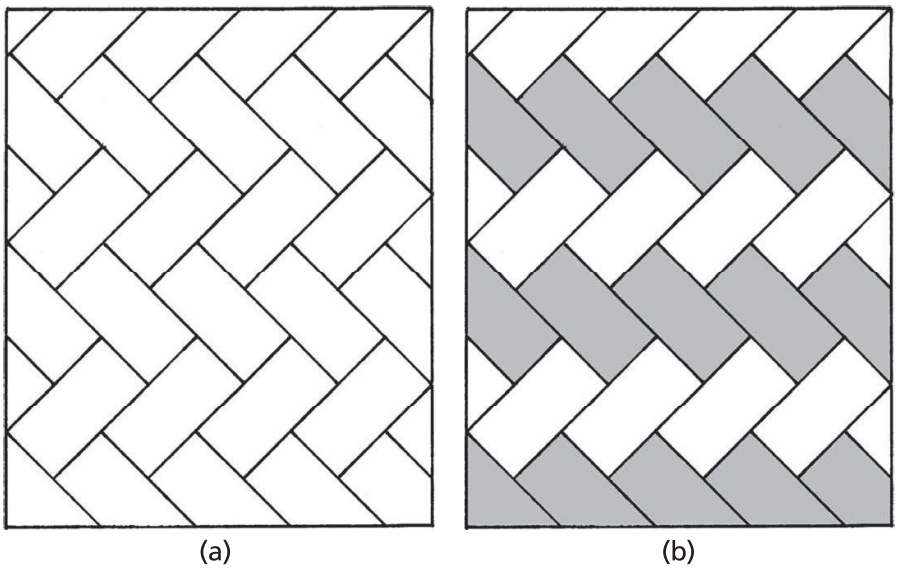

Fig. 2.25. 'Wood block floor' or 'herringbone brickwork' patterns (a) with all blocks the same colour, and (b) with alternating black and white blocks.

3

Bravais lattices and crystal systems

3.1 Introduction

The definitions of the motif, the repeating 'unit of pattern', and the lattice, an array of points in space in which each point has an identical environment, hold in three dimensions exactly as they do in two dimensions. However, in three dimensions there are additional symmetry elements that need to be considered: both **point symmetry elements** to describe the symmetry of the three-dimensional motif (or indeed any crystal or three-dimensional object) and also **translational symmetry elements,** which are required (like glide lines in the two-dimensional case) to describe all the possible patterns which arise by combining motifs of different symmetries with their appropriate lattices. Clearly, these considerations suggest that the subject is going to be rather more complicated and 'difficult'; it is obvious that there are going to be many more three-dimensional patterns (or space groups) than the seventeen two-dimensional patterns (or plane groups or the eighty two-sided patterns—Chapter 2), and to work through all of these systematically would take up many pages! However, it is not necessary to do so; all that is required is an understanding of the principles involved (Chapter 2), the operation and significance of the additional symmetry elements, and the main results. These main results may be stated straight away. The additional point symmetry elements required are centres of symmetry, mirror planes (instead of lines) and inversion axes; the additional translational symmetry elements are glide planes (instead of lines) and screw axes. The application and permutation of all symmetry elements to patterns in space give rise to 230 **space groups** (instead of seventeen plane groups) distributed among fourteen space lattices (instead of five plane lattices) and thirty-two point group symmetries (instead of ten plane point group symmetries).

In this chapter the concept of space (or Bravais) lattices and their symmetries is discussed and, deriving from this, the classification of crystals into seven systems.

3.2 The fourteen space (Bravais) lattices

The systematic work of describing and enumerating the space lattices was done initially by Frankenheim* who, in 1835, proposed that there were fifteen in all. Unfortunately for Frankenheim, two of his lattices were identical, a fact first pointed out by Bravais* in 1848. It was, to take a two-dimensional analogy, as if Frankenheim had failed to notice

* Denotes biographical notes available in Appendix 3.

The Basics of Crystallography and Diffraction. Fourth Edition. Christopher Hammond.

(see Fig. 2.4(b)) that the rhombic or diamond and the rectangular centred plane lattices were identical! Hence, to this day, the fourteen space lattices are usually, and perhaps unfairly, called Bravais lattices.

The unit cells of the Bravais lattices are shown in Fig. 3.1. The different shapes and sizes of these cells may be described in terms of three cell edge lengths or axial

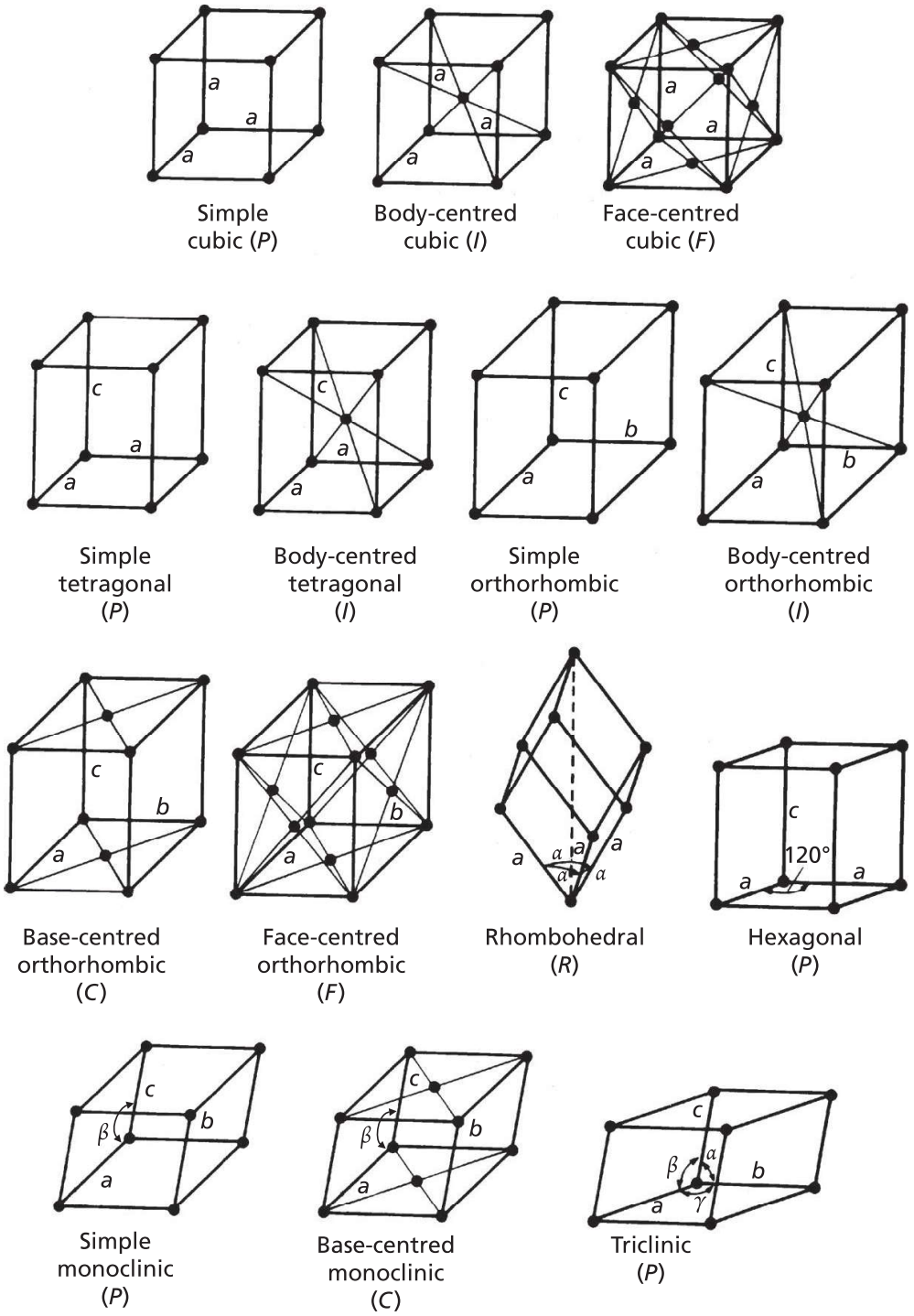

Fig. 3.1. The fourteen Bravais lattices (from *Elements of X-Ray Diffraction,* (2nd edn), by B. D. Cullity, Addison-Wesley, 1978).

distances, *a, b, c,* or lattice vectors **a, b, c** and the angles between them, α, β, γ, where α is the angle between **b** and **c**, β the angle between **a** and **c**, and γ the angle between **a** and **b**. The axial distances and angles are measured from one corner to the cell, i.e. a common origin. It does not matter where we take the origin—any corner will do—but, as pointed out in Chapter 1, it is a useful convention (and helps to avoid confusion) if the origin is taken as the 'back left-hand corner' of the cell, the *a*-axis pointing forward (out of the page), the *b*-axis towards the right and the *c*-axis upwards. This convention also gives a right-handed axial system. If any one of the axes is reversed (e.g. the *b*-axis towards the left instead of the right), then a left-handed axial system results. The distinction between them is that, like left and right hands, they are mirror images of one another and cannot be brought into coincidence by rotation.

The drawings of the unit cells of the Bravais lattices in Fig. 3.1 can be misleading because, as shown in Chapter 2, it is the *pattern* of lattice points which distinguishes the lattices. The unit cells simply represent arbitrary, though convenient, ways of 'joining up' the lattice points. Consider, for example, the three cubic lattices; cubic *P* (for *P*rimitive, one lattice point per cell, i.e. lattice points only at the corners of the cell), cubic *I* (for '*I*nnenzentrierte', which is German for 'body-centred', an additional lattice point at the centre of the cell, giving two lattice points per cell) and cubic *F* (for *F*ace-centred, with additional lattice points at the centres of each face of the cell, giving four lattice points per cell). It is possible to outline alternative primitive cells (i.e. lattice points only at the corners) for the cubic *I* and cubic *F* lattices, as is shown in Fig. 3.2. As mentioned in Chapter 1, these primitive cells are not often used (1) because the inter-axial angles are not the convenient 90° (i.e. they are not orthogonal) and (2) because they do not reveal very clearly the cubic symmetry of the cubic *I* and cubic *F* lattices. (The symmetry of the Bravais lattices, or rather the point group symmetries of their unit cells, will be described in Section 3.3.)

Similar arguments concerning the use of primitive cells apply to all the other centred lattices. Notice that the unit cells of two of the lattices are centred on the 'top' and

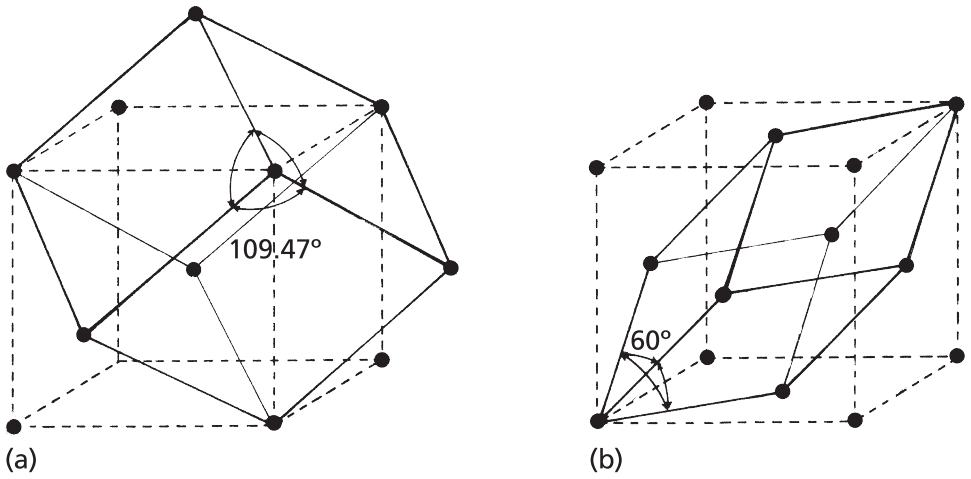

Fig. 3.2. **(a)** the cubic *I*, **(b)** the cubic *F* lattice unit cells (dashed lines), and the corresponding primitive rhombohedral unit cells (full lines) with their inter-axial angles indicated.

'bottom' faces. These are called base-centred or *C*-centred because these faces are intersected by the *c*-axis.

The Bravais lattices may be thought of as being built up by stacking 'layers' of the five plane lattices, one on top of another. The cubic and tetragonal lattices are based on the stacking of square lattice layers; the orthorhombic *P* and *I* lattices on the stacking of rectangular layers; the orthorhombic *C* and *F* lattices on the stacking of rectangular centred layers; the rhombohedral and hexagonal lattice on the stacking of hexagonal layers and the monoclinic and triclinic lattices on the stacking of oblique layers. These relationships between the plane and the Bravais lattices are easy to see, except perhaps for the rhombohedral lattice. The rhombohedral unit cell has axes of equal length and with equal angles (α) between them. Notice that the layers of lattice points, perpendicular to the 'vertical' direction (shown dotted in Fig. 3.1) form triangular, or equivalently, hexagonal layers. The hexagonal and rhombohedral lattices differ in the ways in which the hexagonal layers are stacked. In the hexagonal lattice they are stacked directly one on top of the other (Fig. 3.3(a)) and in the rhombohedral lattice they are stacked such that the next two layers of points lie above the triangular 'hollows' or interstices of the layer below, giving a three layer repeat (Fig. 3.3(b)). These hexagonal and rhombohedral stacking sequences have been met before in the stacking of close-packed layers (Chapter 1); the hexagonal lattice corresponds to the simple hexagonal AAA... sequence and the rhombohedral lattice corresponds to the fcc ABCABC... sequence.

Now observant readers will notice that the rhombohedral and cubic lattices are therefore related. The primitive cells of the cubic *I* and cubic *F* lattices (Fig. 3.2) are rhombohedral—the axes are of equal length and the angles (α) between them are equal. As in the two-dimensional cases, what distinguishes the cubic lattices from the rhombohedral is their symmetry. When the angle α is 90° we have a cubic *P* lattice, when it is 60° we have a cubic *F* lattice and when it is 109.47° we have a cubic *I* lattice (Fig. 3.2). Or, alternatively, when the hexagonal layers of lattice points in the rhombohedral lattice are spaced apart in such a way that the angle α is 90°, 60° or 109.47°, then cubic symmetry results.

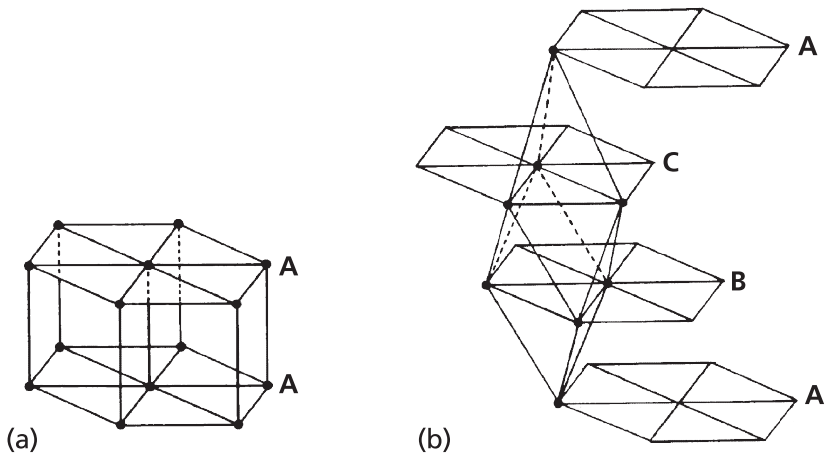

Fig. 3.3. Stacking of hexagonal layers of lattice points in (a) the hexagonal lattice and (b) the rhombohedral lattice.

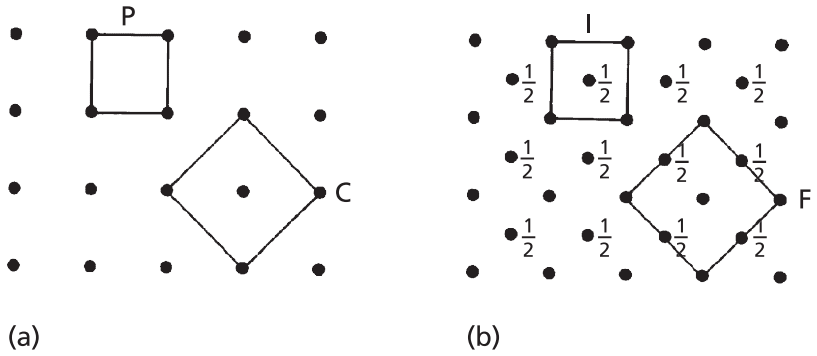

Fig. 3.4. Plans of tetragonal lattices showing (a) the tetragonal $P = C$ lattice and (b) the tetragonal $I = F$ lattice.

Finally, compare the orthorhombic lattices (all sides of the unit cell of different lengths) with the tetragonal lattices (two sides of the cell of equal length). Why are there four orthorhombic lattices, P, C, I and F, and only two tetragonal lattices, P and I? Why are there not tetragonal C and F lattices as well? The answer is that there *are* tetragonal C and F lattices, but by redrawing or outlining different unit cells, as shown in Fig. 3.4, it will be seen that they are identical to the tetragonal P and I lattices, respectively. In short, they represent no new arrangements of lattice points.

3.3 The symmetry of the fourteen Bravais lattices: crystal systems

The unit cells of the Bravais lattices may be thought of as the 'building blocks' of crystals, precisely as Haüy envisaged (Fig. 1.2). Hence it follows that the habit or external shape, or the observed symmetry of crystals, will be based upon the shapes and symmetry of the Bravais lattices, and we now have to describe the point symmetry of the unit cells of the Bravais lattices just as we described the point symmetry of plane patterns and lattices. The subject is far more readily understood if simple models are used (Appendix 1).

First, mirror lines of symmetry become mirror planes in three dimensions. Second, axes of symmetry (diads, triads, tetrads and hexads) also apply to three dimensions. The additional complication is that, whereas a plane motif or object can only have one such axis (perpendicular to its plane), a three-dimensional object can have several axes running in different directions (but always through a point in the centre of the object).

Consider, for example, a cubic unit cell (Fig. 3.5(a)). It contains a total of nine mirror planes, three parallel to the cube faces and six parallel to the face diagonals. There are three tetrad (four-fold) axes perpendicular to the three sets of cube faces, four triad (three-fold) axes running between opposite cube corners, and six diad (two-fold) axes running between the centres of opposite edges. This 'collection' of symmetry elements is called the **point group symmetry** of the cube because all the elements—planes and axes—pass through a point in the centre.

Why should there be these particular numbers of mirror planes and axes? It is because all the various symmetry elements operating at or around the point must be

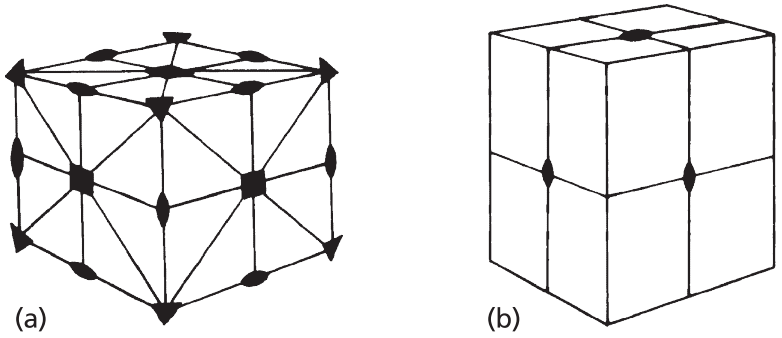

Fig. 3.5. The point symmetry elements in (a) a cube (cubic unit cell) and (b) an orthorhombic unit cell.

consistent with one another. Self-consistency is a fundamental principle, underlying all the two-dimensional plane groups, all the three-dimensional point groups and all the space groups that will be discussed in Chapter 4. If there are two diad axes, for example, then they *have* to be mutually orthogonal, otherwise chaos would result; by the same token they also *must* generate a third diad perpendicular to both of them. It is the necessity for self-consistency which governs the construction of every one of the different combinations of symmetry, controlling the nature of each combination; it is this, also, which limits the total numbers of possible combinations to quite definite numbers such as thirty-two, in the case of the crystallographic point groups (the crystal classes), the fourteen Bravais lattices, and so on.

The cubic unit cell has more symmetry elements than any other: its very simplicity makes its symmetry difficult to grasp. More easy to follow is the symmetry of an orthorhombic cell. Figure 3.5(b) shows the point group symmetry of an orthorhombic unit cell. It contains, like the cube, three mirror planes parallel to the faces of the cell but no more—mirror planes do not exist parallel to the face diagonals. The only axes of symmetry are three diads perpendicular to the three faces of the unit cell.

In both cases it can be seen that the point group symmetry of these unit cells (Figs 3.5(a) and 3.5(b)) is independent of whether the cells are centred or not. All three cubic lattices, P, I and F, have the same point group symmetry; all four orthorhombic lattices, P, I, F and C, have the same point group symmetry and so on. This simple observation leads to an important conclusion: it is not possible, from the observed symmetry of a crystal, to tell whether the underlying Bravais lattice is centred or not. Therefore, in terms of their point group symmetries, the Bravais lattices are grouped, according to the shapes of their unit cells, into seven **crystal systems**. For example, crystals with cubic P, I or F lattices belong to the **cubic system**, crystals with orthorhombic P, I, F or C lattices belong to the **orthorhombic system**, and so on. However, a complication arises in the case of crystals with a hexagonal lattice. One might expect that all crystals with a hexagonal lattice should belong to the hexagonal system, but, as shown in Chapter 4, the external symmetry of crystals may not be identical (and usually is not identical) to the symmetry of the underlying Bravais lattice. Some crystals with a hexagonal lattice, e.g. α-quartz, do not show hexagonal (hexad) symmetry but have triad symmetry. (see Fig. 1.33a, Section 1.11.5) Such crystals are assigned to the **trigonal system** rather than to the hexagonal system. Hence the trigonal

system includes crystals with both hexagonal and rhombohedral Bravais lattices. There is yet another problem which is particularly associated with the trigonal system, which is that the rhombohedral unit cell outlined in Figs 3.1 and 3.3 is not always used—a larger (non-primitive) unit cell of three times the size is sometimes more convenient. The problem of transforming axes from one unit cell to another is addressed in Chapter 5.

The crystal systems and their corresponding Bravais lattices are shown in Table 3.1. Notice that there are no axes or planes of symmetry in the **triclinic system.** The only symmetry that the triclinic lattice possesses (and which is possessed by all the other lattices) is a **centre of symmetry.** This point symmetry element and inversion axes of symmetry are explained in Chapter 4.

3.4 The coordination or environments of Bravais lattice points: space-filling polyhedra

So far we have considered lattices as patterns of points in space in which each lattice point has the same environment in the same orientation. This approach is complete and sufficient, but it fails to stress, or even make clear, the fact that each of these environments is distinct and characteristic of the lattices themselves.

We need therefore a method of clearly and unambiguously defining what we mean by 'the environment' of a lattice point. One approach (which we have used already in working out the sizes of interstitial sites) is to state this in terms of 'coordination'—the numbers and distances of nearest neighbours. For example, in the simple cubic (cubic *P*) lattice each lattice point is surrounded by six other equidistant lattice points; in the bcc (cubic *I*) lattice each lattice point is surrounded by eight equidistant lattice points—and so on. This is satisfactory, but an alternative and much more fruitful approach is to consider the environment or domain of each lattice point in terms of a polyhedron whose faces, edges and vertices are equidistant between each lattice point and its nearest neighbours. The construction of such a polyhedron is illustrated in two dimensions for simplicity in Fig. 3.6. This is a plan view of a simple monoclinic (monoclinic *P*) lattice with the *b* axis perpendicular to the page. The line labelled ① represents the edge or trace of a plane perpendicular to the page and half way between the central lattice point 0 and its neighbour 1. All points lying in this plane (both in the plane of the paper and above and below) are therefore equidistant between the two lattice points 0 and 1. We now repeat the process for the other lattice points 2, 3, 4, etc., surrounding the central lattice point. The planes ①, ②, ③ etc. form the six 'vertical' faces of the polyhedron and in three dimensions, considering the lattice points 'above' and 'below' the central lattice point 0, the polyhedron for the monoclinic *P* lattice is a closed prism, shown shaded in plan in Fig. 3.6. Each lattice point is surrounded by an identical polyhedron and they all fit together to completely fill space with no gaps in between.

In this example (of a monoclinic *P* lattice) the edges of the polyhedron are where the faces intersect and represent points which are equidistant between the central lattice point and *two* other surrounding lattice points. Similarly, the vertices of the polyhedron represent points which are equidistant between the central lattice point and *three* other surrounding points. However, for lattices of higher symmetry this correspondence does

Table 3.1 The seven crystal systems, their corresponding Bravais lattices and symmetries

System	Bravais lattices	Axial lengths and angles	Characteristic (minimum) symmetry	Non-centrosymmetric point groups		Centrosymmetric point groups[a]
				Enantiomorphous[b]	Non-enantiomorphous[c]	Non-enantiomorphous[c]
Cubic	*PIF*	$a = b = c$ $\alpha = \beta = \gamma = 90°$	4 triads equally inclined at 109.47°	23, 432	$\bar{4}3m$	$m\bar{3}$, $m\bar{3}m$
Tetragonal	*PI*	$a = b \neq c$ $\alpha = \beta = \gamma = 90°$	1 rotation tetrad or inversion Tetrad	4^{P}, 422	$\bar{4}$, $4mm^{P}$, $\bar{4}2m$	4/*m*, 4/*mmm*
Orthorhombic	*PICF*	$a \neq b \neq c$ $\alpha = \beta = \gamma = 90°$	3 diads equally inclined at 90°	222	$mm2^{P}$	*mmm*
Trigonal	*R*	$a = b = c$ $\alpha = \beta = \gamma \neq 90°$	1 rotation triad or inversion triad	3^{P}, 32	$3m^{P}$	$\bar{3}$, $\bar{3}m$
Trigonal	*P*	$a = b \neq c$ $\alpha = \beta = 90°$, $\gamma = 120°$	(= triad + centre of symmetry)			
Hexagonal	*P*	$a = b \neq c$ $\alpha = \beta = 90°, \gamma = 120°$	1 rotation hexad or inversion hexad (= triad + perp. mirror plane)	6^{P}, 622	$\bar{6}$, $6mm^{P}$, $\bar{6}m2$	6/*m*, 6/*mmm*
Monoclinic	*PC*	$a \neq b \neq c$ $\alpha = \gamma = 90° \neq \beta \geq 90°$	1 rotation diad or inversion diad (= perp. mirror plane)	2^{P}	m^{P}	2/*m*
Triclinic	*P*	$a \neq b \neq c$ $\alpha \neq \beta \neq \gamma \neq 90°$	None	1^{P}		$\bar{1}$

[a] All the crystals which possess a centre of symmetry and/or a mirror plane are non-enantiomorphous.

[b] The eleven enantiomorphous point groups are those which do not possess a plane or a centre of symmetry. Hence enantiomorphous crystals can exist in right- or left-handed forms.

[c] Eleven of the twenty-one non-enantiomorphous point groups are centrosymmetric. Crystals which have a centre of symmetry do not exhibit certain properties, e.g. the piezoelectric effect.

The ten polar point (non-centrosymmetric) groups (indicated by a superscript P) possess a unique axis not related by symmetry. They are equally divided between the enantiomorphous point groups (1, 2, 3, 4, 6) and non-enantiomorphous point groups (*m*, *mm*2, 3*m*, 4*mm*, 6*mm*).

Trigonal crystals are divided into those which are represented by the hexagonal *P* lattice and those which are represented by the rhombohedral *R* lattice.

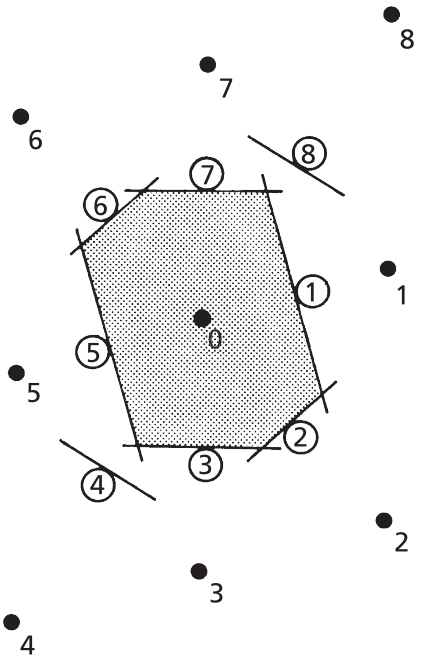

Fig. 3.6. The Voronoi polyhedron (Dirichlet region or Wigner-Seitz cell) for a monoclinic *P* lattice (plan view, *b* axis perpendicular to the page). The lines ①, ② etc. represent the edges or traces of planes which are equidistant between the central lattice point 0 and the surrounding or coordinating lattice points 1, 2, etc. The resulting Voronoi polyhedron is outlined in this two-dimensional section by the shaded area.

not hold. If, for example, we consider a cubic *P* lattice, square in plan, and follow the procedure outlined above, we find that the polyhedron is (as expected) a cube, but the edges of which are equidistant between the central lattice point and *three* surrounding lattice points and the vertices of which are equidistant between the central lattice point and *seven* surrounding lattice points.

The polyhedra constructed in this way and which represent the domains around each lattice point have various names: Dirichlet regions or Wigner-Seitz cells or Voronoi* polyhedra. There are altogether 24 such space-filling polyhedra corresponding to the 14 Bravais lattices; it is not a simple one-to-one correspondence in all cases because the shape of the polyhedron may depend upon the ratios between the axial lengths and angles and whether the Bravais lattice is centred or not. For example, Fig. 3.7(a) and (b) shows the two polyhedra for the tetragonal *I* lattice; Fig. 3.7(a) for the case where the axial ratio, c/a, is less than one and Fig. 3.7(b) for the case where it is greater than one.

The space-filling polyhedra for the cubic *P*, *I* and *F* lattices are particularly interesting. For the cubic *P* lattice it is simply a cube of edge-length equal to the spacing between nearest lattice points (Fig. 3.7(c)). For the cubic *I* lattice it is a truncated octahedron (Fig. 3.7(d), the eight hexagonal faces corresponding to the eight nearest neighbours at the corners of the cube and the six square faces corresponding to the six next-nearest neighbours at the centres of the surrounding cubes. For the cubic *F*

* Denotes biographical notes available in Appendix 3.

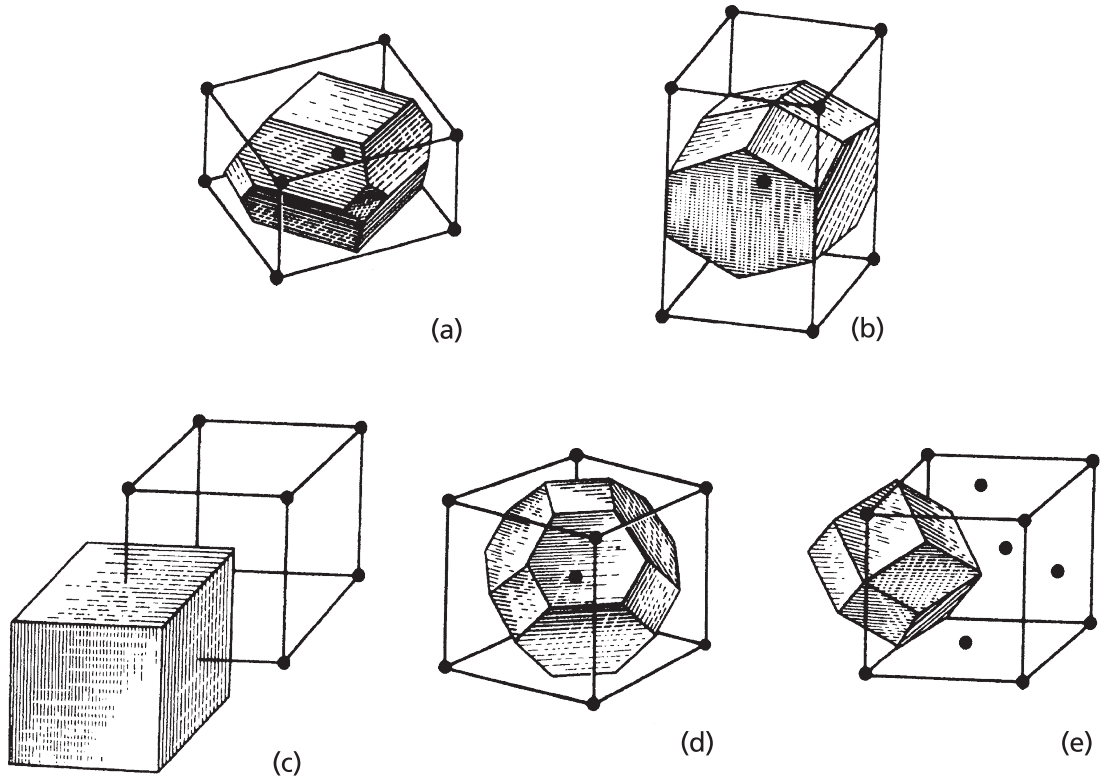

Fig. 3.7. Examples of domains or Voronoi polyhedra outlined around single lattice points (a) tetragonal I lattice, $c/a < 1$; (b) tetragonal I lattice, $c/a > 1$; (c) cubic P lattice; (d) cubic I lattice and (e) cubic F lattice (from *Modern Crystallography* by B. K. Vainshtein, Academic Press, 1981).

lattice it is a rhombic dodecahedron (Fig. 3.7(e)), the twelve diamond-shaped faces corresponding to the twelve nearest neighbours. (see Appendix 2).

It is of interest to compare the space-filling polyhedra for the fcc (cubic F) and hcp close-packing. These are shown in Fig. 3.8(a) and (b) respectively with the positions of the ABC and ABA atom layers indicated. If the 'central' atom is considered to be a B-layer then the 'bottom' three diamond-shaped faces correspond to the coordination of the three A-layer atoms below, the six 'vertical' diamond-shaped faces correspond to the coordination of the six surrounding B-layer atoms and the 'top' three diamond-shaped faces correspond to the coordination of the C-layer atoms for cubic close-packing (Fig. 3.8(a)) or the A-layer atoms for hexagonal close-packing (Fig. 3.8(b)). The polyhedron in Fig. 3.8(a) is a rhombic dodecahedron (as in Fig. 3.7(e)) and in Fig. 3.8(b) it is a trapezorhombic dodecahedron (see also Appendix 2).

The truncated octahedron (the Voronoi polyhedron for the cubic I lattice) also known as a **tetrakaidecahedron**, is of particular interest and is also an Archimedean polyhedron (see Appendix 2). It represents the 'special case' polyhedron for the tetragonal I lattice when the c/a ratio changes from <1 to >1 (compare Figs 3.7(a), (b) and (d)). More importantly, it is the space-filling solid with *plane* faces which has the largest volume-to-surface-area ratio and therefore *approximates* to the shapes of grains in annealed polycrystalline metals or ceramics or the cells in soap-bubble foams (Fig. 3.9). However, the angles between the faces and edges do not satisfy the

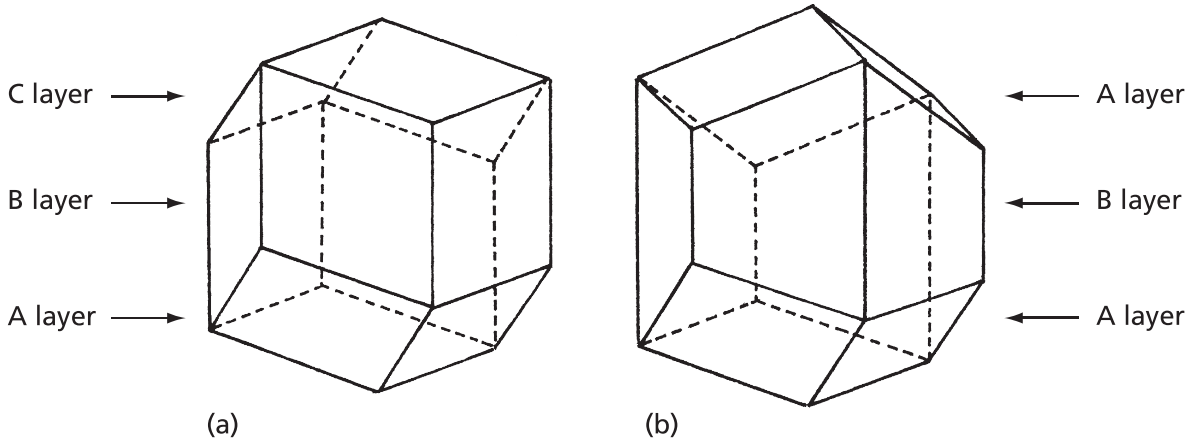

Fig. 3.8. Space filling polyhedra (a) for cubic close-packing (rhombic dodecahedron) and (b) for hexagonal close-packing (trapezorhombic dodecahedron).

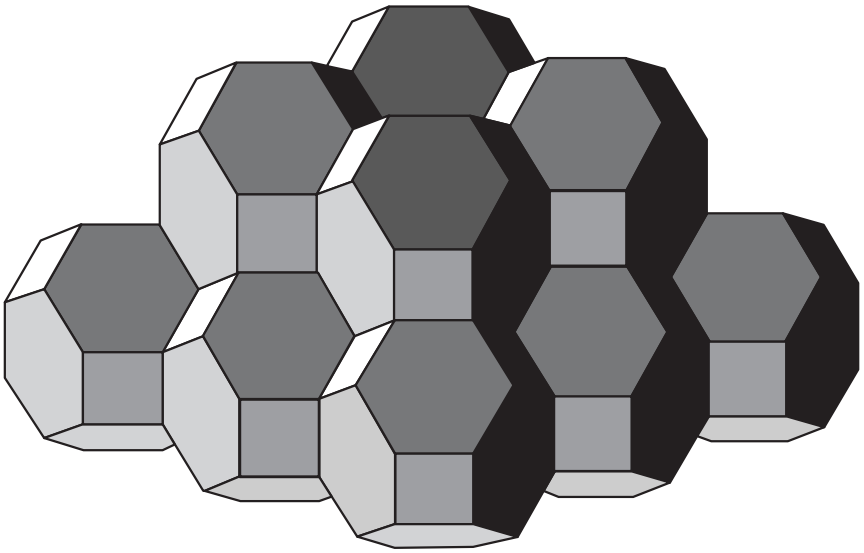

Fig. 3.9. Space-filling by an assembly of truncated octahedra or tetrakaidecahedra (edges of equal length). These polyhedra have 14 faces (6 square plus 8 hexagonal) and are arranged at the points of a cubic *I* lattice. (From *Symmetry* by Hermann Weyl, Princeton University Press, 1952.)

equilibrium requirements for grain boundary energy (e.g. in two-dimensions the grain boundaries must meet at 120°). If, following Lord Kelvin, we (partly) accommodate these requirements by allowing the surfaces and edges to bow in or out, we obtain a (space-filling) solid with curved surfaces and edges called an β-tetrakaidecahedron. This, however, does not represent the 'last word' in the geometry of grain boundaries. If we relax the condition that all the polyhedra have an equal number of faces, then a space-filling structure with a slightly larger volume to surface area ratio can be built up consisting of pentagonal dodecahedra and 14-sided polygons consisting of 12 pentagonal faces and 2 hexagonal faces[1] ('C_{24}' in fullerene notation). However,

[1] D. Weaire (ed.) *The Kelvin Problem: Foam Structures of Minimal Surface Area*. Taylor & Francis, London and Bristol, Pa (1996).

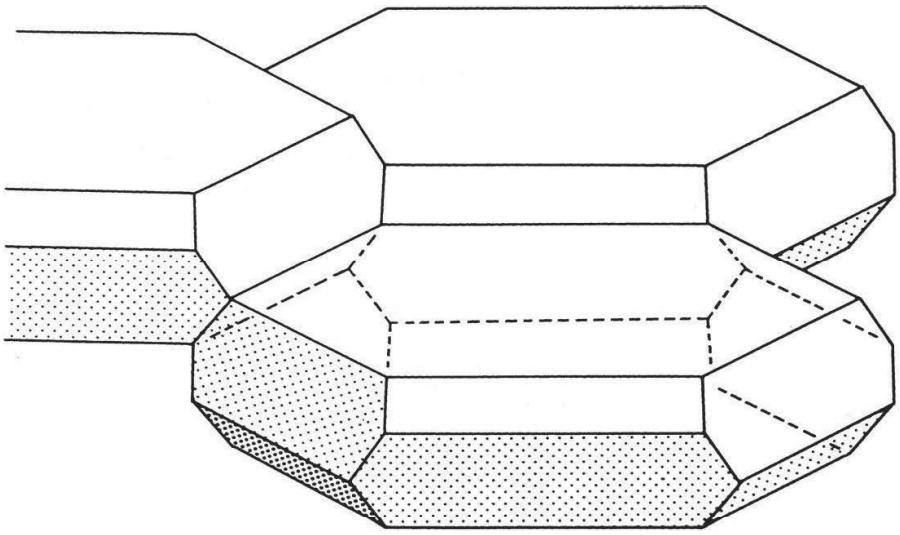

Fig. 3.10. Epidermal cells in mammalian skin which have the shapes of flattened tetrakaidecahedra arranged in vertical columns (compare with Fig. 3.9). (Illustration by courtesy of Professor Honda, Hyogo University, Japan.)

in practice, grains and the cells of soap-films are irregular in shape and size, although they do have on average about fourteen faces, like tetrakaidecahedra. In biological structures, the cells in the epidermis (the outer layer) of mammalian skin have also been shown to have the shape of intersecting flattened tetrakaidecahedra arranged in neat vertical columns (Fig. 3.10). In this case the edges are no longer equal in length; two of the eight hexagonal faces (parallel to the surface of the skin) are large and all the other faces are small and elongated. These epidermal cells are of course space-filling but have much smaller volume-to-surface area ratios.

The Voronoi approach to the partitioning of space may also be applied to the analysis of crystal *structures,* in which one alternative is to draw the planes equidistant between the outer radii of atoms or ions and not their centres—the sizes of the polyhedra being a measure of the relative sizes of the atoms or ions. All the polyhedra (now of different sizes and shapes) are space-filling. It may also be used in entirely non-crystallographic situations to determine, for example, the catchment areas for an irregular distribution of schools; pupils whose homes are on the dividing lines between the irregular polyhedra being equidistant from two schools and those whose homes are at the vertices being equidistant from three schools.

Exercises

3.1 The drawings in Fig. 3.11 show patterns of points distributed in orthorhombic-shaped unit cells. Identify to which (if any) of the orthorhombic Bravais lattices, P, C, I or F, each pattern of points corresponds.

(Hint: It is helpful to sketch plans of several unit cells, which will show more clearly the patterns of points, and then to outline (if possible) a P, C, I or F unit cell.)

3.2 The unit cells of several **orthorhombic** structures are described below. Draw *plans* of each and identify the Bravais lattice, P, C, I or F, in each case.

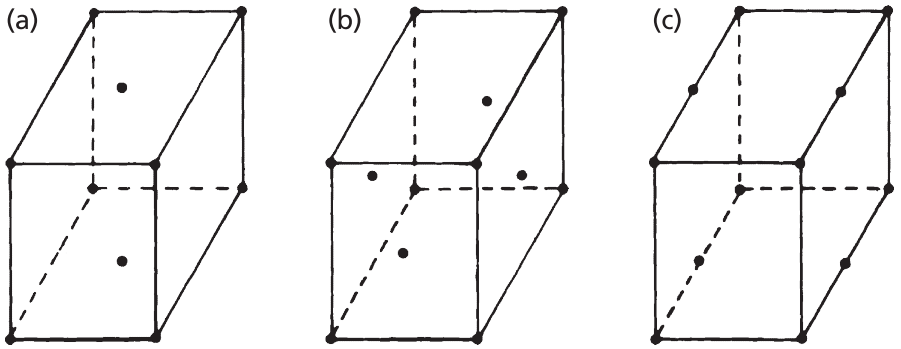

Fig. 3.11. Patterns of points in orthorhombic unit cells.

(a) One atom per unit cell located at $(x'y'z')$.

(b) Two atoms per unit cell of the *same* type located at $(0\frac{1}{2}0)$ and $\left(\frac{1}{2}0\frac{1}{2}\right)$.

(c) Two atoms per unit cell, one type located at $(00z')$ and $\left(\frac{1}{2}\frac{1}{2}z'\right)$ and the other type at $\left(00(\frac{1}{2}+z')\right)$ and $\left(\frac{1}{2}\frac{1}{2}\left(\frac{1}{2}+z'\right)\right)$.

(*Hint*: Draw plans of several unit cells and relocate the origin of the axes, x', y', z' should be taken as small (non-integral) fractions of the cell edge lengths.)

3.3 What are the shapes of the Voronoi polyhedra which correspond to the rhombohedral Bravais lattice?

(*Hint*: recall that the three cubic lattices are 'special cases' of the rhombohedral lattice in which the inter-axial angle α is 90° (cubic *P*), 60° (cubic *F*) or 109.47° (cubic *I*).)

3.4 Calculate the ratio between the 'long' and 'short' diagonals of the diamond-shaped faces in the primitive rhombohedral unit cells of the cubic *I* and cubic *F* lattices (see Fig. 3.2).

4

Crystal symmetry: point groups, space groups, symmetry-related properties and quasiperiodic crystals

4.1 Symmetry and crystal habit

As indicated in Chapter 3, the system to which a crystal belongs may be identified from its observed or external symmetry. Sometimes this is a very simple procedure. For example, crystals which are found to grow or form as cubes obviously belong to the cubic system: the external point symmetry of the crystal and that of the underlying unit cell are identical. However, a crystal from the cubic system may not grow or form with the external shape of a cube; the unit cells may stack up to form, say, an octahedron, or a tetrahedron, as shown in the models constructed from sugar-cube unit cells (Fig. 4.1). These are just two examples of a very general phenomenon throughout all the crystal systems: only very occasionally do crystals grow with the same shape as that of the underlying unit cell. The different shapes or **habits** adopted by crystals are determined by chemical and physical factors which do not, at the moment, concern us; what does concern us as crystallographers is to know how to recognize to which system a crystal belongs even though its habit may be quite different from, and therefore conceal, the shape of the underlying unit cell.

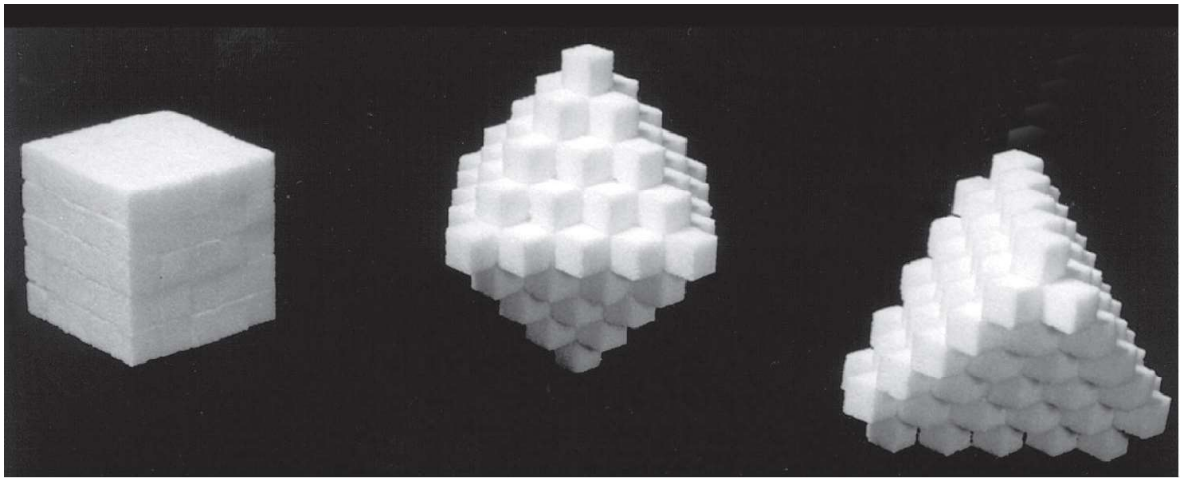

Fig. 4.1. Stacking of 'sugar-cube' unit cells to form (a) a cube, (b) an octahedron and (c) a tetrahedron. Note that the cubic cells in all three models are in the same orientation.

The Basics of Crystallography and Diffraction. Fourth Edition. Christopher Hammond.

The clue to the answer lies in the point group symmetry of the crystal. Consider, for example, the symmetry of the cubic crystals which have the shape or habit of a cube, an octahedron or a tetrahedron (Figs 4.1 and 4.2) or construct models of them (Appendix 1). The cube and octahedron, although they are different shapes, possess the same point group symmetry. The tetrahedron, however, has less symmetry: only six mirror planes instead of nine: only three diads running between opposite edges (i.e. along the directions perpendicular to the cube faces in the underlying cubes) and, as before, four triads running through each corner. The common, unchanged symmetry elements are the four (equally inclined) triads, and it is the presence of these four triads which

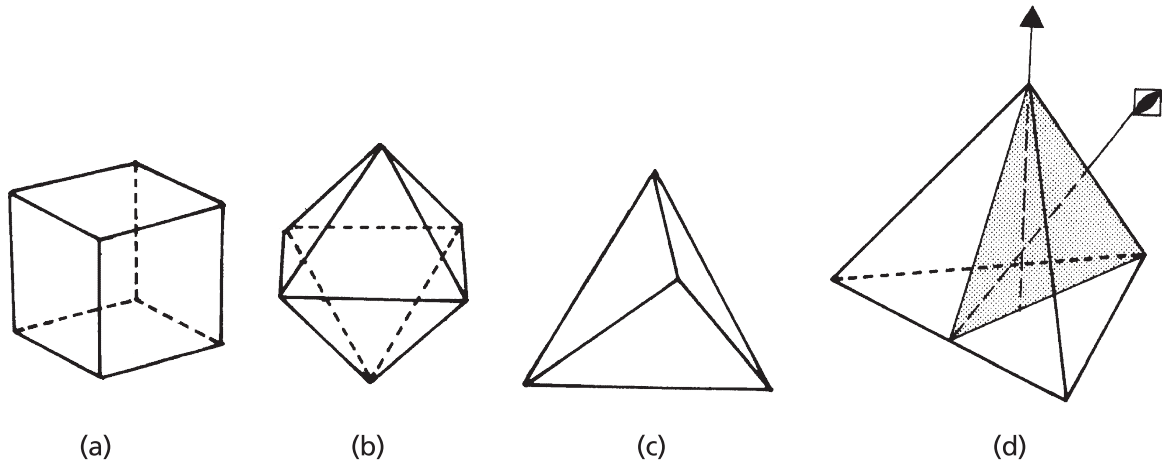

Fig. 4.2. (a) A cube, (b) an octahedron and (c) a tetrahedron drawn in the same orientation as the models in Fig. 4.1. (d) A tetrahedron showing the positions of one variant of the point symmetry elements: mirror plane (shaded) ($\times 6$), triad ($\times 4$) and inversion tetrad (which includes a diad) ($\times 3$).

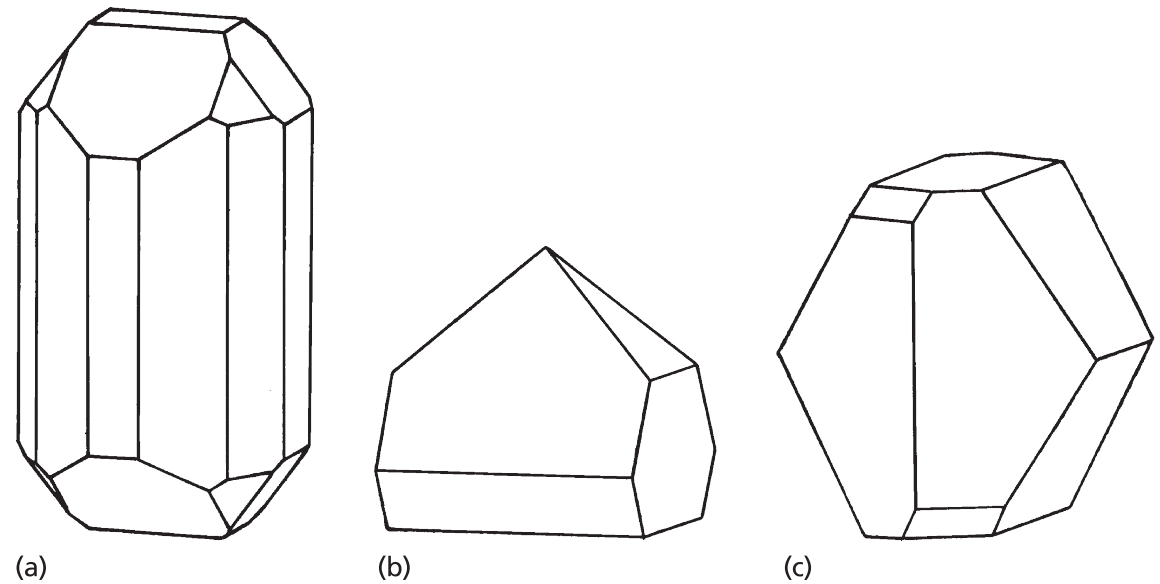

Fig. 4.3. Orthorhombic crystals (a) anglesite $PbSO_4$ (*mmm*), (b) struvite $NH_4MgPO_4 \cdot 6H_2O$ (*mm*2), (c) asparagine $C_4H_4O_3(NH_2)_2$ (222) (from *Introduction to Crystallography,* 3rd edn, by F. C. Phillips, Longmans 1963).

characterizes crystals belonging to the cubic system. Cubic crystals usually possess additional symmetry elements—the most symmetrical cubic crystals being those with the full point group symmetry of the underlying unit cell. But it is the four triads—not the three tetrads or the nine mirror planes—which are the 'hallmark' of a cubic crystal.

Similar considerations apply to all the other crystal systems. For example, Fig. 4.3 shows three orthorhombic crystals. Figure 4.3(a) shows a crystal with the full symmetry of the underlying unit cell—three perpendicular mirror planes and three perpendicular diads. Figure 4.3(b) shows a crystal with only two mirror planes and one diad along their line of intersection. Figure 4.3(c) shows a crystal with three perpendicular diads but no mirror planes.

4.2 The thirty-two crystal classes

The examples shown in Figs 4.1–4.3 are of crystals with different point group symmetries: they are said to belong to different **crystal classes.** Crystals in the same class have the same point group symmetry, so in effect the terms are synonymous. Notice that crystals in the same class do not necessarily have the same shape. For example, the cube and octahedron are obviously different shapes but belong to the same class because their point group symmetry is the same.

In two dimensions (Chapter 2) we found that there were ten plane point groups; in three dimensions there are thirty-two three-dimensional point groups. One of the great achievements of the science of mineralogy in the nineteenth century was the systematic description of the thirty-two point groups or crystal classes and their division into the seven crystal systems. Particular credit is due to J. F. C. Hessel,* whose contributions to the understanding of point group symmetry were unrecognized until after his death. The concept of seven different types or shapes of underlying unit cells then links up with the concept of the fourteen Bravais lattices; in other words, it establishes the connection between the external crystalline form or shape and the internal molecular or atomic arrangements.

It is not necessary to describe all the thirty-two point groups systematically; only the nomenclature for describing their important distinguishing features needs to be considered. This requires a knowledge of additional symmetry elements—centres and inversion axes.

Finally, we come to a 'practical' problem, which those of us who collect minerals or who grow crystals from solutions will immediately recognize. Our crystals are rarely uniformly developed, like those in Figs 4.2 or 4.3, but are irregular in appearance, with faces of different size and shape and from which it is almost impossible to recognize any point symmetry elements at all. Figure 4.4 shows examples of quartz crystals in which the corresponding faces are developed to different extents. It is this problem which hindered the development of crystallography until the discovery of the **Law of Constancy of Interfacial Angles** (Section 1.1) which enables us to focus on the underlying crystal symmetry rather than being diverted by the contingencies of crystal growth.

* Denotes biographical notes available in Appendix 3.

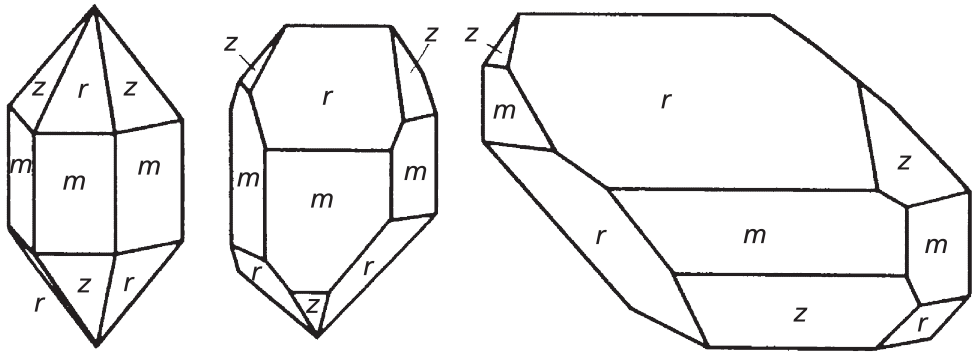

Fig. 4.4. Three quartz crystals with corresponding faces developed differently (from *Modern Crystallography* by B.K. Vainshtein, Springer-Verlag, 1981).

4.3 Centres and inversion axes of symmetry

If a crystal, or indeed any object, possesses a **centre of symmetry,** then any line passing through the centre of the crystal connects equivalent faces, or atoms, or molecules. A familiar example is a right hand and a left hand placed palm-to-palm but with the fingers pointing in opposite directions, as in Fig. 4.5(a). Lines joining thumb to thumb or fingertip to fingertip all pass through a centre of symmetry between the hands. When the hands are placed palm-to-palm but with the fingers pointing in the same direction, as in prayer, then there is no centre of symmetry but a **mirror (or reflection) plane of symmetry** instead, as in Fig. 4.5(b).

Notice the important relationship between these two symmetry elements: a centre of symmetry (Fig. 4.5(a)) *plus* a rotation of 180° (of one hand) is equivalent to a mirror plane of symmetry (Fig. 4.5(b)). Conversely, a mirror plane of symmetry *plus* a rotation of 180° (about an axis perpendicular to the mirror plane) is equivalent to a centre of symmetry. In short, centres and mirror planes of symmetry relate objects which (like hands) do not themselves possess these symmetry elements; conversely objects which themselves possess these symmetry elements do not occur in either right or left-handed forms (see Table 3.1).

In two dimensions a centre of symmetry is equivalent to diad symmetry. (See, for example, the motif and plane molecule shown in Fig. 2.3(4), which may be described as showing diad symmetry or a centre of symmetry.) In three dimensions this is not the case, as an inspection of Fig. 4.5(a) will show.

Inversion axes of symmetry are rather difficult to describe (and therefore difficult for the reader to understand) without the use of the stereographic projection—a method of representing a three-dimensional pattern of planes in a crystal on a two-dimensional plan. This topic is covered in Chapter 12 and the representation of symmetry elements in detail in Section 12.5.1. Geographers have the same problem when trying to represent the surface of the Earth on a two-dimensional map, and they too make use of the stereographic projection. In atlases, the circular maps of the world (usually with the north or south poles in the centre) are often stereographic projections.

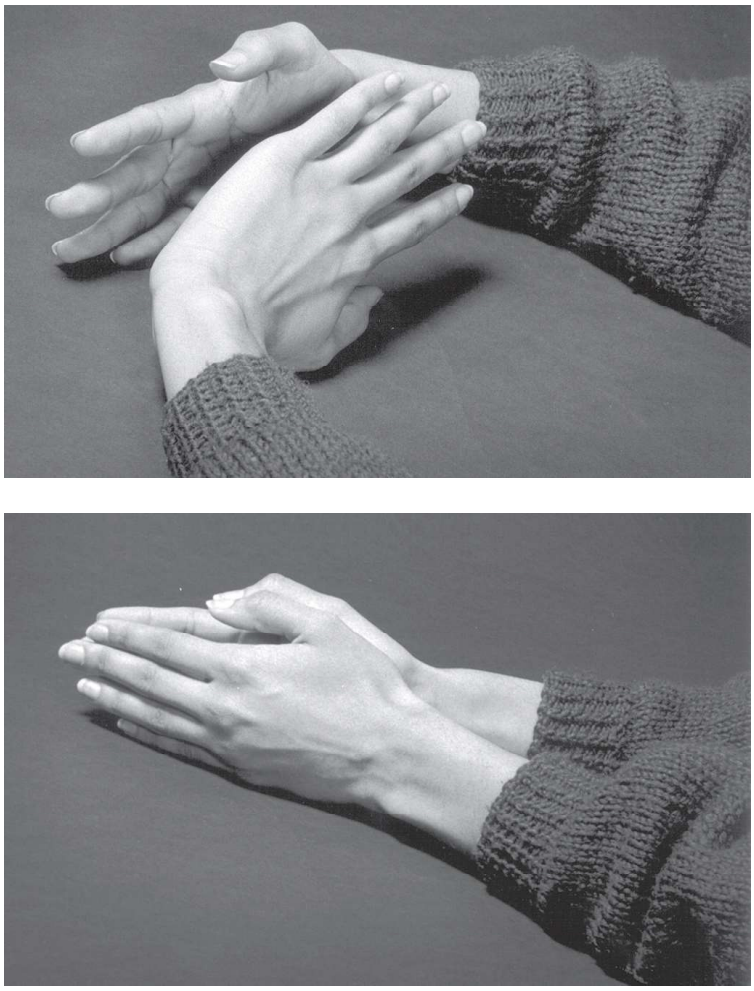

Fig. 4.5. Right and left hands (a) disposed with a centre of symmetry between them and (b) disposed with a mirror plane between them.

Inversion axes are *compound* symmetry elements, consisting of a rotation followed by an inversion. For example, as described in Chapter 2, the operation of a tetrad (fourfold) rotation axis is to repeat a crystal face or pattern every 90° rotation, e.g. in two dimensions giving four repeating **R**s or the four-fold pattern of faces in a cube. The operation of an inversion tetrad, symbol ◪ or $\bar{4}$, is to repeat a crystal face or pattern every 90° rotation-plus-inversion through a centre. What results is a four-fold pattern of faces around the inversion axis, but with each alternate face inverted. Examples of a crystal and an object with inversion tetrad axes are shown in Figs 4.6(a) and (b). The tennis ball has, in fact, the same point group symmetry as the crystal. Notice that when it is rotated 90° about the axis indicated, the 'downwards' loop in the surface pattern is replaced by an 'upwards' loop. Another 90° rotation brings a 'downwards' loop and so on for the full 360° rotation. Notice also that the inversion tetrad includes a diad, as is indicated by the diad (lens) symbol in the inversion tetrad (open square) symbol, ◪ or $\bar{4}$.

Finally, compare the symmetry of the tetragonal crystal in Fig. 4.6(a) with that of the tetrahedron (Fig. 4.2(d)): the diad axes which we recognized passing through the centres of opposite edges in the tetrahedron are, in fact, inversion tetrad axes or, to

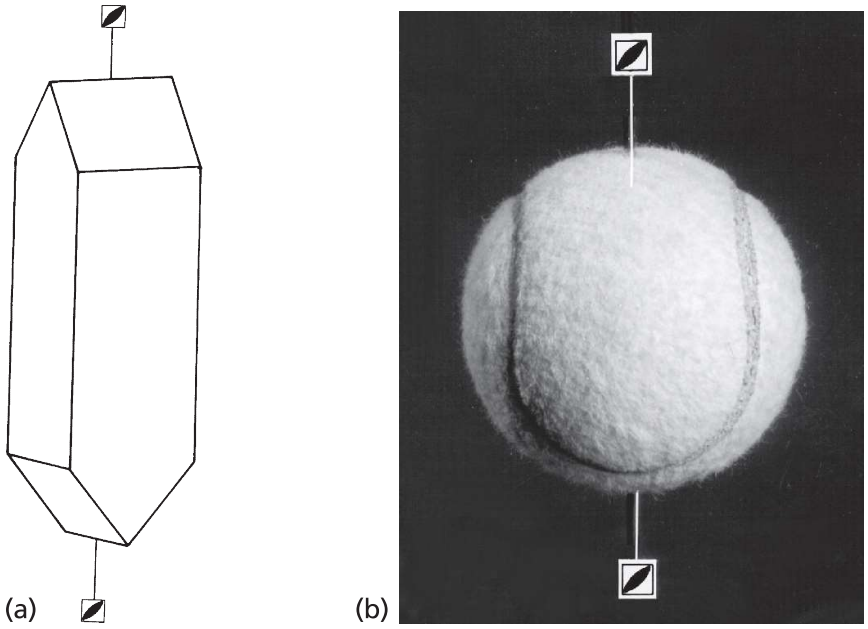

Fig. 4.6. Examples of a crystal and an object which have inversion tetrad axes (both point group $\bar{4}2m$). (a) Urea $CO(NH_2)_2$ and (b) a tennis ball.

develop one of the points made in Section 4.1, stacking the cubes into the form of a tetrahedron reduces the symmetry element along the cube axis directions from rotation to inversion tetrad.

There are also inversion axes corresponding to rotation monads diads, triads and hexads. The operation of an inversion hexad, for example, is a rotation of 60° plus an inversion, this compound operation being repeated a total of six times until we return to the beginning. However, for a beginner to the subject, these axes may perhaps be regarded as being of lesser importance then the inversion tetrad because they can be represented by combinations of other (better-understood) symmetry elements.

An inversion monad, symbol ○ or $\bar{1}$ is equivalent to a centre of symmetry.
An inversion diad, symbol $\bar{2}$ is equivalent to a perpendicular mirror plane.
An inversion triad, symbol △ or $\bar{3}$ is equivalent to a triad plus a centre of symmetry—which is the symmetry of a rhombohedral lattice (see Fig. 3.1). Notice that the 'top' three faces of the rhombohedron are related to the 'bottom' three faces by a centre of symmetry.
An inversion hexad, symbol ⬢ or $\bar{6}$ is equivalent to a triad plus a perpendicular mirror plane.

Again, these equivalences are best understood with the use of the stereographic projection (Chapter 12). The important point is that only inversion tetrads are unique (i.e. they cannot be represented by a combination of rotation axes, centres of symmetry or mirror planes) and therefore need to be considered separately.

The point group symmetries of the thirty-two classes are described by a 'short-hand' notation or **point group symbol** which lists the main (but not necessarily all) symmetry elements present. For example, the presence of centres of symmetry is not recorded

because they may arise 'automatically' from the presence of other symmetry elements, e.g. the presence of an inversion triad axis mentioned above. This notation for the thirty-two crystal classes or point groups, and their distribution among the seven crystal systems, is fully worked out in the *International Tables for Crystallography* published for the International Union of Crystallography and in F. C. Phillips' *Introduction to Crystallography*. Altogether there are five cubic classes, three orthorhombic classes, three monoclinic classes and so on. They are all listed in Table 3.1 (p. 93). The order in which the symmetry elements are written down in the point group symbol depends upon the crystal system.

In the cubic system the first place in the symbol refers to the axes parallel to, or planes of symmetry perpendicular to, the *x*-, *y*- and *z*-axes, the second refers to the four triads or inversion triads and the third the axes parallel to, or planes of symmetry perpendicular to, the face diagonal directions. Hence the point group symbol for the cube or the octahedron—the most symmetrical of the cubic crystals—is $4/m\bar{3}\,2/m$. This full point group symbol is usually (and rather unhelpfully) contracted to $m\bar{3}m$ because the operation of the four triads and nine mirror planes (three parallel to the cube faces and six parallel to the face diagonals) 'automatically' generates the three tetrads, six diads, and a centre of symmetry. The symbol for the tetrahedron is $\bar{4}3m$, the $\bar{4}$ referring to the three inversion tetrad axes along the *x*-, *y*- and *z*-axes together with the *m* referring to the face-diagonal mirror planes. The least symmetric cubic class has point group symbol 23, i.e. it only has diads along the *x*-, *y*- and *z*-axes and the characteristic four triads.

In the orthorhombic system the three places in the point group symbol refer to the symmetry elements associated with the *x*-, *y*- and *z*-axes. The most symmetrical class (Fig. 4.3(a)), which has the full point group symmetry of the underlying orthorhombic unit cell (Fig. 3.5), has the full point group symbol $2/m2/m2/m$, but this is usually abbreviated to *mmm* because the presence of the three mirror planes perpendicular to the *x*-, *y*- and *z*-axes 'automatically' generates the three perpendicular diads. The other two classes are *mm*2 (Fig. 4.3(b))—a diad along the intersection of two mirror planes—and 222 (Fig. 4.3(c))—three perpendicular diads.

In the monoclinic system the point group symbol simply refers to the symmetry elements associated with the *y*-axis. This may be a diad (class 2), an inversion diad (equivalent to a perpendicular mirror plane (class $\bar{2}$ or *m*)), or a diad plus a perpendicular mirror plane (class $2/m$).

In the tetragonal, hexagonal and trigonal systems, the first position in the point group symbol refers to the 'unique' *z*-axis. For example, the tetragonal crystals in Fig. 4.6 have point group symmetry $\bar{4}2m$; $\bar{4}$ referring to the inversion tetrad along the *z*-axis, 2 referring to the diads along the *x*- and *y*-axes and *m* to the mirror planes which bisect the *x*- and *y*-axes (which you will find by examining the model!). One of the trigonal classes has point group symbol 32 (not to be confused with cubic class 23!), i.e. a single triad along the *z*-axis and (three) perpendicular diads.

Not all classes are of equal importance; in 432 and $\bar{6} = 3/m$ there is only one example of a crystal structure (Li Fe_5 O_8 and LiO_2, respectively). On the other hand, the two monoclinic classes *m* and $2/m$ contain about 50 per cent of all inorganic crystalline materials on a 'crystal counting' basis, including feldspar, the commonest mineral in

nature, and many other economically important minerals. As for the crystals of organic compounds, class 2/*m* is by far the most important, while crystals of biologically important substances which contain chiral (right- or left-handed enantiomorphic molecules) have a predilection for class 2. The commonest class in any system is the **holosymmetric** class, i.e. the class which shows the highest symmetry. The holosymmetric cubic class $m\bar{3}m$, the most symmetrical of all, contains only a few per cent of all crystals on this basis, but these also include many materials and ceramics of economic and commercial importance.

It is a great help in an understanding of point group symmetry simply to identify the symmetry elements of everyday objects such as clothes pegs, forks, pencils, tennis balls, pairs of scissors, etc. Or, one step further, you could make models showing the point group symmetries of all the 32 crystal classes as described in Appendix 1.

A note on alternating or rotation-reflection axes

These compound symmetry elements were used by Schönflies in his derivation of the 230 space groups. They are used in the description of layer-symmetry (Section 2.8) but are otherwise little used today. They consist of rotation plus a **reflection** in a plane perpendicular to the axis, rather than an **inversion**. Hence a monad alternating axis is equivalent to a perpendicular mirror plane (or inversion diad); a diad alternating axis is equivalent to a centre of symmetry (or inversion monad); a triad alternating axis is equivalent to an inversion hexad; a tetrad alternating axis is equivalent to an inversion tetrad and a hexad alternating axis is equivalent to an inversion triad.

4.4 Crystal symmetry and properties

The quantities which are used to describe the properties of materials are, as we know, simply represented as *coefficients,* i.e. as one measured (or measurable) quantity divided by another. For example, the property (coefficient) of electrical conductivity is given by the amount of electrical current flowing between two points (which may be measured in various ways) divided by the electrical potential gradient; the pyroelectric effect—the property of certain crystals of developing electrical polarization when the temperature is changed—is given by the polarization divided by the temperature change; the heat capacity is given by the quantity of heat absorbed or given out divided by the temperature change, and so on.

In many (in fact most) cases the measured quantities depend on direction and are called **vectors**.[1] In the examples above, electrical current flow, potential gradient and polarization are all vectors. The other quantities in the examples above, temperature change, quantity of heat, do not depend on direction and are called **scalars**. Finally, many quantities which are of importance in the description of the physical properties of crystals are described by **tensors**, a subject which is introduced in Chapter 14.

[1] See Appendix 5.

The important point is that, in those cases where one or more of the measured quantities vary with direction, so also do the crystal properties; they are said to be *anisotropic* (from the Greek tropos, direction or turn; (an)iso, (not the) same). Anisotropy clearly arises because the arrangements of atoms in crystals vary in different directions—you would intuitively *expect* crystals to be anisotropic, the only exceptions being those properties (the heat capacity) which are direction independent. You would also intuitively expect cubic crystals to be 'less anisotropic' than, say, monoclinic ones because of their greater symmetry, and this intuition would also be correct. For many properties, but not all, cubic crystals are isotropic—the property (and property coefficient) is direction independent. In the example given above, cubic crystals are isotropic with respect to electrical conductivity. They are also isotropic with regard to the pyroelectic effect, i.e. cubic crystals do not exhibit electrical polarization when the temperature is changed; the pyroelectric coefficient is zero. But cubic crystals are not isotropic with respect to all properties. For example, their elastic properties, which determine the mechanical properties of stiffness, shear and bulk moduli, are direction dependent and these are very important factors with respect to the properties of metals and alloys.

Hence, one major use of point groups is in relating crystal symmetry and properties; as the external symmetry of crystals arises from the symmetry of the internal molecular or atomic arrangements, so also do these in turn determine or influence crystal properties. Some examples have already been alluded to. For example, the pyroelectric effect cannot exist in a crystal possessing a centre of symmetry, and the pyroelectric polarization can only lie along a direction in a crystal that is *unique,* in the sense that it is not repeated by any symmetry element. There are only ten point groups or crystal classes which fulfil these conditions and they are called the **ten polar point groups:**

1	2	3	4	6
m	*mm*2	3*m*	4*mm*	6*mm.*

Hence, pyroelectricity or the pyroelectric effect can only occur in these ten polar point groups or classes.

A very closely related property to pyroelectricity, and of great importance in electroceramics, is ferroelectricity. A ferroelectric crystal, like a pyroelectric crystal, can also show polarization, but in addition the direction of polarization may be reversed by the application of an electric field. Most ferroelectric crystals have a transition temperature (Curie point) above which their symmetry is non-polar and below which it is polar.

One such example is barium titanate, $BaTiO_3$, which has the perovskite structure (Fig. 1.17). Above the Curie temperature barium titanate has the fully symmetric cubic structure, point group $m\bar{3}m$, but below the Curie temperature, when the crystal becomes ferroelectric, distortions occur—a small expansion occurs along one cell edge and small contractions along the other two, changing the crystal system symmetry from cubic to tetragonal and the point group symmetry from $m\bar{3}m$ to 4*mm*. As the temperature is further lowered below the Curie point, further distortions occur and the point group symmetry changes successively to *mm*2 and 3*m*—all of them, of necessity, being polar point groups (see Section 1.11.1).

Another very important crystal property is piezoelectricity—the development of an electric dipole when a crystal is stressed, or conversely, the change of shape of a crystal when it is subjected to an electrical field. At equilibrium the applied stress will be centrosymmetrical, so if a crystal is to develop a dipole, i.e. develop charges of opposite sign at opposite ends of a line through its centre, it cannot have a centre of symmetry. There are twenty-one non-centrosymmetric point groups (Table 3.1), all of which, except one, point group 432, may exhibit piezoelectricity. It is the presence of the equally inclined triads, tetrads and diads in this cubic point group which in effect cancel out the development of a unidirectional dipole.

The optical properties of crystals—the variation of refractive index with the vibration and propagation direction of light (double refraction or birefringence), the variation of refractive index with wavelength or colour of the light (dispersion), or the associated variations of absorption of light (pleochroism)—are all symmetry dependent. The complexity of the optical properties increases as the symmetry decreases. Cubic crystals are optically isotropic—the propagation of light is the same in all directions and they have a single refractive index. Tetragonal, hexagonal and trigonal crystals are characterized by two refractive indices. For light travelling in a direction *perpendicular* to the principal (tetrad, hexad or triad) axis, such crystals exhibit two refractive indices—one for light vibrating along the principal axis, and another for light vibrating in a plane perpendicular to the principal axis. For light travelling *along* the principal axis (and therefore vibrating in the planes parallel to it), the crystal exhibits only one refractive index, and therefore behaves, for this direction only, as an optically isotropic crystal. Such crystals are called *uniaxial* with respect to their optical properties, and their principal symmetry axis is called the *optic axis.* Crystals belonging to the remaining crystal systems—orthorhombic, monoclinic and triclinic—are characterized by three refractive indices and two, not one, optic axes. Hence they are said to be biaxial since there are two, not one, directions for the direction of propagation of light in which they appear to be optically isotropic. It should be noted, however, that unlike uniaxial crystals, there is no simple relationship between the two optic axes of biaxial crystals and the principal symmetry elements; nor are they fixed, but vary as a result of dispersion, i.e. the variations in the values of the refractive indices with wavelength.

Finally, there is the phenomenon or property of optical activity or rotatory polarization, which should not be confused with double refraction. It is a phenomenon in which, in effect, the vibrational direction of light rotates such that it propagates through the crystal in a helical manner either to the right (dextrorotatory) or the left (laevorotatory). Now right-handed and left-handed helices are distinct in the same way as a right and left hand (Fig. 4.5) or the two parts of a twinned crystal (Fig. 1.18) and therefore optical activity would be expected to occur only in those crystals which occur in right-handed or left-handed forms, i.e. those which do not possess a mirror plane or a centre (or inversion axis) of symmetry. Such crystals are said to be enantiomorphous and there are altogether eleven enantiomorphous classes or point group symmetries (Table 3.1).

A famous example is sodium ammonium tartrate, a salt of tartaric acid (Fig. 4.7). In 1848 Louis Pasteur* first noticed these two forms 'hemihedral to the right' and 'hemihedral to the left' under the microscope and, having separated them, found that their solutions were optically active in opposite senses.

The study of enantiomorphism, or chirality, from the Greek word *chiros,* meaning hand, is becoming increasingly important. Louis Pasteur, as a result of his work on tartaric acid, was the first to suggest that the molecules themselves could be chiral—i.e. that they could exist in either right-handed or left-handed forms. The basic constituents of living things are chiral, including the amino acids[2] present in proteins, the nucleotides present in nucleic acids and the DNA double helix itself. But *only one* enantiomorph is ever found in nature—only L-amino acids are present in proteins and only D-nucleotides are present in nucleic acids (L stands for laevo—or left-rotating, and D stands for dextro—or right-rotating). Why this should be so is one of the mysteries surrounding the origin of life itself and for which many explanations or hypotheses have been offered. If, as many hypotheses suppose, it was the result of a chance event which was then consolidated by growth, then we might reasonably suppose that on another

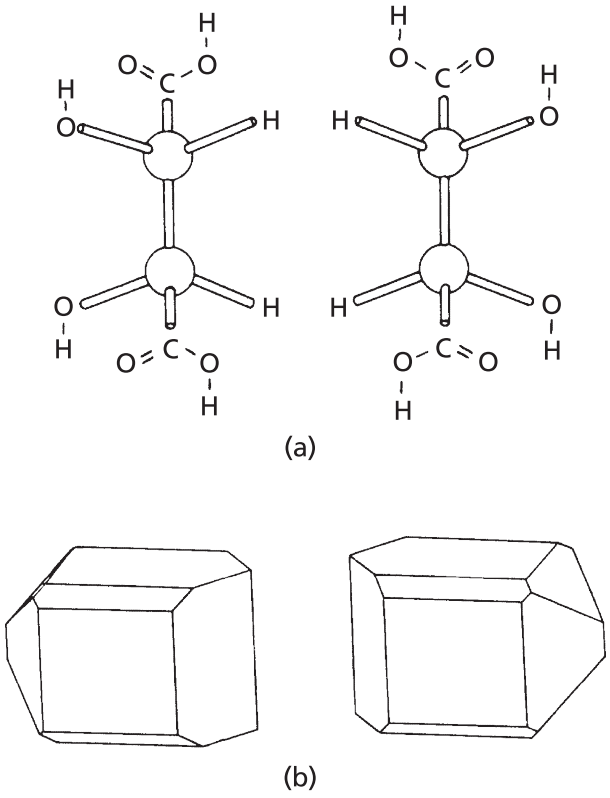

Fig. 4.7. (a) Left- and right-handed forms of tartaric acid molecules (from *Crystals: their Role in Nature and Science* by C. W. Bunn, Academic Press, New York, 1964); and (b) the left- and right-handed forms of tartaric acid crystals (from F. C. Phillips, loc. cit.).

* Denotes biographical notes available in Appendix 3.

[2] Except glycine, the simplest amino acid.

planet such as ours the *opposite* event might have occurred and that there exist living creatures, in every way like ourselves, but who are constituted of D-amino acids and L-nucleotides!

However, to return to earth, once our basic chirality has been established, the D- and L- (enantiomorphous) forms of many substances, including drugs in particular, may have very different chemical and therapeutic properties. For example, the molecule asparagine (Fig 4.3(c)) occurs in two enantiomorphous forms, one of which tastes bitter and the other sweet. Thalidomide also; the right-handed molecule of which acts as a sedative but the left-handed molecule of which gave rise to birth defects. Hence chiral separation, and the production of enantiomorphically pure substances, is of major importance.

4.5 Translational symmetry elements

The thirty-two point group symmetries (Table 3.1) may be applied to three-dimensional patterns just as the ten plane point group symmetries are applied to two-dimensional patterns (Chapter 2). As in two dimensions where translational symmetry elements or glide lines arise, so also in three dimensions do **glide planes** and also **screw axes** arise. It is only necessary to state the symmetry properties of patterns that are described by these translational symmetry elements. Glide planes are the three-dimensional analogues of glide lines; they define the symmetry in which mirror-related parts of the motif are shifted half a lattice spacing. In Fig. 2.5(b) the figures are related by glide lines, which can easily be visualized as glide-plane symmetry. Glide planes are symbolized as a, b, c (according to whether the translation is along the x-, y- or z-axes), n or d (diagonal or diamond glide—special cases involving translations along more than one axis).

Screw axes (for which there is no two-dimensional analogue—except for screw diads which arise in layer-symmetry patterns (see Section 2.8))—essentially describe helical patterns of atoms or molecules, or the helical symmetry of motifs. Several types of helices are possible and they are all based upon different combinations of rotation axes and translations. Figure 4.8 shows the possible screw axes (the direction of translation out of the plane of the page) with the heights **R** of the asymmetrical objects represented as fractions of the lattice repeat distance (compare to Fig. 2.3). Screw axes are represented in writing by the general symbol N_m, N representing the rotation (2, 3, 4, 6) and the subscript m representing the pitch in terms of the number of lattice translation or repeat distances for one complete rotation of the helix. m/N therefore represents the translation for each rotation around the axis. Thus the 4_1 screw axis represents a rotation of 90° followed by a translation of $\frac{1}{4}$ of the repeat distance, which repeated three times brings **R** to an identical position but displaced one lattice repeat distance; the 4_3 screw axis represents a rotation of 90° followed by a translation of $\frac{3}{4}$ of the lattice repeat distance, which repeated three times gives a helix with a pitch of three lattice repeat distances. This is equivalent to the 4_1 screw axis but of opposite sign: the 4_1 axis is a right-handed helix and 4_3 axis is a left-handed helix. In short they are enantiomorphs of each other. Similarly the 3_1 and 3_2 axes, the 6_1 and 6_5 axes, and the 6_2 and 6_4 axes are enantiomorphs of each other. In diagrams, screw axes are represented by the symbol for the

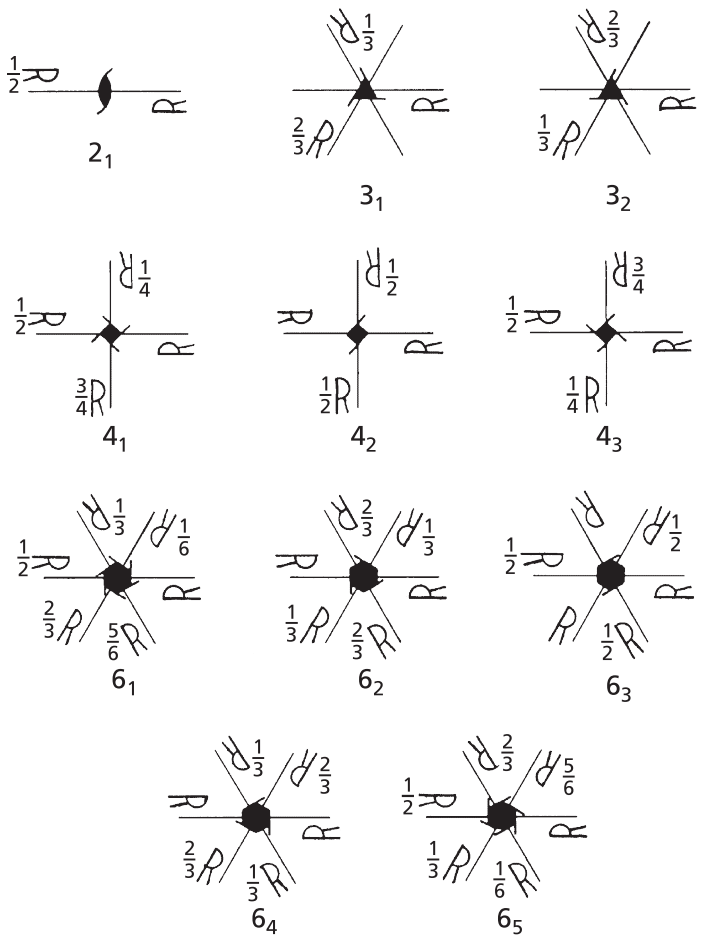

Fig. 4.8. The operation of screw axes on an asymmetrical motif, **R**. The fractions indicate the 'heights' of each motif as a fraction of the repeat distance.

rotation axis with little 'tails' indicating (admittedly not very satisfactorily) the pitch and sense of rotation (see Fig. 4.8). Screw axes have, of course, their counterparts in nature and design—the distribution of leaves around the stem of a plant, for example, or the pattern of steps in a spiral (strictly helical) staircase. Figure 4.9 shows two such examples. Figure 4.10 shows the 6_3 screw hexads which occur in the hcp structure; notice that they run parallel to the *c*-axis and are located in the 'unfilled' channels which occur in the hcp structure. They do not pass through the atom centres of either the A layer or the B layer atoms; these are the positions of the triad (not hexad) axes in the hcp structure.

Just as the external symmetry of crystals does not distinguish between primitive and centred Bravais lattices, so also it does not distinguish between glide and mirror planes, or screw and rotation axes. For example, the six faces of an hcp crystal show hexad, six-fold symmetry, whereas the underlying structure possesses only screw hexad, 6_3, symmetry.

In many crystals, optical activity arises as a result of the existence of enantiomorphous screw axes. For example, in α-quartz (enantiomorphous class 32), the SiO_2 structural units which are not themselves asymmetric, are arranged along the *c*-axis

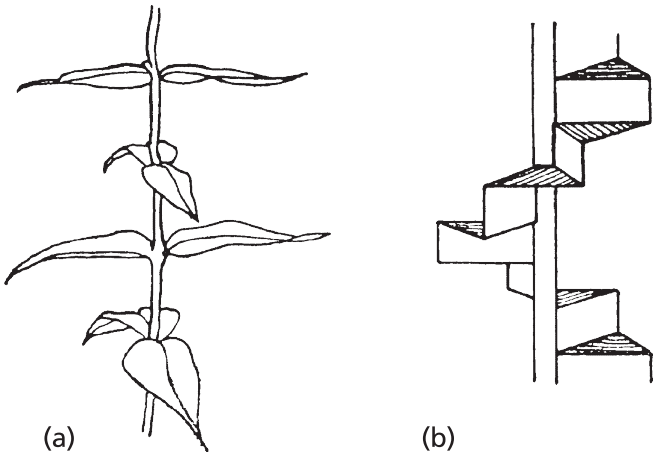

Fig. 4.9. (a) The 4_2 screw axis arrangement of leaves round a stem of pentstemon (after Walter Crane); and (b) a 6_1 screw axis spiral (helical) staircase (from *The Third Dimension in Chemistry* by A. F. Wells, Clarendon Press, Oxford, 1968).

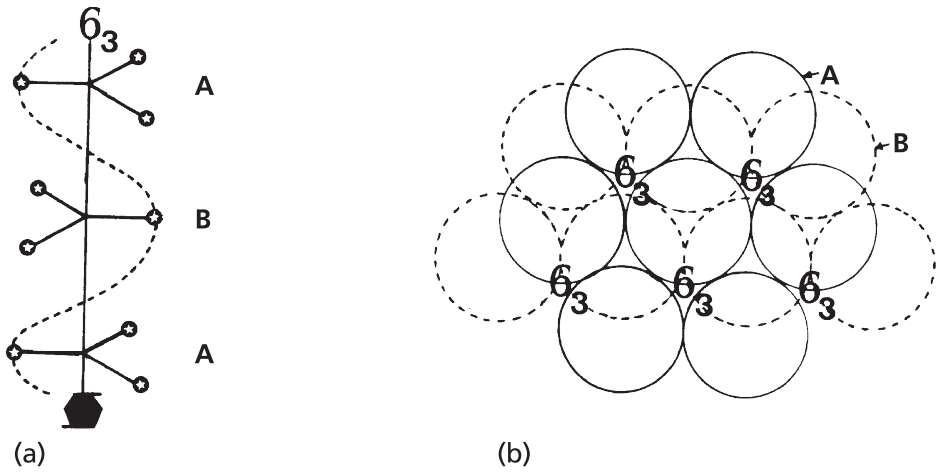

Fig. 4.10. (a) A screw hexad (6_3) axis; and (b) location of these axes in the hcp structure. Notice that they pass through the 'unfilled channels' between the atoms in this structure.

(which is also the optic axis) in either a 3_1 or a 3_2 screw orientation (see Figure 1.33(a), Section 1.11.5). This gives rise to the two enantiomorphous crystal forms of quartz (class 32, Fig. 4.11). The plane of polarization of plane-polarized light propagating along the optic axis is rotated to right or left, the angle of rotation depending on the wavelength of the light and the thickness of the crystal. This is not, to repeat, the same phenomenon as birefringence; for the light travelling along the optic axis the crystal exhibits (by definition) one refractive index. If the 3_1 or 3_2 helical arrangement of the SiO_2 structural units in quartz is destroyed (e.g. if the crystal is melted and solidified as a glass), the optical activity will also be destroyed.

However, in other crystals such as tartaric acid (Fig. 4.7) and its derivatives, the optical activity arises from the asymmetry—the lack of a mirror plane or centre of symmetry—of the molecule itself (Fig. 4.7(a)). In such cases the optical activity is not destroyed if the crystal is melted or dissolved in a liquid. The left or right handedness of

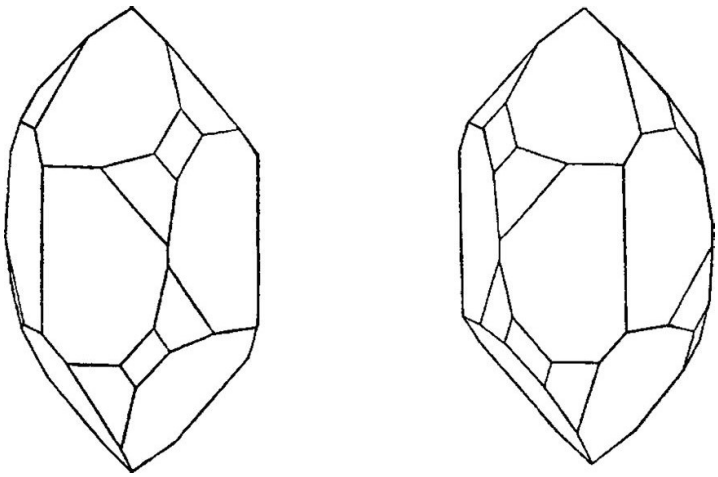

Fig. 4.11. The enantiomorphic (right- and left-handed) forms of quartz. The optic axis is in the vertical (long) direction in each crystal (from F. C. Phillips, loc. cit).

the molecules, even though they are randomly orientated in a solution, is communicated at least in part, to the plane-polarized light passing through it. Unlike quartz, in which the optical activity depends on the direction of propagation of the light with respect to the optic axis, the optical activity of a solution such as tartaric acid is unaffected by the direction of propagation of the light. In summary, the optical activity of solutions arises from the asymmetry of the molecule itself; the optical activity which is shown in crystals, but not their solutions or melts, arises from the enantiomorphic screw symmetry of the arrangement of molecules in the crystal.

4.6 Space groups

In Section 2.4 it is shown how the seventeen possible two-dimensional patterns or plane groups (Fig. 2.6) can be described as a combination of the five plane lattices with the appropriate point and translational symmetry elements. Similarly, in three dimensions, it can be shown that there are 230 possible three-dimensional patterns or **space groups,** which arise when the fourteen Bravais lattices are combined with the appropriate point and translational symmetry elements. It is easy to see why there should be a substantially larger number of space groups than plane groups. There are fourteen space lattices compared with only five plane lattices, but more particularly there is a greater number of combinations of point and translational symmetry elements in three dimensions, particularly the presence of inversion axes (point) and screw axes (translational) which do not occur in two-dimensional patterns.

The first step in the derivation of 230 space groups was made by L. Sohncke* (who also first introduced the notion of screw axes and glide planes described in Section 4.5). Essentially, Sohncke relaxed the restriction in the definition of a Bravais lattice—that the environment of each point is identical—by considering the possible arrays of points which have identical environments when viewed from *different* directions, rather than from the *same* direction as in the definition of a Bravais lattice. This is equivalent to

combining the fourteen Bravais lattices with the appropriate translational symmetry elements, and gives rise to a total of sixty-five space groups or Sohncke groups.

The second, final, step was to account for inversion axes of symmetry which gives rise to a further 165 space groups. They were first worked out by Fedorov* in Moscow in 1890 (who drew heavily on Sohncke's work) and independently by Schönflies* in Göttingen in 1891 and Barlow* in London in 1894—an example of the frequently occurring phenomenon in science of progress being made almost at the same time by people approaching a problem entirely independently. (see Appendix 7)

The 230 space groups are systematically drawn and described in the *International Tables for Crystallography* Volume A, which is based upon the earlier *International Tables for X-ray Crystallography* Vol. 1 compiled by N. F. M. Henry* and Kathleen Lonsdale*—a work of great crystallographic scholarship. The space groups are arbitrarily numbered 1 to 230, beginning with triclinic crystals of lowest symmetry and ending with cubic crystals of highest symmetry. There are two space group symbols, one due to Schönflies* used in spectroscopy and the other, which is now generally adopted in crystallography, due to Hermann* and Mauguin.*

The Hermann–Mauguin space group symbol consists first of all of a letter *P, I, F, R, C, B or A* which describes the Bravais lattice type (Fig. 3.1) (the alternatives *C*, *B* or *A* being determined as to whether the unit cell axes are chosen such that the *C*, *B* or *A* faces are centred); then a statement, rather like a point group symbol, of the essential (not all) symmetry elements present. For example, the space group symbol *Pba*2 represents a space group which has a primitive (*P*) Bravais lattice and whose point group is *mm*2 (the *a* and *b* glide planes being simple mirror planes in point group symmetry). This is one of the point groups of the orthorhombic system (Fig. 4.3) and the lattice type is orthorhombic *P*. Similarly, space group $P6_3/mmc$ has a primitive (*P*) (hexagonal) Bravais lattice with point group symmetry 6/*mmm.*

The space group itself is represented by means of two diagrams or projections, one showing the symmetry elements present and the other showing the operation of these symmetry elements on an asymmetric 'unit of pattern' represented by the circular symbol ◯ and its mirror-image by ⊙: a circle with a comma inside. These symbols, which may represent an asymmetric molecule, a group of molecules, or indeed any asymmetrical structural unit, correspond to the **R** and **Я** of our two-dimensional patterns. The choice of a *circle* to represent an *asymmetric* object might be thought to be inadequate—surely a symbol such as **R** or, better still, a right hand would be more appropriate? In a sense it would, but there would then arise a serious problem of typography, of clearly and unambiguously representing the operation of all the symmetry elements in the projection. For example, in the case where a mirror plane lies *in* the plane of projection a right hand (palm-down) would be mirrored by a left hand (palm-up)—and the problem would be to represent clearly these two superimposed hands in a plan view. In the case of a circle this situation is easily represented by ⏀ —a circle divided in the middle with the mirror-image indicated in one half. Similarly, the use of a symbol such as **R** would

* Denotes biographical notes available in Appendix 3.

lead to ambiguity. For example, a diad axis *in* the plane of projection would rotate an **R** 180° out of the plane of projection into an **Я**—which would be indistinguishable from an **R** reflected to an **Я** in a mirror plane perpendicular to the plane of projection—i.e. as for mirror-lines in the two-dimensional case. In the case of a circle there is no such ambiguity; in the former case we have

(diad axis in plane of paper—no change of hand of motif)

and in the latter case

(mirror plane perpendicular to plane of paper—a change of hand of motif)

The representation of space groups and some, but not all of the associated crystallographic information, is best described by means of four examples *Pba*2 (No. 32), $P2_1/c$ (No. 14), $P6_3/mmc$ (No. 194) and $P4_12_12$ (No. 92).

Figure 4.12, from the *International Tables for X-ray Crystallography,* shows space group No. 32, *Pba*2 with the Hermann–Mauguin and Schoenflies symbols shown top left and the point group and crystal system top right. The two diagrams are projections in the $x - y$ plane, the right-hand one shows the symmetry elements present—the diads parallel to the z-axis at the corners, edges and centre of the unit cell and the a and b glide planes shown as dashed lines in between. It would be perfectly possible to draw the origin of the unit cell at an intersection of the glide planes—but to choose it, as shown, at a diad axis is more convenient, hence the note 'origin on 2'.

In the left-hand diagram the ◯ is placed at (small) fractions, x, y, z of the cell edge lengths away from the origin, the z parameter or 'height' being represented by a plus (+) sign. This is called a 'general equivalent position' because the ◯ does not lie on any of the symmetry elements present and the resulting pattern is known as the set of 'general equivalent positions'. The coordinates of these positions are listed below together with the total number of them, 4, the 'Wyckoff letter', c and the symbol 1 for a monad, indicating the asymmetry of the ◯ (and its glide plane image ⊙).

If the pattern unit ◯ were to be placed not in a general position but in a 'special position', on a diad axis in this example, then a simpler pattern results. The four asymmetric pattern units 'merge together' to give two units with diad symmetry and these are called 'special equivalent positions'. There are in fact two possibilities, denoted by the Wyckoff letters a and b and their co-ordinates are listed in the table on the left. The Wyckoff letters are purely arbitrary, like the numbering of the space groups themselves.

The table on the right lists the conditions (on the Laue indices *hkl*) limiting possible reflections, those not meeting these conditions being known as *systematic absences* in X-ray diffraction. These topics are covered in Chapter 9 and Appendix 6. Finally, the 'symmetry of special projections' shows the plane groups corresponding to the space group projected on different planes (just as in our projections of crystal structures in Chapter 2). For example, the projection on the (001) plane (which is that of the diagrams) corresponds to plane groups *pgg* (or *p*2*gg*—see Fig. 2.6).

$P\,b\,a\,2$ C_{2v}^{8} No. 32 $P\,b\,a\,2$ $m\,m\,2$ Orthorhombic

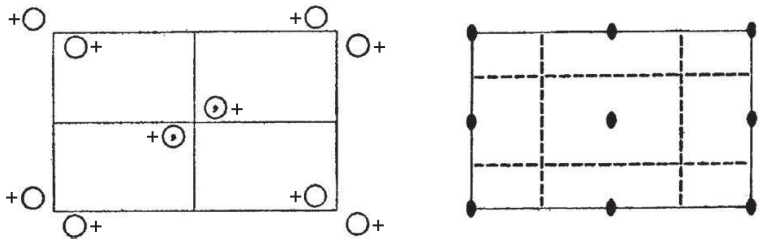

Origin on 2

Number of positions, Wyckoff notation, and point symmetry			Co-ordinates of equivalent positions	Conditions limiting possible reflections
				General:
4	*c*	1	x,y,z; $\bar{x},\bar{y},z$; $\frac{1}{2}-x,\frac{1}{2}+y,z$; $\frac{1}{2}+x,\frac{1}{2}-y,z$.	*hkl*: No conditions 0*kl*: $k=2n$ *h*0*l*: $h=2n$ *hk*0: No conditions *h*00: $(h=2n)$ 0*k*0: $(k=2n)$ 00*l*: No conditions
				Special: as above, plus
2	*b*	2	$0,\frac{1}{2},z$; $\frac{1}{2},0,z$.	*hkl*: $h+k=2n$
2	*a*	2	$0,0,z$; $\frac{1}{2},\frac{1}{2},z$.	

Symmetry of special projections

(001) *pgg*; $a'=a$, $b'=b$ (100) *pm*1; $b'=b/2$, $c'=c$ (010) *p*1*m*; $c'=c$, $a'=a/2$

Fig. 4.12. Space group *Pba*2 (No. 32) (from the *International Tables for X-ray Crystallography*).

Figure 4.13 is extracted from the entry for the most frequently occurring space group No. 14 ($P2_1/c$) in the *International Tables for Crystallography* in which two choices for the unique axis *b* or *c* (parallel to the (screw) diad axes) and three choices of unit cell are available. Figure 4.13(a) shows the usual choice of the *b* (or *y*-axis) parallel to the (screw) diad axes as indicated by the monoclinic point group symbol 2/*m* (see Section 4.3) and 'cell choice 1'. The pattern of general equivalent positions is shown in the lower right diagram and the symmetry elements (screw diads, centres of symmetry and glide planes) are shown in three different projections. The centres of symmetry are indicated by small circles, the glide planes by dashed or dotted lines depending as to whether the glide direction is in, or perpendicular to, the plane of the diagram, and similarly the screw diad axes normal to or in the plane of the projection are indicated by ◖ or single-headed arrow symbols respectively. Figure 4.13(b) shows the three possible cell choices and the tables of the coordinates of the general and special equivalent positions (with their Wyckoff letters running from bottom to top) and the reflection conditions as before.

(a) $P\,2_1/c$ C_{2h}^5 2/*m* Monoclinic

No. 14 $P\,1\,2_1/c\,1$ Patterson symmetry $P\,1\,2/m\,1$

UNIQUE AXIS *b*, CELL CHOICE 1

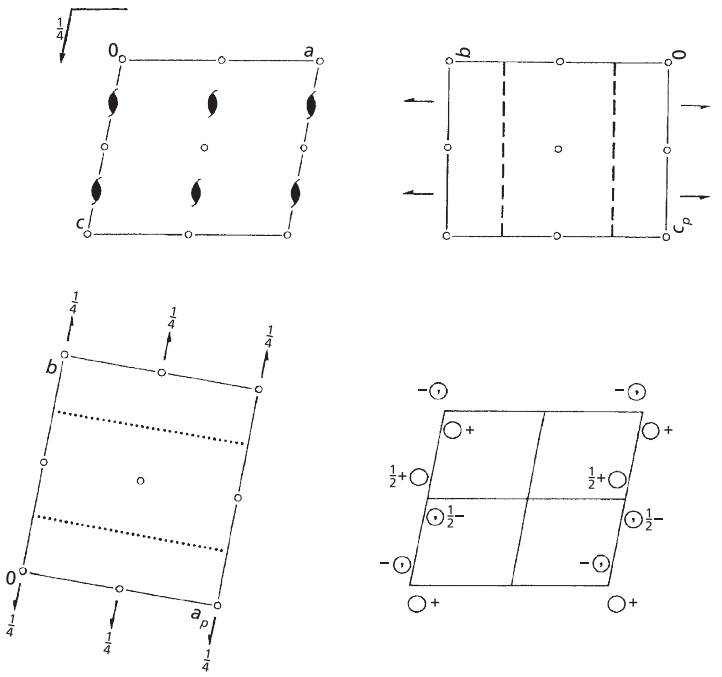

Origin at $\bar{1}$

Asymmetric unit $0\leq x\leq 1;\ 0\leq y\leq \frac{1}{4};\ 0\leq z\leq 1$

Symmetric operations

(1) 1 (2) $2(0,\frac{1}{2},0)$ $0,y,\frac{1}{4}$ (3) $\bar{1}$ 0,0,0 (4) *c* $x,\frac{1}{4},z$

Fig. 4.13. (*continued*)

Figure 4.14 is extracted from the entry for space group $P6_3/mmc$, No. 194 in the *International Tables for X-ray Crystallography;* this is the space group for the hcp metals (Fig. 1.5(b)), $A1B_2$, WC (Fig. 1.15) and wurtzite (Figs 1.26 and 1.36(b)). Notice that there is a greater number of special equivalent positions (Wyckoff letters running from *a* to *k*) than in the two lower-symmetry space groups we have just looked at and that the coordinates of the pattern units are much reduced—from 24 for the general case to 2 for positions with Wyckoff letters *a, b, c, d.* In hcp metals the A and B layer atoms (Fig. 1.5(b)) are in the special equivalent positions denoted by Wyckoff letters *c* and *d*. Notice that if the origin of the unit cell is shifted so as to coincide with one of these atoms then their coordinates become (000), (2/3 1/3 1/2) *and* (000), (1/3 2/3 1/2) (see Exercise 1.6 and Section 9.2, Example 4). Finally, having studied Fig. 4.14 it is a good test of your powers of observation to turn back to Fig. 4.10(b) and fill in all the symmetry elements in addition to the 6_3 axes already indicated.

(b) $P\,2_1/c$ C_{2h}^5 2/*m* Monoclinic

No. 14

UNIQUE AXIS *b*, DIFFERENT CELL CHOICES

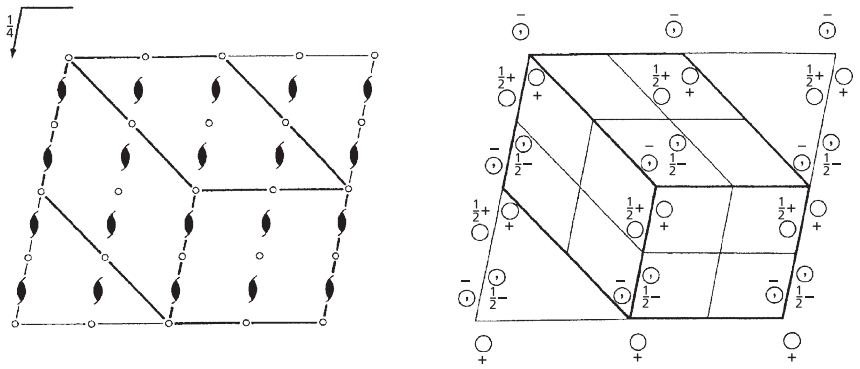

$P\,12_1/c\,1$

UNIQUE AXIS *b*, CELL CHOICE 1

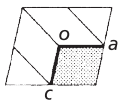

Origin at $\bar{1}$

Asymmetric unit $0\leq x\leq 1;\ 0\leq y\leq \frac{1}{4};\ 0\leq z\leq 1$

Generators selected (1); *t*(1,0,0); *t*(0,1,0); *t*(0,0,1); (2); (3)

Positions

Multiplicity, Wyckoff letter, Site symmetry			Coordinates				Reflection conditions
							General:
4	*e*	1	(1) *x*,*y*,*z*	(2) $\bar{x}$,*y* + $\frac{1}{2}$,$\bar{z}$ + $\frac{1}{2}$	(3) $\bar{x}$,$\bar{y}$,$\bar{z}$	(4) *x*,$\bar{y}$ + $\frac{1}{2}$,*z* + $\frac{1}{2}$	*h*0*l*: *l* = 2*n* 0*k*0: *k* = 2*n* 00*l*: *l* = 2*n*
							Special: as above, plus
2	*d*	$\bar{1}$	$\frac{1}{2}$,0,$\frac{1}{2}$	$\frac{1}{2}$,$\frac{1}{2}$,0			*hkl* : *k* + *l* = 2*n*
2	*c*	$\bar{1}$	0,0,$\frac{1}{2}$	0,$\frac{1}{2}$,0			*hkl* : *k* + *l* = 2*n*
2	*b*	$\bar{1}$	$\frac{1}{2}$,0,$\frac{1}{2}$	$\frac{1}{2}$,$\frac{1}{2}$,$\frac{1}{2}$			*hkl* : *k* + *l* = 2*n*
2	*a*	$\bar{1}$	0,0,0	0,$\frac{1}{2}$,$\frac{1}{2}$			*hkl* : *k* + *l* = 2*n*

Fig. 4.13. Space group $P2_1/c$ (No. 14) (from the *International Tables for Crystallography*), (a) unique axis *b*, cell choice 1, (b) unique axis *b*, different cell choices.

Figure 4.15 is extracted from the entry for space group $P4_12_12$ (No. 92) in the *International Tables for Crystallography*, Volume A. This space group contains principally 4_1 (screw tetrad) axes of symmetry but no glide, mirror planes or inversion axes of symmetry. It is enantiomorphous with space group $P4_32_12$ (No. 96). In the left-hand diagram two neighbouring cells are drawn to show clearly the operation of the 4_1 (right-handed) screw axes along the cell edges. To these two space groups belong the α (low-temperature) form of cristobalite (see Section 1.11.5) in which the distortion from the high temperature β (cubic) form gives rise to the enantiomorphous tetragonal forms.

$P\,6_3/m\,m\,c$ — D_{6h}^4

No. 194 — $P\,6_3/m\,2/m\,2/c$ — $6/m\,m\,m$ — Hexagonal

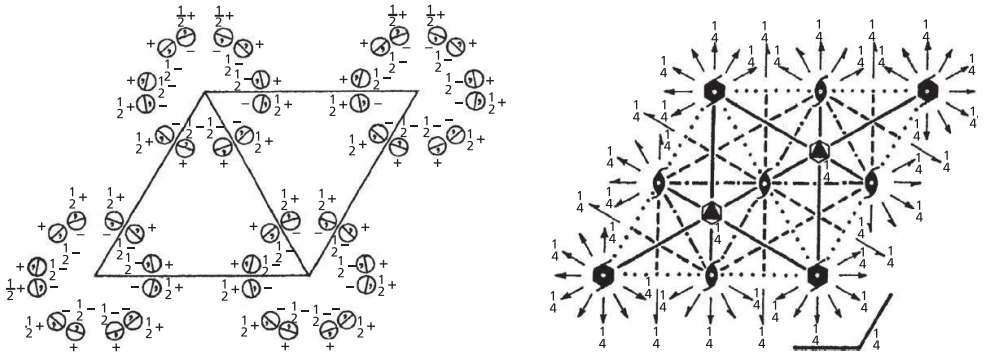

Origin at centre ($\bar{3}m1$)

Number of positions, Wyckoff notation, and point symmetry			Co-ordinates of equivalent positions	Conditions limiting possible reflections
				General:
24	*l*	1	x,y,z; $\bar{y},x-y,z$; $y-x,\bar{x},z$; $\bar{y},\bar{x},z$; $x,x-y,z$; $y-x,y,z$; $\bar{x},\bar{y},\bar{z}$; $y,y-x,\bar{z}$; $x-y,x,\bar{z}$; $y,x,\bar{z}$; $\bar{x},y-x,\bar{z}$; $x-y,\bar{y},\bar{z}$; $\bar{x},\bar{y},\frac{1}{2}+z$; $y,y-x,\frac{1}{2}+z$; $x-y,x,\frac{1}{2}+z$; $x,y,\frac{1}{2}-z$; $\bar{y},x-y,\frac{1}{2}-z$; $y-x,\bar{x},\frac{1}{2}-z$; $y,x,\frac{1}{2}+z$; $\bar{x},y-x,\frac{1}{2}+z$; $x-y,\bar{y},\frac{1}{2}+z$; $\bar{y},\bar{x},\frac{1}{2}-z$; $x,x-y,\frac{1}{2}-z$; $y-x,y,\frac{1}{2}-z$.	*hkil*: No conditions *hh*2$\bar{h}$*l*: *l*=2*n* *h*$\bar{h}$0*l*: No conditions
				Special: as above, plus
12	*k*	*m*	$x,2x,z$; $2\bar{x},\bar{x},z$; $x,\bar{x},z$; $\bar{x},2\bar{x},\bar{z}$; $2x,x,\bar{z}$; $\bar{x},x,\bar{z}$; $\bar{x},2\bar{x},\frac{1}{2}+z$; $2x,\bar{x},\frac{1}{2}+z$; $\bar{x},x,\frac{1}{2}+z$; $x,2x,\frac{1}{2}-z$; $2\bar{x},\bar{x},\frac{1}{2}-z$; $x,\bar{x},\frac{1}{2}-z$.	no extra conditions
12	*j*	*m*	$x,y,\frac{1}{4}$; $\bar{y},x-y,\frac{1}{4}$; $y-x,\bar{x},\frac{1}{4}$; $\bar{y},\bar{x},\frac{1}{4}$; $x,x-y,\frac{1}{4}$; $y-x,y,\frac{1}{4}$; $\bar{x},\bar{y},\frac{3}{4}$; $y,y-x,\frac{3}{4}$; $x-y,x,\frac{3}{4}$; $y,x,\frac{3}{4}$; $\bar{x},x-y,\frac{3}{4}$; $x-y,\bar{y},\frac{3}{4}$.	no extra conditions
12	*i*	2	$x,0,0$; $0,x,0$; $\bar{x},\bar{x},0$; $x,0,\frac{1}{2}$; $0,x,\frac{1}{2}$; $\bar{x},\bar{x},\frac{1}{2}$; $\bar{x},0,0$; $0,\bar{x},0$; $x,x,0$; $\bar{x},0,\frac{1}{2}$; $0,\bar{x},\frac{1}{2}$; $x,x,\frac{1}{2}$.	*hkil*: *l*=2*n*
6	*h*	*mm*	$x,2x,\frac{1}{4}$; $2\bar{x},\bar{x},\frac{1}{4}$; $x,\bar{x},\frac{1}{4}$; $\bar{x},2\bar{x},\frac{3}{4}$; $2x,x,\frac{3}{4}$; $\bar{x},x,\frac{3}{4}$.	no extra conditions
6	*g*	2/*m*	$\frac{1}{2},0,0$; $0,\frac{1}{2},0$; $\frac{1}{2},\frac{1}{2},0$; $\frac{1}{2},0,\frac{1}{2}$; $0,\frac{1}{2},\frac{1}{2}$; $\frac{1}{2},\frac{1}{2},\frac{1}{2}$.	*hkil*: *l*=2*n*
4	*f*	3*m*	$\frac{1}{3},\frac{2}{3},z$; $\frac{2}{3},\frac{1}{3},\bar{z}$; $\frac{2}{3},\frac{1}{3},\frac{1}{2}+z$; $\frac{1}{3},\frac{2}{3},\frac{1}{2}-z$.	*hkil*: If *h*–*k*=3*n*, then *l*=2*n*
4	*e*	3*m*	$0,0,z$; $0,0,\bar{z}$; $0,0,\frac{1}{2}+z$; $0,0,\frac{1}{2}-z$;	*hkil*: *l*=2*n*
2	*d*	$\bar{6}m2$	$\frac{1}{3},\frac{2}{3},\frac{3}{4}$.	*hkil*: If *h*–*k*=3*n*, then *l*=2*n*
2	*c*	$\bar{6}m2$	$\frac{1}{3},\frac{2}{3},\frac{1}{4}$; $\frac{2}{3},\frac{1}{3},\frac{3}{4}$.	
2	*b*	$\bar{6}m2$	$0,0,\frac{1}{4}$; $0,0,\frac{3}{4}$.	*hkil*: *l*=2*n*
2	*a*	$\bar{3}m$	$0,0,0$; $0,0,\frac{1}{2}$.	

Fig. 4.14. Space group $P6_3/mmc$ (No. 194) (from the *International Tables for X-ray Crystallography*).

$P\,4_1\,2_1\,2$ D_4^4 Tetragonal

No. 92 $P\,4_1\,2_1\,2$ Patterson symmetry $P\,4/m\,m\,m$

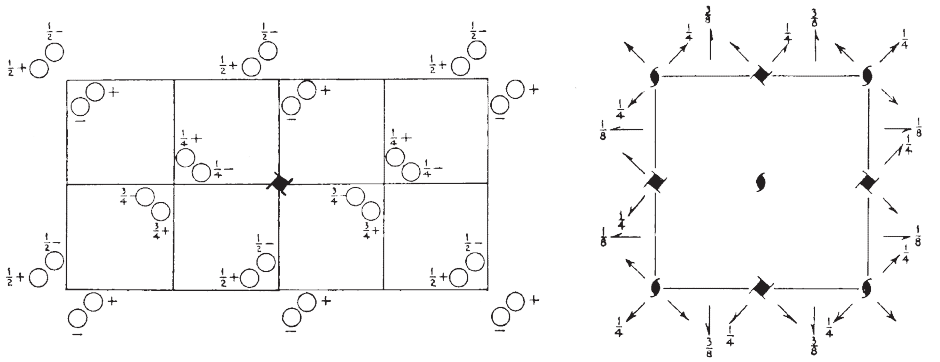

Origin on $2[1\,1\,0]$ at $2_1\,1(1,2)$

Asymmetric unit $0\le x\le 1;\ 0\le y\le 1;\ 0\le z\le \frac{1}{8}$

Symmetry operations

(1) 1 (2) $2(0,0,\frac{1}{2})$ $0,0,z$ (3) $4^+(0,0,\frac{1}{4})$ $0,\frac{1}{2},z$ (4) $4^-(0,0,\frac{1}{4})$ $\frac{1}{2},0,z$
(5) $2(0,\frac{1}{2},0)$ $\frac{1}{4},y,\frac{1}{8}$ (6) $2(\frac{1}{2},0,0)$ $x,\frac{1}{4},\frac{3}{8}$ (7) 2 $x,x,0$ (8) 2 $x,\bar{x},\frac{1}{4}$

Generators selected (1); $t(1,0,0)$; $t(0,1,0)$; $t(0,0,1)$; (2); (3); (5)

Positions

Multiplicity, Wyckoff letter, Site symmetry	Coordinates				Reflection conditions
					General:
8 b 1	(1) x,y,z	(2) $\bar{x},\bar{y},z+\frac{1}{2}$	(3) $\bar{y}+\frac{1}{2},x+\frac{1}{2},z+\frac{1}{4}$	(4) $y+\frac{1}{2},\bar{x}+\frac{1}{2},z+\frac{3}{4}$	$00l$: $l=4n$
	(5) $\bar{x}+\frac{1}{2},y+\frac{1}{2},\bar{z}+\frac{1}{4}$	(6) $x+\frac{1}{2},\bar{y}+\frac{1}{2},\bar{z}+\frac{3}{4}$	(7) $y,x,\bar{z}$	(8) $\bar{y},\bar{x},\bar{z}+\frac{1}{2}$	$h00$: $h=2n$
					Special: as above, plus
4 a $..2$	$x,x,0$	$\bar{x},\bar{x},\frac{1}{2}$	$\bar{x}+\frac{1}{2},x+\frac{1}{2},\frac{1}{4}$	$x+\frac{1}{2},\bar{x}+\frac{1}{2},\frac{3}{4}$	$0kl$: $l=2n+1$ or $2k+l=4n$

Symmetry of special projections

Along [001] $p\,4\,g\,m$
$\boldsymbol{a}'=\boldsymbol{a}$ $\boldsymbol{b}'=\boldsymbol{b}$
Origin at $0,\frac{1}{2},z$

Along [100] $p\,2\,g\,g$
$\boldsymbol{a}'=\boldsymbol{b}$ $\boldsymbol{b}'=\boldsymbol{c}$
Origin at $x,\frac{1}{4},\frac{3}{8}$

Along [110] $p\,2\,g\,m$
$\boldsymbol{a}'=\frac{1}{2}(-\boldsymbol{a}+\boldsymbol{b})$ $\boldsymbol{b}'=\boldsymbol{c}$
Origin at $x,x,0$

Fig. 4.15. Space group $P4_12_12$ (No. 92) (from the *International Tables for Crystallography*, Volume A—partly redrawn and data relating to sub-groups omitted).

4.7 Bravais lattices, space groups and crystal structures

In the simple cubic, bcc and ccp structures of the elements, the three cubic lattices (Fig. 3.1) have exactly the same arrangement of lattice points as the atoms, i.e. in these examples the motif is just one atom. In more complex crystals the motif consists of more than one atom and, to determine the Bravais lattice of a crystal, it is necessary first to identify the motif and then to identify the arrangement of the motifs. In crystals consisting of two or more different types of atoms this procedure may be quite difficult, but fortunately simple examples best illustrate the procedure and the principles involved. For example, in NaCl (isomorphous with TiN; see Fig. 1.14(a)), the motif is one sodium and one chlorine ion and the motifs are arranged in an fcc array. Hence the Bravais lattice of NaCl and TiN is cubic F.

In Li_2O (isomorphous with TiH_2; see Fig. 1.14(b)) the motif is one oxygen and two lithium atoms; the motifs are arranged in an fcc array and the Bravais lattice of these compounds is cubic *F*. In ZnS (isomorphous with TiH; see Fig. 1.14(c)) the motif is one zinc and one sulphur atom; again, these are arranged in an fcc array and Bravais lattice of these compounds is cubic *F*. All the crystal structures illustrated in Fig. 1.14 have the cubic *F* Bravais lattice. They are called face-centred cubic structures not because the arrangements of atoms are the same—clearly they are not—but because they all have the cubic *F* lattice.

In CsC1 (Fig. 1.12(b)), the motif is one caesium and one chlorine ion; the motifs are arranged in a simple cubic array and the Bravais lattice is cubic *P*. To be sure, the arrangement of ions in CsCl (and compounds isomorphous with it) is such that there is an ion or atom at the body-centre of the unit cell, but the Bravais lattice is *not* cubic *I* because the ions or atoms at the corners and centre of the unit cell are different. Nor, for the same reason, should CsCl and compounds isomorphous with it be described as having a body-centred cubic structure.

In the case of hexagonal structures the arrangements of lattice points in the hexagonal *P* lattice (Fig. 3.1) corresponds to the arrangement of atoms in the simple hexagonal structure (Fig. 1.5(a)) and *not* the hcp structure (Fig. 1.5(b)). In the simple hexagonal structure the environment of all the atoms is identical and the motif is just one atom. In the hcp structure the environment of the atoms in the A and B layers is different. The motif is a pair of atoms, i.e. an A layer and a B layer atom per lattice point. The environment of these pairs of atoms (as for the pairs of ions or atoms in the NaCl, or CsCl or ZnS structures) is identical and they are arranged on a simple hexagonal lattice. Notice that in these examples the motif is either asymmetric or has a mirror plane or centre of symmetry. These are further instances of the situation which we found in two-dimensional patterns (Section 2.5). It is the repetition of the motif by the lattice which generates the crystal structures.

The space groups of the simple cubic bcc and ccp structures of the elements are those of maximum symmetry, namely $Pm\bar{3}m$, $Im\bar{3}m$ *and* $Fm\bar{3}m$, and in which the atoms are all at the special positions 000 etc. Similarly, CsCl (Fig. 1.12(b)) and the cubic forms of perovskite $CaTiO_3$ (Fig. 1.17) or barium titanate $BaTiO_3$, in which all the atoms are in special positions, also belong to space group $Pm\bar{3}m$. All these space groups or structures have a centre of symmetry (at the origin) as indicated by the inversion triad axis, $\bar{3}$, symbol.

In all the examples above, the (special) atom positions are fixed or 'pinned down' by the symmetry elements. For example, in the CaF_2 (fluorite) or Li_2O (antifluorite) structures the space group, as with fcc metals, is of maximum symmetry $Fm\bar{3}m$ (point group $m\bar{3}m$) and the symmetry elements fix the positions of the atoms in their special positions precisely as shown in Figs 1.16(c) and (d). For example, an atom or ion must either be evenly bisected by a mirror plane or must be arranged in pairs equidistant each side of it: it cannot occupy an 'in between' position because the mirror symmetry would be violated. It is in crystals of lower symmetry that the positions of the atoms are not completely fixed. The 'classic' example is the structure of iron pyrites, FeS_2, which at first glance might be thought to have the same structure as CaF_2, the S atoms

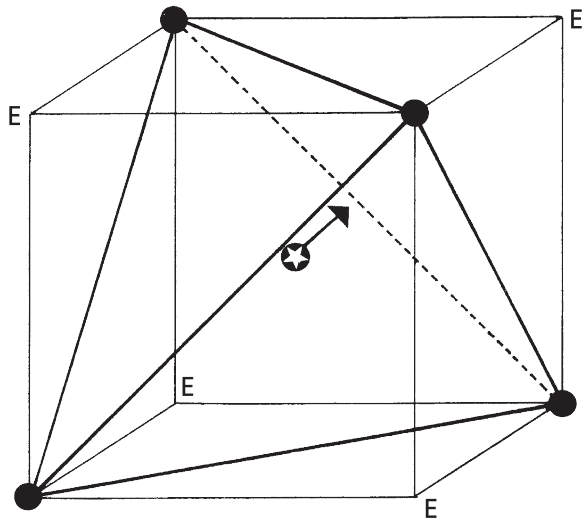

Fig. 4.16. A tetrahedral site in FeS_2 outlined within a cube. The Fe atoms are situated at four corners of the cube, the other four corners are 'empty' (denoted by E). The S atom (starred) is shifted from the centre of the tetrahedron/cube towards one of the four 'empty' corners as indicated by the arrow.

situated precisely at the centres of the tetrahedral sites co-ordinated by the Fe atoms. But this is not so: the S atoms do not lie in the centres of the tetrahedra but are shifted in a body-diagonal (triad axis) direction; in short, they lie in special positions in the structure. The geometry, just for one S atom, is shown in Figure 4.16. Within the whole unit cell the shifts of the S atoms are towards different 'empty' corners, preserving the cubic symmetry but reducing the space group symmetry from $Fm\bar{3}m$ to $Pa\bar{3}$ (point group symmetry reduced from $m\bar{3}m$ to $m\bar{3}$ (or $2/m\bar{3}$)).[3]

The 'amount' of shift of the S atoms in FeS_2, a single parameter, was deduced by W. L. Bragg in 1913 from the intensities of the X-ray reflections. It was the first structure to be analysed in which the atom positions are not fixed by the symmetry and provided Bragg, as he records long afterwards 'with the greatest thrill'.[4] Today of course the number of parameters required to be determined for the far more complex inorganic and especially organic crystals runs into the thousands and constitutes the major task in crystal structure determination.

Zinc blende, ZnS, and isomorphous structures such as TiH (Fig. 1.14(c)) and the technologically important gallium arsenide, GaAs, have the cubic F Bravais lattice, the atoms are again in special positions but the structure does not have a centre of symmetry; the space group in this case is $F\bar{4}3m$. This lack of a centre of symmetry, which is the origin, or crystallographic basis of the important electrical and physical properties in these structures, may be visualized with reference to Fig. 1.14(c). The TiH, ZnS or GaAs atoms are arranged in pairs in the body-diagonal directions of the cube (symbolized by ⟨111⟩—see Section 5.2) and the sequence of the atoms is either, e.g. ••• GaAs ••• GaAs ••• GaAs •••, or the reverse, i.e. ••• AsGa ••• AsGa ••• AsGa •••

[3] See Appendix 1 for illustrative models of the five cubic point groups.
[4] W. L. Bragg *The development of X-ray analysis*, Proc. Roy. Soc. **A262**, 145 (1961).

The body-diagonal directions are *polar* axes and the faces on he opposite sides of the crystal are terminated either by Ga or by As atoms.

In silicon, germanium and the common (cubic) form of diamond (see Section 1.11.6), the pattern of the atoms is the same as in ZnS or GaAs but of course all the atoms are of the same type (see Fig. 1.36). The body-diagonal directions are no longer polar because the sequence of pairs of atoms, e.g. ••• SiSi ••• SiSi ••• SiSi ••• , is obviously the same either way. These structures are centro-symmetric, the centres of symmetry lying half-way between the pairs of atoms.The space group in these cases is $Fd\bar{3}m$, the *d* referring to the special type of glide plane. Graphite and hcp metals, as mentioned above, belong to space group $P6_3/mmc$, as does also wurtzite, the hexagonal form of ZnS (Fig. 1.26) and the common crystal structure of ice (see Section 1.11.5) in which the oxygen atoms lie in the same atomic positions as the carbon atoms in the hexagonal form of diamond (Fig. 1.36(b)) and in which the H atoms are between (but not equidistant between) neighbouring O atoms.

There are (Table 3.1) eleven enantiomorphous point groups (i.e. without a centre or mirror plane of symmetry) and upon which are based the 65 space groups first derived by L. Sohncke and in which there are eleven enantiomorphous pairs. We have already noticed the enantiomorphous pair for α-cristobalite ($P4_12_12$ and $P4_32_12$) based on the tetragonal point group 422. The others of particular interest are those for α-quartz ($P3_121$ and $P3_221$) based on the trigonal point group 32 and for β-quartz ($P6_222$ and $P6_422$) based on the hexagonal point group 622.

Not all the 230 space groups are of equal importance; for many of them there are no examples of real crystals at all. About 70% of the elements belong to the space groups $Fm\bar{3}m$, $Im\bar{3}m$ and $Fd\bar{3}m$ (all based on point group $m\bar{3}m$), $F\bar{4}3m$ (based on point group $\bar{4}3m$) and $6_3/mmc$ (based on point group $6/mmm$). Over 60% of organic and inorganic crystals belong to space groups $P2_1/c$, $C2/c$, $P2_1$, $P\bar{1}$, $Pbca$ and $P2_12_12_1$ and of these space group $P2_1/c$ (based on point group $2/m$, Fig. 4.12) is by far the commonest (see Table 4.1, p. 125).

4.8 The crystal structures and space groups of organic compounds

As mentioned in Section 1.10.1, the stability of inorganic molecules arises primarily from the strong, directed, covalent bonds which bind the atoms together. In comparison, the forces which bind organic molecules together are weak (in the liquid or solid states) or virtually non-existent (as in the gaseous state). The strongest of the intermolecular forces are hydrogen bonds, which link polar groups (as in water or ice, Section 1.11.5) or hydroxyl groups as in sugars. Indeed, organic crystals in which hydrogen bonds dominate are hard and rigid, like inorganic crystals. The remaining intermolecular forces are short-range and are generally described as van der Waals bonds. Apart from residual polarity, organic molecules are generally electrically neutral, and intermolecular ionic bonds, such as occur between atoms or groups of atoms in ionic crystals, do not exist.

The crystal structures which occur (if they occur at all) are largely determined by the ways in which the molecules pack together most efficiently: it is the 'organic equivalent'

of Robert Hooke's packing together of 'bullets' described at the very beginning of this book—except of course that organic molecules have far more complex shapes, or envelopes, than simple spheres.

As described below, it is from such packing considerations that the space groups of organic crystals can be predicted. However, it should be recognized at the outset that the determination of the space group provides little information on the positions of the atoms within the molecules themselves and which, particularly in macromolecules, are nearly all in general positions. The importance of crystallization (apart from its role in purification) lies in the fact that the structure of organic molecules may then be investigated by X-ray diffraction techniques: the space group determines the geometry of the pattern but it is the intensities of the X-ray reflections which ultimately determine the atom positions (see Chapters 6–10 and Chapter 13).

However, there is a further desideratum. Organic molecules which constitute living tissue—proteins, DNA, RNA—do not generally occur *in vivo* as crystals but are separated in an aqueous environment. The process of crystallization may not only reduce or eliminate the aqueous environment but may also distort the molecules away from their free-molecule geometry. An historically important example is the structure of DNA (see Section 10.5). Only when the parallel-orientated strands of DNA are examined in the wet or high-humidity condition (the B form) does the double-helical structure correspond to that which occurs *in vivo*. In the low-humidity or 'dry' condition (the A form) the repeat distance and conformation of the helices is changed—but at the same time giving rise to much sharper diffraction patterns. F.H.C. Crick realized that the transformation was in effect displacive rather than reconstructive (see Section 1.11.5) and that from the A form the double helical B form could be deduced.

4.8.1 The close packing of organic molecules

The first detailed analysis of the close (and closest) packing of organic molecules was made by A.I. Kitaigorodskii* who predicted the possible space groups arising from the close packing of 'molecules of arbitrary form'.[5] He proceeded on the principle that all the molecules were in contact, none interpenetrated, but rather that the 'protrusions' of one molecule fitted into the 'recesses' of a neighbouring molecule such that the amount of empty space was the least possible. He found, in summary, that the deviations from close-packing were small and that (as in the close-packing of spheres) a twelve-fold coordination was the general rule. No assumptions were made as to the nature of the intermolecular forces—the analysis is purely geometrical and must of course be modified when, for example, hydrogen bonding between molecules is taken into account.

The crystallographic interest of the analysis lies in its development from plane group symmetry (Section 2.5) to layer-group symmetry (Section 2.8) and then to space-group symmetry (Section 4.7). We shall follow these steps in outline (omitting the details of the analysis).

* Denotes biographical notes available in Appendix 3.

[5] A I Kitaigorodskii *Organic Chemical Crystallography*, USSR Academy of Sciences, Moscow, 1955; Eng. Trans (revised) Consultants Bureau Enterprises, New York, 1961.

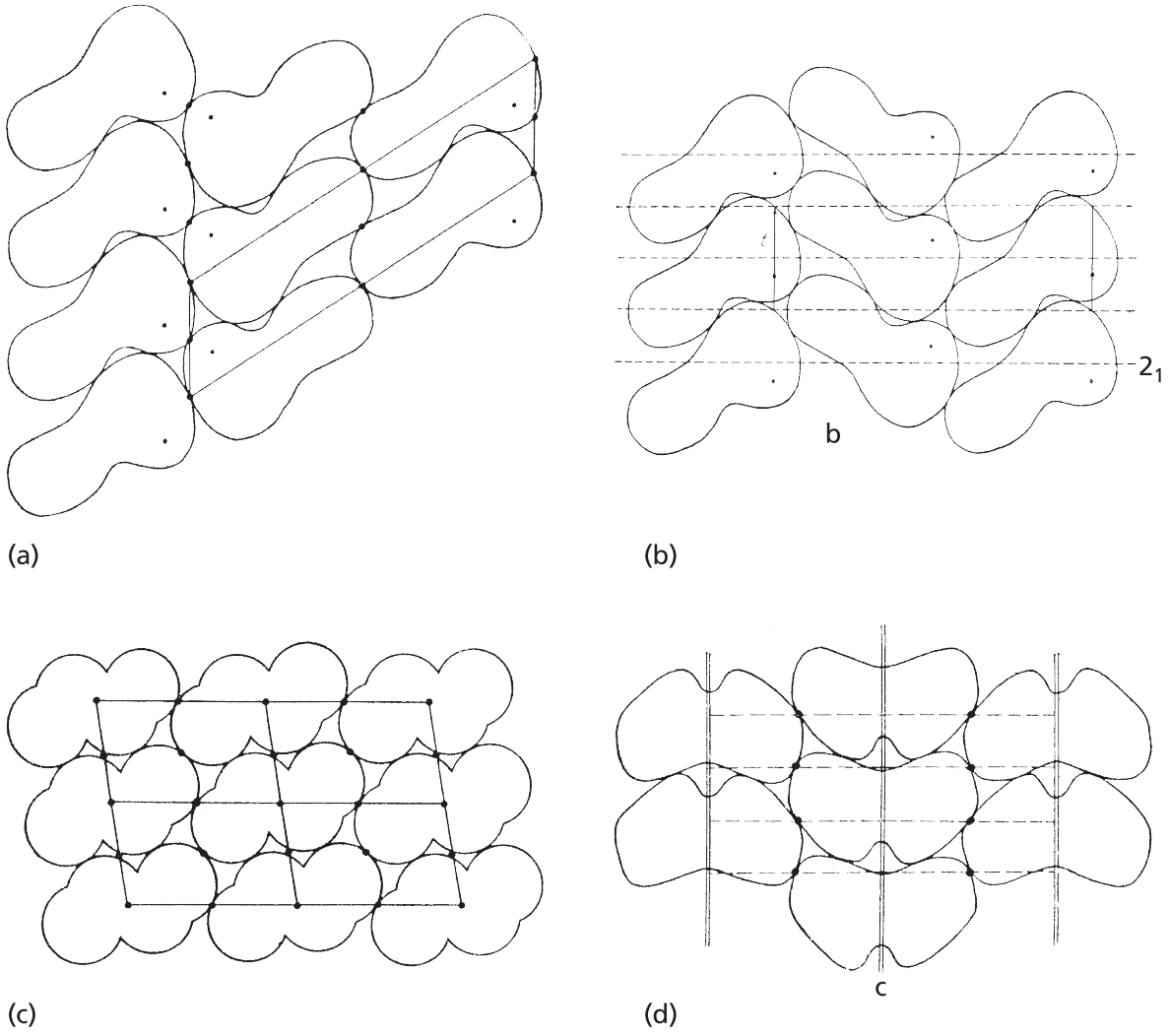

Fig. 4.17. Close-packing of two-dimensional motifs of 'arbitrary form' in oblique and rectangular unit cells. Motifs with point group symmetry 1 (a) and (b), 2 (c) and m (d) (from *Organic Chemical Crystallography* by A.I. Kitaigorodskii, Consultants Bureau, New York, 1961).

For plane molecules (or motifs) of arbitrary form having point group symmetry 1, 2 or *m* (see Fig. 2.3) it turns out that the requirement of close or closest-packing limits the plane groups to those with either oblique or rectangular unit cells (see Fig. 2.6). Figure 4.17 shows four examples to illustrate the motifs of 'arbitrary form' and the packing principles involved.

We now consider molecules or motifs which are three-dimensional, i.e. having 'top' and 'bottom' faces (as represented in Section 2.8, Fig. 2.15 by black and white **R**'s).

As in the two-dimensional case, such motifs can only be arranged with a minimum of empty space in layers in which the unit cells are oblique (total 7) or rectangular (total 41), i.e. a total of 48 out of the 80 possible layer symmetry groups (see Section 2.8). However, there are further restrictions. Layer symmetry groups with horizontal mirror planes are unsuitable for the close packing of such motifs since such planes would double the layers and cause protrusions to fall on protrusions and recesses on recesses.

Similarly, horizontal glide planes parallel to, or mirror planes perpendicular to, the axes of rectangular cells lead to four-fold, not six-fold coordination in the plane. Taking all these restrictions into account we are left with only ten layer symmetry groups which allow six-fold coordination close packing within the plane. These ten groups are shown in Fig. 4.18 where the black and white triangles indicate the 'top' and 'bottom' faces of the 'molecules of arbitrary form'.

Now we need to stack these layers upon each other to create a close-packed structure. Four of these layers are polar—the molecules all face the same way (all black triangles, Fig. 4.18 (a), (d), (f), (i)), represented diagrammatically in Fig. 4.19(a). The rest are non-polar, (Fig. 4.19(b)) and clearly only these non-polar layers can in principle give rise to close packing. Further, the presence of diad axes normal to the layers prohibit the close-packing of arbitrary shapes which just leaves us with layer-symmetry groups b, c, g and h (Fig. 4.18). Finally Kitaigorodskii concludes that close-packing can be achieved with molecules with monad symmetry (1) or a centre of symmetry ($\bar{1}$) but that for molecules with diad (2) or a single mirror plane (m) symmetry there is a reduction in full packing density; such structures he called 'limitingly close packed'.[5] Finally, he established those space groups which he termed 'permissible'. The space groups thus derived are listed in Table 4.1.

It is of interest to compare these predicted space groups with those of the molecular solids listed in the *Cambridge Structural Database* which (in 2009) had a total of 460,000 entries. Of this number, eight space groups account for 84% of all the

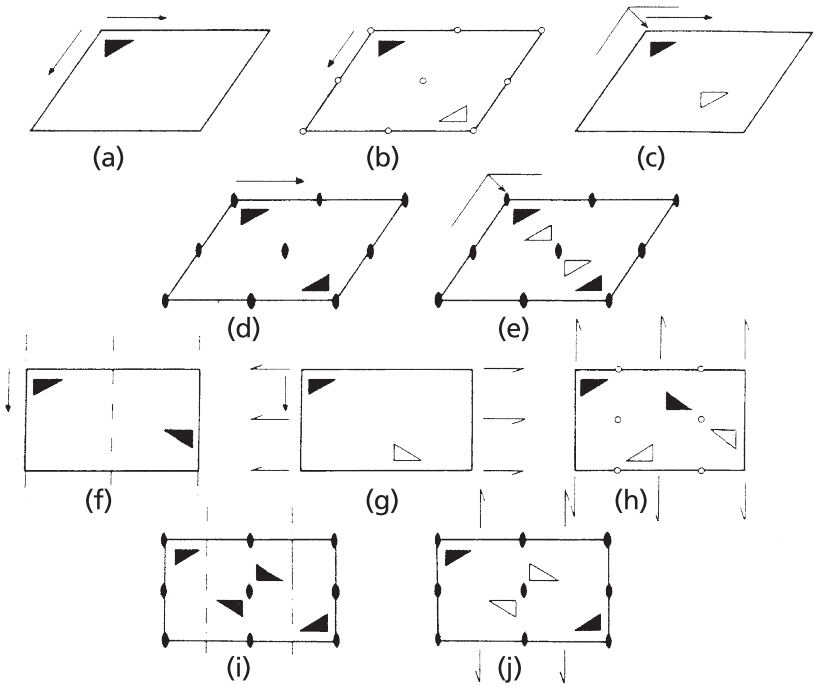

Fig. 4.18. Representation of the ten-layer symmetry groups allowing coordination close packing of three-dimensional motifs in a plane. Single-headed arrows indicate in-plane screw diads, dashed lines indicate vertical glide planes (from *Macromolecular Physics*, Volume 1, by B. Wunderlich, Academic Press, New York and London, 1973).

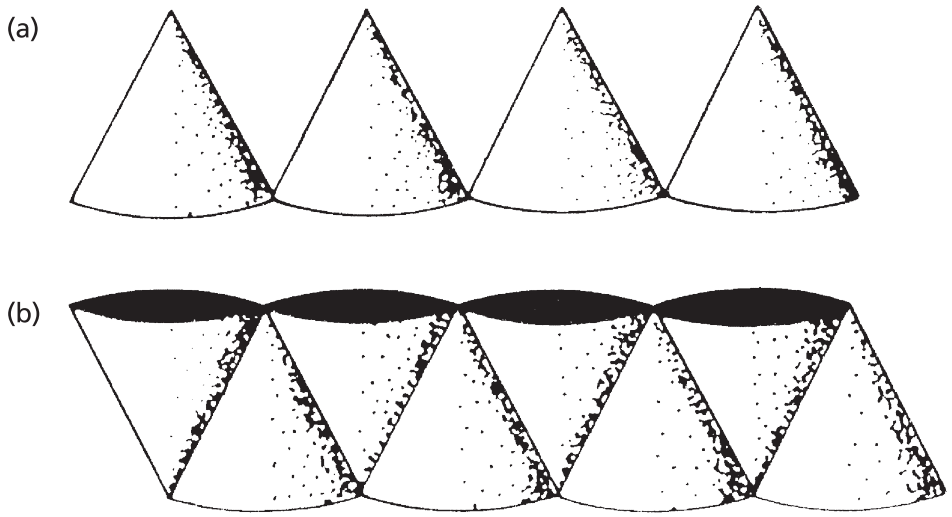

Fig. 4.19. Representation using a cone as a motif of the packing of (a) polar and (b) non-polar layers (from *Macromolecular Physics*, Volume 1, by B. Wunderlich, Academic Press, New York and London, 1973).

Table 4.1 Space groups for closest, limitingly and permissible close packing.

Motif symmetry	Closest packed	Limitingly close packed	Permissible
1	$P\bar{1}, P2_1, P2_1/c, Pca2_1, Pna2_1, P2_12_12_1$	None	$P1$, C_c, $C2$, $P2_12_12$, $Pbca$
$\bar{1}$	$P\bar{1}, P2_1/c, C2/c, Pbca$	None	$Pccn$
2	None	$C2/c, P2_12_12, Pbcn$	$C2, Aba2$
m	None	$Pmc2_1, Cmc2_1, Pnma$	C_m, $P2_1/m$, $Pmn2_1$, $Abm2, Ima2, Pbcm$

entries, viz. $P2_1/c$ (36%), $P\bar{1}$ (17.6%), $P2_12_12_1$ (10.2%), $C2/c$ (7.0%), $P2_1$ (5.7%), *Pbca* (4.1%), *Pnma* (1.7%) and $Pna2_1$ (1.7%). All these space groups are included in Table 4.1—a remarkable predictive achievement when one considers how little chemistry was involved!

4.8.2 Long-chain polymer molecules

The crystal structures and space groups formed by long-chain polymer molecules are also in accord with the principles outlined above.

In the case of *atactic* polymers (i.e. those in which the side-groups are large and/or randomly distributed along the chain), crystal structures rarely occur—the side-groups keep the chains well apart—hence the name atactic. Crystal structures only occur in *tactic* polymers in which the side-groups are regularly distributed on one side of the chain (*isotactic*) or alternatively each side (*syndiotactic*). We shall consider just two polymers—polyethylene (polythene) and isotactic polypropylene (polypropene).

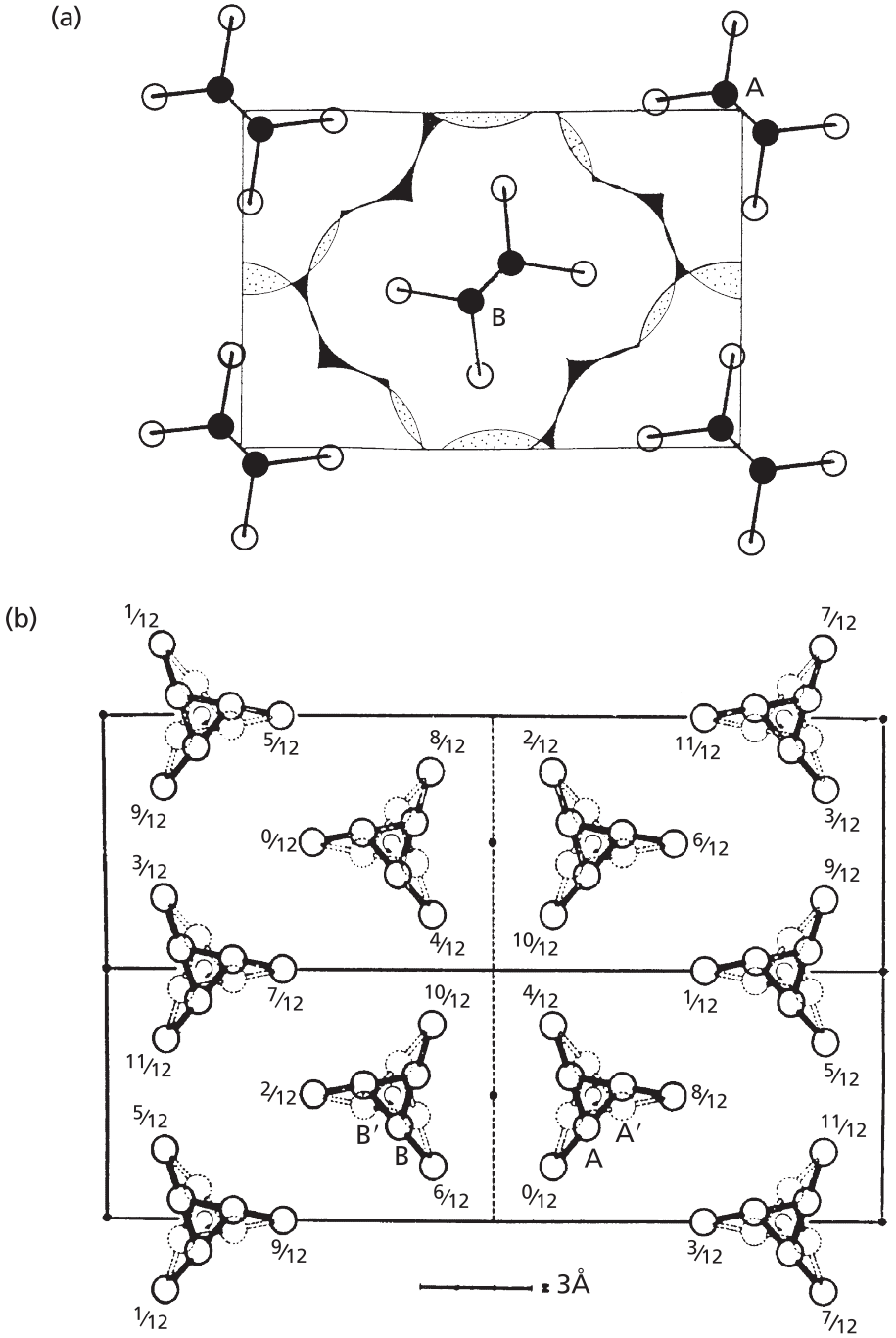

Fig. 4.20. Projections of polymer unit cells perpendicular to the chain axes. (a) Polyethylene, space group P*nam*, the centres of the carbon and hydrogen atoms in the planar zig-zag chains are shown by black and open circles respectively; the envelopes of the molecules show clearly the close packing (from *Macromolecular Physics*, Volume 1, by B. Wunderlich, Academic Press, New York and London, 1973). (b) Isotactic polypropylene, space group P $2_1/c$; the senses of the helices are indicated by the ↺ and ↻ symbols (from *Structure and properties of isotactic polypropylene* by G. Natta and P. Corradini, *Nuovo Cimento*, Suppl. to Vol **15** 1, 40, 1960).

Polyethylene n(CH_2) is the simplest polymer, made up of a planar zig-zag chain of carbon atoms, each carbon tetrahedrally coordinated to two hydrogen atoms. Two crystal structures occur, polyethylene I (orthorhombic, space group P*nam*—equivalent to P*nma* by change of axes) and polyethylene II (monoclinic, space group C2/*m*). Polyethylene I is the common, stable form and the arrangement of the chains in the unit cell is shown in Fig. 4.20(a). The zig-zag planes of the chains are at 45° to the unit cell axes and are so arranged that the protrusions of one chain fit into the 'hollow' or recess formed by three neighbouring chains as is also shown in Fig. 4.20(a) by the outlines or the envelopes of the molecules. Screw diad axes of symmetry run in the directions of all three axes in the unit cell—principally along and through the centres of the chains.

In polypropylene (polypropene), n(CH_2-$CHCH_3$), the CH_3 side-groups approach too closely for the backbone to remain planar and their efficient packing results in the backbone being twisted into a helical conformation, both right and left handed. In isotactic polypropylene the crystal structure is monoclinic and the space group is $P\,2_1/c$—the commonest space group of all. Figure 4.20(b) shows a projection of the unit cell perpendicular to the chain axes. The packing together of the helices is dictated by the intermeshing of the CH_3 side-groups and this occurs most efficiently when the rows of helices along the *c*-axis are alternatively right and left handed as shown in Fig. 4.20(b). The packing is, in fact, very close to hexagonal, like a bundle of pencils, and an hexagonal unit cell may also occur. (Figure 10.11(b) shows a fibre photograph of isotactic polypropylene and Exercise 10.4 shows how the orientation of the chains in the unit cell may be determined.)

4.9 Quasicrystals (quasiperiodic crystals or crystalloids)

The 230 space groups represent all the possible combinations of symmetry elements, and therefore all the possible patterns which may be built up by the repetition, without any limit, of the structural units of atoms and molecules which constitute crystals. But real crystals are finite and the atoms or molecules at their surfaces obviously do not have the same environment as those inside. Moreover, crystals nucleate and grow not according to geometrical rules as such but according to the local requirements of atomic and molecular packing, chemical bonding and so on. The resulting repeating pattern or space group is the usual consequence of such requirements, but it is not a necessary one. We will now consider some such cases where 'crystals' nucleate and grow such that the resulting pattern of atoms or molecules is non periodic and does not conform to any of the 230 space groups—in short the three-dimensional analogy to the non-periodic patterns and tilings discussed in Section 2.9. But first we need to adopt a new name for such structures and, following Shechtman[6] can call them **quasiperiodic crystals** or **materials**, or following Mackay[7] call them **crystalloids** or simply, call them **quasicrystals**.

[6] D. Shechtman, I. Blech, D. Gratias, and J.W. Cahn (1984) *Metallic phase with long-range orientational order and no translational symmetry*. Phys. Rev. Lett. **53**, p. 1951.

[7] A.L. Mackay (1976) *De nive quinquangula*, Phys. Bull. p. 495.

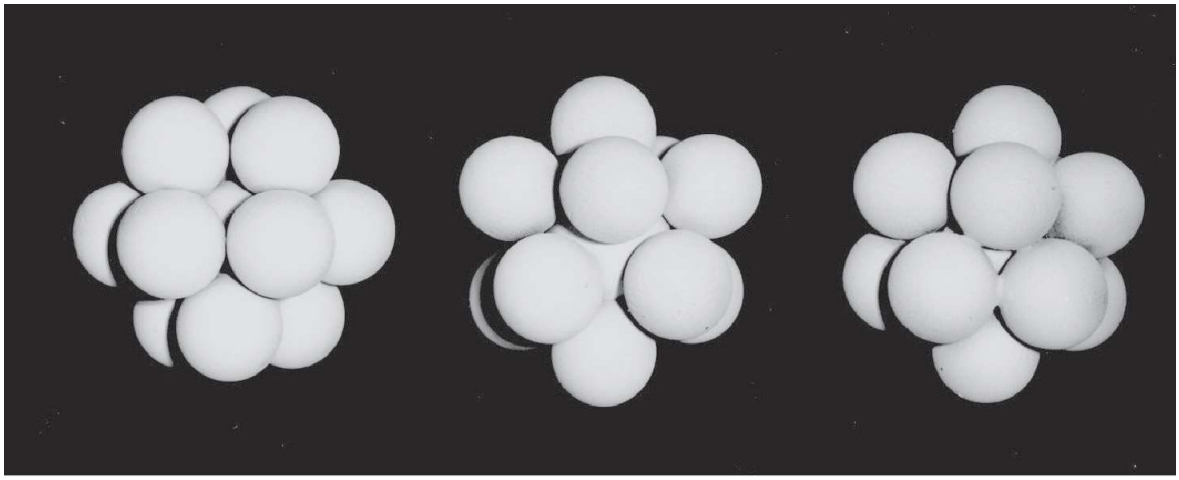

(a) (b) (c)

Fig. 4.21. (a) The close packing of 12 spheres around a central sphere as in the ccp structure. The solid is a cubeoctahedron; note that the spheres are not *evenly* distributed round the central sphere, some of the interstices are square, some triangular, (b) The twelve spheres shifted to obtain an *even* distribution; note that the spheres are surrounded by, but not in contact with, five others. (c) The spheres brought together such that they are now in contact; the central sphere is now ∼10% smaller. The solid now has the 20 triangular faces of an icosahedron (see also note on pp. 129–30).

We will start 'where we began' in Section 1.1 of this book by model-building with equal size closely packed spheres. In the ccp structure, as we have seen, each sphere is surrounded or coordinated by 12 others as shown in Fig. 4.21(a). The polyhedron formed around the central sphere is a cubeoctahedron. It is one of the thirteen semi-regular or Archimedean solids (see Sections 3.4 and Appendix 2). However, even though all the spheres are close-packed, they are not all *evenly distributed* around the central sphere the interstices between them are different: some 'square', some 'triangular'.

Now, we can shift the spheres around the central sphere to obtain an even distribution and as we see (Fig. 4.21(b)), this occurs when each sphere is surrounded by (but not now touching) five others and with 'open' triangular interstices between them. (This operation is best carried out by making the central sphere out of soft modelling clay and using pegs sticking from the spheres into the clay to keep them in place.) Finally, we can squeeze the whole model (i.e. compress the central sphere) in our cupped hands to bring all the spheres into contact and make a close-packed shell of 12 spheres as shown in Fig. 4.21(c). We have created icosahedral packing because the solid has the 20 triangular faces of an icosahedron. The central sphere or interstice now has a radius some 10% smaller than the 12 surrounding spheres.

The icosahedron can be extended by adding a second icosahedral shell of 42 atoms, twice the size of the first, then a third shell of 92 atoms, as shown in Fig. 4.22. The atoms in the surfaces of the 20 triangular faces are clearly close-packed but they are not close-packed with the atoms in the underlying shells. As further shells are added, Mackay shows that the packing density converges to 0.688—a value only a little greater

than the packing density for a (monoatomic) bcc structure (see Section 2.9)—which is often the high temperature structure of metals and alloys.

Mackay[8] also shows that the structure of quasicrystals may be understood by an extension of Penrose tiling from two to three dimensions (see Section 2.9), using obtuse and acute rhombohedra (instead of 'wide' and 'narrow' rhombs) and corresponding matching rules. Again, the Golden Ratio occurs as the limit of the ratio of the occurrence of these two types of rhombohedra. Icosahedral packing is not the densest packing (cubeoctahedral packing is the densest—packing density 0.7405—see Section 1.4), nor is it crystallographic packing—the non-repeating pattern of the shells of spheres constitutes a crystalloid with point group symmetry $2\bar{3}\bar{5}$ indicating the presence of 30 two-fold, 20 three-fold and 12 five-fold axes of symmetry. It is, however, an extremely stable structure (the spheres naturally 'lock' together during the squeezing operation) and it is the basis of Buckminster Fuller's construction of geodesic domes (Section 1.11.6) as well as being characteristic of many virus structures (e.g. the polio virus) which makes them so indestructible.

Icosahedral structures also occur in several metallic alloys, in particular those based on aluminium with copper, iron, ruthenium, manganese, etc. These quasicrystals were first recognized in an Al-25wt% Mn(Al_6Mn) alloy by Dan Shechtman (see Section 11.4.3) from the ten-fold symmetry of their electron diffraction patterns (i.e. five-fold symmetry) plus a centre of symmetry resulting from diffraction—Friedel's

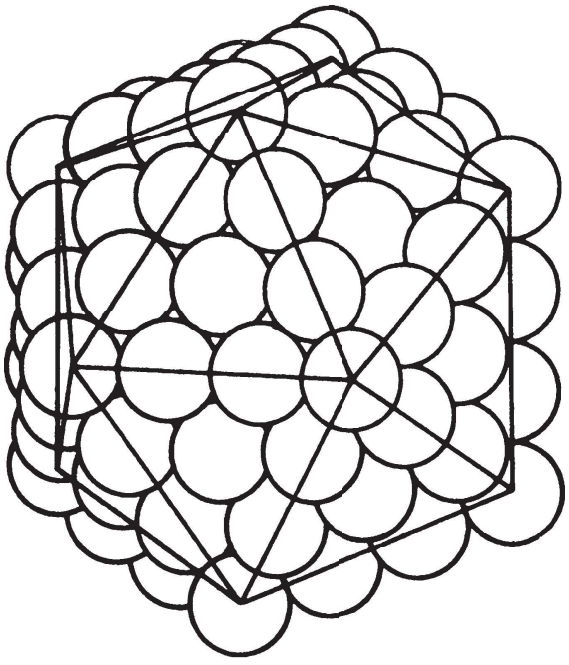

Fig. 4.22. Icosahedral packing of spheres showing close-packing on each of the 20 triangular faces (from 'A dense non-crystallographic packing of equal spheres', by A. L. Mackay (1962), Acta. Cryst. **15,** 916).

[8] A.L. Mackay (1982) *Crystallography and the Penrose Pattern*, Physica **114A**.

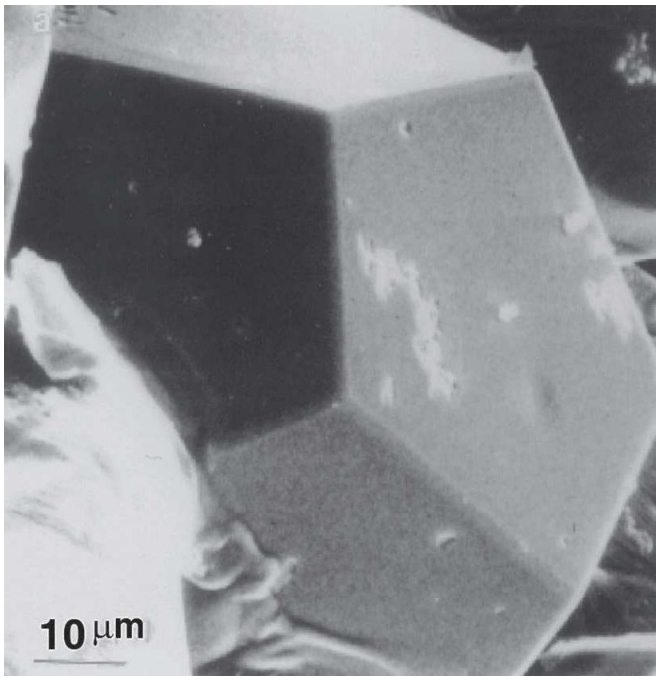

Fig. 4.23. A quasicrystal of a 63% Al, 25% Cu-11% Fe alloy showing pentagonal dodecahedral faces (from 'A stable quasicrystal in Al-Cu-Fe system' by An-Pang Tsai, Akihisa Inoue and Tsuyoshi Masumoto, *Jap. J. Appl. Phys.* **26**, 1505, 1987).

law—see Section 9.2). Many such quasicrystals, formed by rapid solidification from the melt, are metastable and revert to crystalline structures on heating, but stable quasicrystals as large as a few millimetres in size have been prepared. Figure 4.23 is a scanning electron micrograph of a 63% Al-25% Cu-11% Fe alloy quasicrystal showing the existence of beautiful pentagonal dodecahedral faces. The pentagonal arrangement of atoms in such a face can be revealed by scanning tunnelling microscopy of carefully prepared surfaces and Fig. 4.24 shows such a (Fourier filtered) image of the quasicrystalline alloy Al_{70} Pd_{21} Mn_9.

Icosahedral shells of atoms may also occur as the motif within crystal structures. For example, the alloy $MoAl_{12}$ consists of Mo atoms surrounded by icosahedral shells of 12 Al atoms, the icosahedra themselves being packed together in a bcc array. Similarly, the so-called complex alloy Frank–Caspar phases (with 162 atoms per unit cell) consist of clusters of atoms of icosahedral shape (or parts of icosahedra) which are assembled to form a periodic lattice.

Icosahedral groups of molecules also occur in a number of gas hydrates which can be crystallized in the form of highly hydrated solids, called clathrates. For example, chlorine hydrate, Cl_2nH_2O, has a body-centred cubic structure at the centre and corners of which the water molecules are arranged at the corners of pentagonal dodecahedra—an arrangement analogous to dodecahedrene (see Section 1.11.6). Further water molecules occupy the interstices between four such dodecahedra and the chlorine molecules are 'imprisoned' within this framework—hence the name clathrate, meaning latticed or screened.

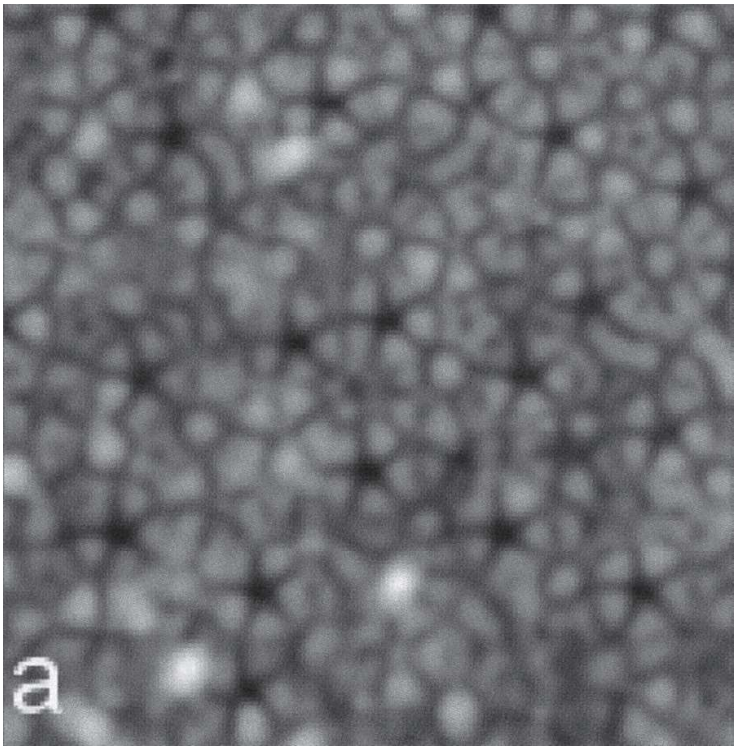

Fig. 4.24. Image (10 nm × 10 nm) of a surface of the alloy Al_{70} Pd_{21} Mn_9 showing the five-fold 'dark star' quasiperiodic pattern. (Photograph by courtesy of Prof. Ronan McGrath, University of Liverpool.)

It was the known existence of such phases which led some crystallographers, Linus Pauling in particular, to question the existence of quasicrystals. The arguments are complex but may be (partly) understood by the tetrahedron models shown in Fig. A1.4 (Appendix 1): a multiply twinned crystal may exhibit a symmetry very close to that of (true) pentagonal symmetry.

Quasicrystallography has an important role in the new science of nanomaterials. As particle size decreases, surface energy terms increasingly dominate and determine the relative stability of different crystal/quasicrystal structures. For example, W, Mo, and Nb, which are all bcc in the bulk, have fcc or hcp structures at particle sizes 5∼10 nm. All particles assume polyhedral shapes and small (<5 nm) clusters may be quasicrystalline.

A note on the transformation from crystallographic to quasiperiodic atom packing

The transformation from the cubeoctahedron to the icosahedron (Fig 4.21 and the front cover illustration of this book) may be described in another way. In cubic close-packing the 'middle' ring of six atoms is *planar* with a group of three close-packed atoms above and three below. In icosahedral packing the corresponding ring of six atoms is *puckered* (resulting in a ∼10% smaller central cavity) with again three close-packed atoms above and three below. Hence, the transformation may proceed by such small displacive atom movements.

Exercises

4.1 Draw the space group *Pba*2 with the pattern unit ◯ at the following positions:

(a) on the *b* glide plane, i.e. at $\left(\frac{1}{4}y'z'\right)$;

(b) at the intersections of the *a* and *b* glide planes, i.e. at $\left(\frac{1}{4}\,\frac{1}{4}z'\right)$;

(c) on a diad axis through the origin, i.e. at (00z′);

(d) on a diad axis through the mid-points of the cell edges, i.e. at $\left(\frac{1}{2}0z'\right)$.

Hence, show that only (c) and (d) constitute special positions.

4.2 Make and examine the crystal models of NaCl, CsCl, diamond, ZnS (sphalerite), ZnS (wurtzite), Li_2O or CaF_2 (fluorite), $CaTiO_3$ (perovskite). Identify the Bravais lattice and describe the motif of each structure.

4.3 Figure 1.33 shows the pattern of silicon atoms in one enantiomorphous form of α-quartz (trigonal) and the corresponding form in β-quartz. Identify the space groups of these two forms and describe the structural relationships between them.